

# Review of Electrochemical Hydrogen Sensors

Ghenadii Korotcenkov,<sup>‡</sup> Sang Do Han,<sup>†</sup> and Joseph R. Stetter<sup>\*,§,||</sup>

Gwangju Institute of Science and Technology, Gwangju, Republic of Korea, Technical University of Moldova, Chisinau, Republic of Moldova, Korea Institute of Energy Research, Daejeon, Republic of Korea, and Microsystems Innovation Center, SRI International, Menlo Park, California USA

Received May 6, 2008

## Contents

1. Introduction and Background	1402	6.5.1. Solid Electrolytes for High-Temperature H <sub>2</sub> Sensors	1424
2. Fundamentals of Electrochemical H <sub>2</sub> Sensors	1404	6.5.2. Practical High-Temperature H <sub>2</sub> Sensors	1424
2.1. Amperometric H <sub>2</sub> Sensors	1404	6.5.3. Role of Sensing Electrodes in High-Temperature H <sub>2</sub> Sensors	1425
2.2. Potentiometric H <sub>2</sub> Sensors	1406	6.5.4. Advantages of High-Temperature Solid Electrolyte H <sub>2</sub> Sensors	1427
2.3. Conductometric Sensors	1407	6.6. Conductometric Solid Electrolyte H <sub>2</sub> Sensors	1428
3. Electrochemical H <sub>2</sub> Sensor Designs and Materials	1407	7. Outlook	1429
3.1. Membranes	1407	8. Acknowledgments	1430
3.2. Electrolytes	1408	9. References	1430
3.3. Electrodes	1408		
3.3.1. Materials for Electrodes	1409		
3.3.2. Fabrication of Electrodes	1410		
3.3.3. Mechanism of Electrode Reactions	1410		
3.4. Bias Control of Selectivity and Sensitivity	1410		
4. Practical Electrochemical H <sub>2</sub> Sensors with Liquid Electrolytes	1410		
4.1. Details of Electrode and Sensor Fabrication	1411		
4.2. Design of Electrochemical Sensors for Field Applications	1412		
4.2.1. Temperature	1412		
4.2.2. Humidity	1412		
4.2.3. Pressure	1413		
4.2.4. Calibration	1413		
4.2.5. Potential Failure Mechanisms	1413		
4.2.6. Sensor Life	1413		
5. Amperometric and Potentiometric H <sub>2</sub> Sensors with Polymer Electrolytes	1414		
5.1. Advantages/Limitations of Polymer Electrolyte H <sub>2</sub> Sensors	1414		
5.2. Response Characteristics of Polymer H <sub>2</sub> Sensors	1414		
5.3. Methods to Improve H <sub>2</sub> Sensor Performance	1417		
6. Solid Electrolyte H <sub>2</sub> Sensors	1419		
6.1. Solid Electrolytes Used in H <sub>2</sub> Sensors	1419		
6.2. Solid Electrolyte H <sub>2</sub> Sensors: Fundamentals of Operation	1420		
6.3. Low-Temperature Solid Electrolyte H <sub>2</sub> Sensors	1421		
6.4. Performance of Mixed-Potential H <sub>2</sub> Sensors	1423		
6.5. High-Temperature Solid Electrolyte H <sub>2</sub> Sensors	1424		

## 1. Introduction and Background

Hydrogen, H<sub>2</sub>, is one of the most important of the reducing gases and is used in many chemical processes and various industries including aerospace, medical, petrochemical, transportation, and energy.<sup>1–6</sup> The use of hydrogen in fuel cells for transportation and power generation applications has renewed interest today and can lead to less polluting vehicles where the emissions are only water.<sup>7</sup> Hydrogen finds extensive application as a cryogenic-fuel in rockets and as a lift gas in weather balloons. Hydrogen batteries and fuel cells are used in satellites. In power plants, gaseous hydrogen is used for removing friction-heat in turbines. Hydrogen is involved as a product in many chemical reactions including the charging of acid electrolyte batteries.

Hydrogen is a colorless, odorless gas which, when mixed with air, is flammable/explosive in the 4–75% (by volume) concentration range. The minimum energy for hydrogen gas ignition in air at atmospheric pressure is about 0.02 mJ, and it has been shown that escaped hydrogen can be very easily ignited; the ignition temperature in air is 520–580 °C. Hydrogen gas is the lightest element, having a relative density of 0.07, and is extremely buoyant and will accumulate near the ceiling of an airtight room. Moreover, in high concentrations, hydrogen will exclude an adequate supply of oxygen, causing asphyxiation.

Hydrogen must be monitored for many reasons. Under process conditions, monitoring is important to provide control of reactions. The measurement of diffusible hydrogen is important in the certification of welds. Accumulation can be dangerous, and safety monitoring of confined spaces is important. Transportation applications will further increase the demand for cheap, simple, reliable, and low-cost hydrogen gas sensors to guard against possible accidents. The emergence of a safety sensor is vital to the widespread use and the public acceptance of hydrogen as a fuel.

The required sensor(s) for hydrogen will need to have a sensitivity that can range from the detection of trace amounts of hydrogen (on the order of parts per million [ppm]) to levels

\* To whom correspondence should be addressed. E-mail: joseph.stetter@SRI.com.

<sup>†</sup> Korea Institute of Energy Research, Daejeon, Republic of Korea. E-mail: sdhan@kier.re.kr.

<sup>‡</sup> Gwangju Institute of Science and Technology, Gwangju, Republic of Korea, and Technical University of Moldova, Chisinau, Republic of Moldova. E-mail: ghkoro@yahoo.com.

<sup>§</sup> SRI International.

<sup>||</sup> New address: KWJ Engineering Inc., 8440 Central Ave, Newark, CA 94560, USA. E-mail: jrstetter@kwjengineering.com.



Ghenadii Korotcenkov is a chief scientific researcher of the Technical University of Moldova and the head of the Gas Sensor Group. Currently, he is a research Professor at Gwangju Institute of Science and Technology. He received his Ph.D. in Physics and Technology of Semiconductor Materials and Devices from the Technical University of Moldova in 1976, and his Habilitat Degree (DSc) in Physics and Mathematics from the Academy of Science of Moldova in 1990. G. Korotcenkov has experience in the design and study of solid state gas sensors based on metal oxide thin films. His current research interests include material science focused on metal oxide deposition and characterization, surface science, and gas sensing effects. Structural engineering of metal oxide films to prepare low-cost and low-power,  $\text{SnO}_2$ - and  $\text{In}_2\text{O}_3$ -based sensors for  $\text{CO}$ ,  $\text{CH}_4$ ,  $\text{H}_2$ , smoke, ozone, and vapors of organic solvents has been developed. The fundamental challenge of his research is both to establish the relation between structure/composition and gas sensor's analytical performance on both atomic and mesoscopic scales, and to understand the mechanism of metal oxide gas sensor response. G. Korotcenkov is an internationally known expert in the field of metal oxide gas sensors. He is the author of five books and special issues, five invited review papers, and several book chapters. He has coauthored more than 180 peer-reviewed articles and has 15 patents. He has presented more than 200 reports at national and international conferences. His research activities are honored by the Award of the Supreme Council of Science and Advanced Technology of the Republic of Moldova (2004), the Prize of the Presidents of Ukrainian, Belarus, and Moldovan Academies of Sciences (2003), the Senior Research Excellence Award of the Technical University of Moldova (2001; 2003; 2005), a Fellowship from the International Research Exchange Board (1998), and the National Youth Prize of the Republic of Moldova (1980).



Sang-Do Han received his Ph.D. degree in Solid State Chemistry from University of Bordeaux, France. He worked at LG Semiconductor Co. Ltd. and is currently a principal researcher in the photoelectromaterial center at the Korea Institute of Energy Research (KIER) since 1980. His areas of interest are (i) electronic and electrolyte nanomaterials, (ii) advanced chemical sensors and MEMS devices, (iii) hydrogen, oxygen, and ozone production technologies, and (iv) inorganic/organic phosphor materials. Currently, he is president of (the Journal of) the Korean Sensors Society. He has more than 320 published and presented research results including papers, patents, reports, and books. He is also coworking as a professor in electronic materials and devices at the Chungnam National University, Daejeon.



Dr. Joseph R. Stetter is currently CTO at KWJ Engineering Inc., in Newark, CA, and up to 2008 was the Director of the Microsystems Innovation Center at SRI International in Menlo Park, CA. Stetter obtained a Ph.D. in Physical Chemistry from the University at Buffalo (SUNY, 1975) and in the 1970s was Director of Chemical Research at the Energetics Sciences Division of Becton Dickinson and Company, where he developed the first diffusion-type electrochemical  $\text{CO}$  sensors, the earliest diffusion  $\text{CO}$  dosimeters, solid-state gas sensors for  $\text{CO}$ ,  $\text{NO}_x$ ,  $\text{SO}_2$ , and other toxic gases, and an electrochemical hydrazine sensor still in use. While at the Argonne National Laboratory in the 1980s, he led the organic analysis group, wherein laboratory and field GC, GC/MS, FTIR, and TOFMS analytical techniques were developed and applied to environmental biological and energy-related complex mixture analysis. His team codeveloped bio-directed chemical characterization methods for isolation and identification of carcinogens in coal tars. He also developed of the first integrated and operational "sensor-array-based" instrument with pattern recognition (now called an electronic nose). Dr. Stetter founded Transducer Research, Inc. (1983), where he developed portable instruments and sensors for  $\text{CO}$  and  $\text{CO}_2$ , end of service filter indicators, chlorinated hydrocarbon sensors,  $\text{NO}_x$  sensors, personal protection instruments, and low-cost, effective-protection equipment for human health and environmental applications. In the 1990s, he sold TRI and became Professor of Chemistry at the Illinois Institute of Technology, started the sensor research group, taught in both chemistry and business schools, founded the International Center for Sensor Research and Engineering at IIT, and mentored both M.S. and Ph.D. students in analytical, environmental, and electrochemical sciences. He founded Transducer Technology Inc. (TTI) a start up company focusing on nanotechnology enabled sensors and instruments in 1999. In 2007 TTI merged with KWJ Engineering, Inc. of Newark, CA, making nanosensors for health, safety, and process control applications. Currently, Dr. Stetter's research work is focused on new commercially viable MEMS Chemical sensors, analytical methods, unique structures/materials, artificial senses, chem/bio sensors, MEMS for drug and vaccine delivery, micro/nanostructures, and bio-MEMS. Dr. Stetter has published more than 200 technical articles, has written book chapters, and has more than 30 domestic and foreign patents. He has served as Chairman of the Electrochemical Society Sensor Division and on the boards of national and international technical societies. He has organized national and international scientific meetings and symposia and frequently serves as editor and reviewer for scientific and engineering journals. His awards include three IR-100 Awards for new product development; the Federal Laboratory Consortium Special Award for Excellence in Technology Transfer; the Argonne National Laboratory Inventor's award; the Technology Management Association of Chicago's 2002 "Entrepreneur-of-the-Year" award, and two NASA New Technology Awards. He has been elected "Fellow" of the Electrochemical Society (2008) and is also on the board of directors for several start-up companies. There are commercial products based on Dr. Stetter's work that are in worldwide use today, protecting human health and the environment as well as providing industrial and environmental analysis.

near the lower explosive limit, or LEL (4%  $\text{H}_2$  in air), and to concentrations near 100%. The sensor(s) will need to function in ambient air, in cryogenic and high-temperature process environments. The  $\text{H}_2$  sensor will be most valuable if it can provide its measurements with high sensitivity, high selectivity, and fast response time but even more important

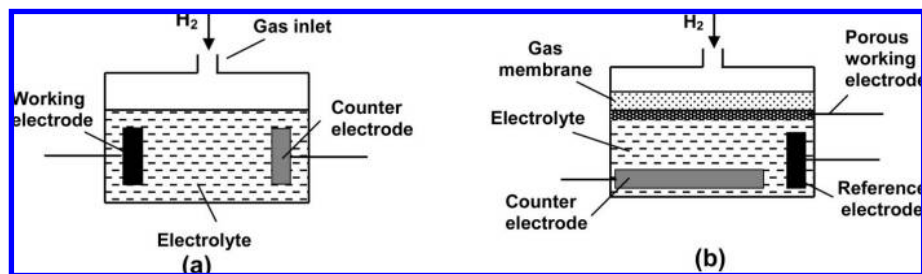


**Figure 1.** Schematic diagram of  $H_2$  sensors with (a) two- and (b) three-electrode configurations.

are logistical properties of long-term stability, low cost, and simple operation in all applications.

Many different hydrogen sensor technologies have been reported. Hydrogen sensors based on thermoelectric effects, thermal conductivity, catalytic combustion (combustible gas sensors), surface plasmon resonance, both aqueous and solid-state electrochemistry, heated metal-oxide (HMOX) electronic devices, surface acoustic wave or cantilever mechanical devices, optical and electronic effects in carbon nanotubes,<sup>9</sup> optical and electronic palladium film technology, and other techniques have been reported for various applications.<sup>3,10–18</sup> However, in this review, we consider electrochemical sensors including amperometric, potentiometric, and conductometric devices, their mechanism of operation and performance to the need for improved hydrogen sensing capability.<sup>19</sup>

Hydrogen sensors are needed that can operate at temperatures from  $-30$  to  $1000$  °C, and this results in the use of unique designs and new materials. Some applications demand extremely high selectivity over a wide concentration range from 10 ppm to 100% in many different background gases. For many widespread applications, a sensor with simplicity and low cost as well as small size and minimal power consumption is desired. Electrochemical approaches to sensing  $H_2$  can provide one of the lowest power approaches for gas monitoring combined with good analytical performance.

Potentiometric sensors can be fabricated with very small size, since the generated voltage can be easily measured with very high precision and the potentials generated are independent of the dimensions of the sensor. In contrast, the amperometric sensor's signal (current) is proportional to the electrode area and will get smaller as the size is reduced. However, small amperometric sensors with improved signal/noise ratio are becoming available through the use of nanostructured electrodes and high-precision electronics.<sup>9</sup>

The possibility to work at room temperatures (RT) is an important advantage of liquid electrolyte electrochemical hydrogen sensors, since a power consuming heater is not needed and the gas sample and sensing environment are unperturbed by the measuring device.<sup>20,21</sup> The RT operation is also an important criterion to achieve intrinsically safe performance in potentially hazardous situations.

Liquid and polymer electrolyte gas sensors are not yet as robust as those devices that can be made with solid state materials such as the heated metal oxide (HMOX) sensors based on the conductivity change. But the amperometric and potentiometric devices typically offer higher selectivity than the chemi-resistor semiconductor sensors. In general, electrochemical sensors are reported to last for years, and as is typical for all sensors, the actual lifetime will depend upon the conditions of use, but 5 years is not unusual.<sup>22</sup>

The overall electrochemical sensing approach including the potentiometric, amperometric, and conductometric sen-

sors, offers an attractive package of combined analytical and logistical characteristics that result in being able to provide relatively high analytical performance at modest cost for many applications.<sup>23–25</sup> Therefore, a variety of electrochemical sensors are found in real-world gas detection process, stationary, and portable applications. These hydrogen sensors and hydrogen sensing technologies are reviewed in the following sections.

## 2. Fundamentals of Electrochemical $H_2$ Sensors

Understanding the electrochemistry is only the first step in understanding a sensor. After understanding the principles, the sensor's performance must be linked to the operating environment, the device design, and the specific materials and structures used. Trying to link the fundamental electrochemical theory to the observed analytical performance is a challenge often met only by a careful synthesis of empirical and theoretical work and is not complete for many sensors.

Electrochemical hydrogen gas sensors can be divided into three main classes according to the operating principle: amperometric, potentiometric, and conductometric sensors.<sup>19,23–26</sup> Operation at low temperature typically utilizes liquid or polymer electrolytes while high temperature requires solid state materials for sensor component parts. The general characteristics of many  $H_2$  sensing systems have been reported, but hydrogen sensors generally demand electrolytes with specific proton ( $H^+$ ) or mixed conductivity.<sup>23</sup> Due to the large number of related publications, this review will consider selected results that are important for understanding the principles of operation of hydrogen gas sensors, and a more detailed discussion of general principles of a broad range of electrochemical sensors for detection of gases other than hydrogen can be found elsewhere.<sup>19,23,27–40</sup>

### 2.1. Amperometric $H_2$ Sensors

The amperometric gas sensor, or AGS,<sup>23,28,38,40,41</sup> combines versatility, sensitivity, and ease of use in common gas detection situations with a relatively low cost and, recently, with the possibility for miniaturization.<sup>9,42</sup> The simplest amperometric cell consists of two electrodes (see Figure 1a), i.e., a working electrode and a counter electrode, and the electrolyte solution in which the two electrodes are immersed. The amperometric gas sensor is operated under an externally applied voltage, which drives the electrode reaction in one direction. This two electrode detection principle presupposes that the potential of the counter electrode remains constant. A potentiostat is usually used to fix this working electrode potential. In reality, the surface reactions at each electrode cause them to polarize, and significantly limit the concentrations of reactant gas they can be used to measure. Therefore, in practice many amperometric sensors have a more com-



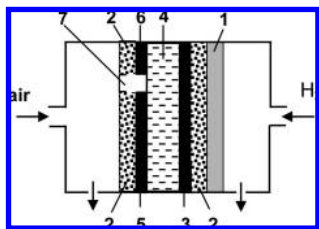


**Figure 2.** Schematic diagram of the hydrogen AGS thin film structure, operated in a fuel cell mode: (1) PTFE membrane; (2) Pt/Ru mesh (embedded into the catalyst layer); (3) working electrode (Pt/C catalyst thin layer); (4) Nafion-117 membrane; (5) counter electrode; (6) reference electrode; (7) insulator. (Adapted from ref 43, Copyright 2005, with permission from Elsevier.)

plicated physical configuration and, specifically, are built according to the three-electrode scheme illustrated in Figure 1b. In three electrode designs, it is still the current between working and counter electrodes that is measured and the reference electrode maintains the thermodynamic potential of the working electrode constant during sensing. Since the reference electrode is often shielded from reactions, it maintains a constant thermodynamic potential during sensing.

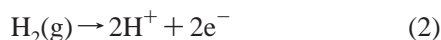
The inlet shown in Figure 1 can be simple diffusion or aided by a small air pump that transports the sample to the gas porous membrane through which the analyte diffuses/permeates to the sensing electrode. Figure 2 illustrates an H<sub>2</sub> AGS in a thin film “fuel-cell” configuration.

In this variant of AGS, the current generated by reaction of hydrogen at the sensing or working electrode is measured as the sensor signal and it can be measured at a fixed or variable electrode potential. Electroactive analyte, i.e. the H<sub>2</sub> participating in electrochemical reaction, diffuses from the surrounding gas to the cell, through the porous layers, and dissolves in the electrolyte, through which it proceeds to diffuse to the working electrode surface. The reaction rate, reflected by the current at the sensing electrode, can be limited by the rate of reaction at the surface or the rate of diffusion of the H<sub>2</sub> to the electrode surface. If operated under diffusion-limited conditions, the current is proportional to the concentration of the analyte in the surrounding gas.<sup>23</sup> Application of Faraday’s law relates the observed current (sensor signal) to the number of reacting molecules (concentration) by

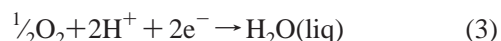
$$I = nFQC \quad (1)$$

where  $I$  = current in coulombs/s,  $Q$  = the rate of gas consumption in m<sup>3</sup>/s,  $C$  = the concentration of analyte in mol/m<sup>3</sup>,  $F$  = Faraday’s constant ( $9.648 \times 10^4$  coulombs/mol), and  $n$  = the number of electrons per molecule participating in the reaction.

In general, the Nafion electrolyte H<sub>2</sub> sensor electrode processes include the anode reaction<sup>44</sup>



and the cathode reduction reaction<sup>45</sup>



Under short-circuit conditions, reaction 2 occurs at the sensing or working electrode, WE, whereas reaction 3 occurs at the counter, or CE, electrode. Simultaneously, the protons move toward the counter electrode through the proton conducting electrolyte. This process results in a flow of an equivalent number of electrons in an external electrical circuit. The anodic oxidation reaction of hydrogen is often

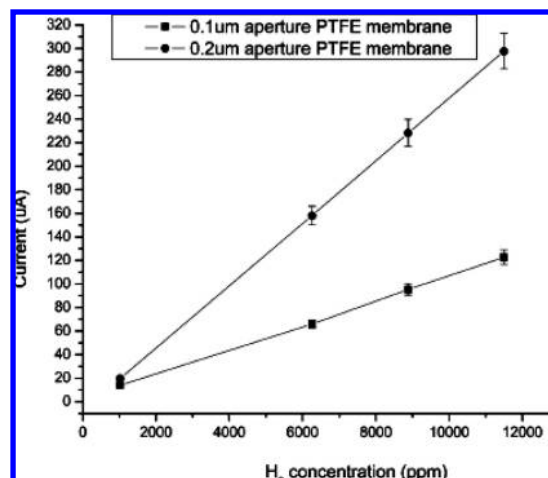


**Figure 3.** Calibration curves for the Pt/Nafion-based H<sub>2</sub> sensors with different aperture PTFE diffusion membranes. (Reprinted from ref 43, Copyright 2005, with permission from Elsevier.)

limited by the diffusion process to the sensing electrode by the sensor design. The number of protons produced is proportional to the hydrogen concentration. Since, the number of H<sub>2</sub> molecules reaching the WE are limited by diffusion of H<sub>2</sub> from the air to the WE surface, the external current is proportional to the hydrogen concentration in the gas phase,<sup>45</sup> which can be derived from combining Fick’s law and Faraday’s law, correlating the flux/number,  $J_{\text{H}_2}$ , of hydrogen molecules being pumped per second to the current  $I$ :

$$J_{\text{H}_2} = I/2q \quad (4)$$

where  $I$  = current in coulombs/s and  $q$  = the electric charge of an electron ( $1.6 \times 10^{-19}$  coulombs).

The flux of hydrogen diffusing through the aperture of an amperometric sensor is given by Fick’s first law:

$$J_{\text{H}_2} = A \cdot D_{\text{H}_2} \frac{\partial P_{\text{H}_2}}{\partial x} \quad (5)$$

where  $A$  is the area of the diffusion barrier in m<sup>2</sup>,  $D$  is the diffusion coefficient in m<sup>2</sup>/s,  $P_{\text{H}_2}$  is the hydrogen concentration in mol/m<sup>3</sup>, and  $x$  is the thickness of the barrier in m. Thus, eqs 4 and 5 can be rearranged to give the current:

$$I = 2qAD_{\text{H}_2} \frac{\partial P_{\text{H}_2}}{\partial x} \quad (6)$$

It is necessary to note that, in a “fuel cell” mode, the same reactions (eqs 2 and 3) take place on the electrodes with one distinction: reaction 3 takes place with participation of oxygen from the gas phase. As derived from eq 6, the properly designed diffusion limited amperometric gas sensor has a linear relationship between the H<sub>2</sub> partial pressure and the generated electrical current, which can be easily measured with very high precision (see Figure 3).

Linear response is often an advantage in a sensor, since sensitivity is constant over a broad range of concentrations, and electronics and compensation are simplified. However, a sensor with an exponential response can sometimes provide advantages like sensitivity at the lowest levels.<sup>46</sup> However, the AGS for hydrogen can detect low levels (see Figure 4) when optimized,<sup>47</sup> and the AGS with Nafion and liquid electrolytes has been demonstrated for ppm and subppm level detection in various applications.<sup>48–51</sup>

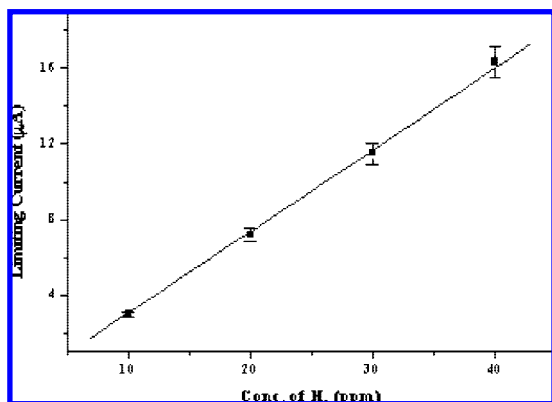


**Figure 4.** Calibration plot for Pd/PVA-H<sub>3</sub>PO<sub>4</sub>/Pt-based amperometric sensors showing the dependence of limiting current against hydrogen concentration. (Reprinted from ref 47, Copyright 2003, with kind permission from Springer Science+Business Media.)

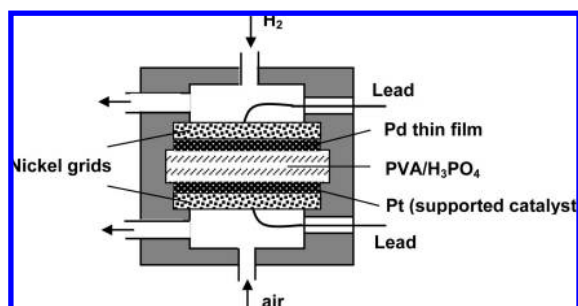


**Figure 5.** Schematic diagram of the polymer/acid electrolyte AGS (Adapted from ref 47, Copyright 2003, with kind permission from Springer Science+Business Media.)

The specific configuration of a hydrogen sensor having a very low limit of detection is shown in Figure 5. This sensor uses PVA-H<sub>3</sub>PO<sub>4</sub> electrolyte and functions like an H<sub>2</sub>/air fuel cell.

The reference electrode in this AGS can be Pt/air; that is, the hydrogen activity (or combined water and oxygen activities) in air is used as a reference. While this is not the most reversible of systems, the thermodynamic potential of the Pt in this case remains stable over long periods and allows the cell to run for long periods. Under potentiostatic control, the sensor response/current is controlled by the rate of bulk hydrogen diffusion to the WE surface when the oxidation rate of hydrogen at the WE surface is much higher than the diffusion rate. This diffusion-limited process is the condition that often provides the most stability for sensing hydrogen in the surrounding gas.<sup>52</sup>

The mechanism of a hydrogen gas sensor can be described in four steps:

- (i) the gas (H<sub>2</sub>) diffuses through the gas-diffusion barrier to the electrode and is then absorbed on the sensing electrode H<sub>2</sub>(ads),
- (ii) the electrochemical reaction (eq 2) occurs with electron transfer and generation of H<sup>+</sup>,
- (iii) the protons move toward the counter electrode through the proton-conducting membrane,
- (iv) the resulting reaction (eq 3) occurs with electron transfer, and the product desorbs from the counter electrode and diffuses away. The electronic charge is transferred to or from the electrodes in steps ii and iv and is observed as a current through the external circuit.<sup>52,53</sup>

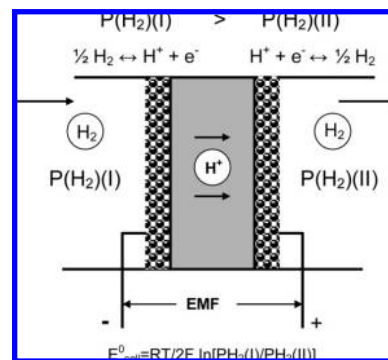


**Figure 6.** Working principle of a hydrogen concentration cell using a proton-conducting membrane. Reprinted with permission from Elsevier. (Adapted from ref 54, Copyright 2005, with permission from Elsevier.)

## 2.2. Potentiometric H<sub>2</sub> Sensors

Potentiometric sensors are thermodynamic equilibrium sensors for specific electrochemical reactions involving a redox reaction. Examples include ion sensors or ion-selective electrodes (ISEs) that are based on redox or ion exchange reactions.<sup>33,34,39</sup> The simplest configuration of potentiometric gas sensors consists of two electrodes in contact with an electrolyte, similar in arrangement to the two electrode version of an amperometric sensor except that the measurement is taken at zero current (or as near to zero as possible) and all reactions must be in equilibrium to observe the thermodynamic potential. In the simplest concept, the operation of a potentiometric gas sensor is based on the concentration dependence of a potential ( $E$ ) of a sensing electrode compared to a reference electrode (RE). The chemical concentration effect on the potential of an electrode is given by the Nernst equation as

$$E = E^\circ + \frac{RT}{nF} \ln a \quad (7)$$

where  $E^\circ$  = the standard electrode potential in volts,  $R$  = the universal gas constant ( $8.314472 \text{ J} \cdot \text{K}^{-1} \cdot \text{mol}^{-1}$ ),  $T$  = the absolute temperature in kelvin,  $F$  = Faraday's constant ( $9648 \times 10^4 \text{ coulombs/mol}$ ),  $n$  = the number of electrons participating in the electrochemical reaction, and  $a$  = the chemical activity of the analytes;  $a_X = \gamma_X[X]$ , where  $\gamma_X$  is the activity coefficient of species X. (Since the activity coefficient tends to unity at low concentrations, activities in the Nernst equation are frequently replaced by simple concentrations.) The Nernst equation expresses the chemical concentration effect on the observed electrical potential; for example, for a reaction involving 1 electron, a change in potential of 59.1 mV is observed for each order of magnitude change in the activity of analyte  $a$ . The "ln  $a$ " term is derived by writing the Nernst equation for the chemical reaction at the sensing electrode. Since activity is often approximated by concentration, the measured value of  $E$  is a measure of the concentration of target analyte  $a$ . In the more general Nernst equation, ln  $a$  is expressed as ln  $K$ , where  $K$  is the equilibrium constant for the reaction under consideration.

In most cases, modern potentiometric sensors function as concentration cells (see Figure 6).

The potential observed between the two electrodes is given by the Nernst equation summed for the two reactions, i.e.

$$\text{sum of } E_a = E^\circ + RT/F \ln[H^+]/[H_{2a}]^{1/2} \text{ and} \quad (8)$$

$$E_b = E^\circ + RT/F \ln[H^+]/[H_{2b}]^{1/2} \quad (9)$$

where a and b represent each side of the membrane with a different concentration of  $H_2$  as above. So, for the concentration cell the Nernst equation is written

$$E_a = E^\circ + RT/F \ln[H_{2b}]/[H_{2a}]^{1/2} \quad (10)$$

and the potential depends upon the difference in the pressure of the  $H_2$  on each side of the membrane.

A potentiometric sensor can measure analyte concentrations over a very wide range,<sup>23,34</sup> often more than 10 decades. In potentiometry, the chemical and diffusion processes must be at equilibrium conditions in the sensor for a thermodynamically accurate signal to be observed, while the amperometric sensors rely on Faraday's law and a dynamic reaction achieving a steady-state condition in the sensor. In potentiometric sensors where equilibrium is not obtained or several reactions are involved, deviations from Nernstian behavior are observed and these systems are often called "mixed" potential sensors. These sensors are often able to be calibrated and provide useful sensing performance, but understanding the molecular and chemical reaction basis for the signal is more difficult.

Interestingly, the amperometric sensor signal will get smaller with the size of the electrode and the decreasing rate of analyte reaction at the electrode surface, while the potentiometric sensor has no such dependence on geometry. This situation becomes most interesting in nanostructures wherein the thermodynamic potential can be characteristic of aggregates of atoms and different from a bulk system of components. The amperometric sensor reaction rate is typically enhanced by the high surface areas afforded by nanostructured electrode materials.

It is necessary to note that, during the past decade, the chemical sensing abilities of ISEs have been improved to such an extent that it has resulted in a "new wave of ion-selective electrodes".<sup>55,56</sup> This can be attributed to the considerable improvement in the lower detection limit of ISEs, new membrane materials, new sensing concepts, and a deeper theoretical understanding and modeling of the potentiometric response of ISEs.<sup>34</sup> The response of potentiometric ion sensors, i.e., ion-selective electrodes (ISEs) and/or ion-sensitive sensors (ISSs) and sensors with solid-state contact made of conducting polymer films, is a complex time-dependent phenomenon that depends on the electroactive material (membrane/film) and the electrolyte solution as well as the specific membrane-solution interface's composition and thermodynamics and kinetics of reactions.<sup>34</sup> This technology is relevant to understanding the fundamentals of all potentiometric sensors, including hydrogen sensors.

### 2.3. Conductometric Sensors

In conductometric sensors, the measurement of solution resistance is not inherently species-selective. Therefore, this approach to design of a  $H_2$  sensor, based on liquid electrolytes, would observe conductivity changes, and the difference for hydrogen is the large conductivity of the proton as compared to other ions. This results in a similar selectivity performance to the gas phase thermal conductivity measurement wherein hydrogen has a thermal conductivity many times higher than that of other gases. The conductometric detectors can be useful in situations where it is necessary to

ascertain, for example, whether the total ion concentration is below a certain permissible maximum level or for use as an online detector after separation by ion chromatography.<sup>19</sup> Such situations can arise in electroremediation technologies.

Some people consider all resistance measurements and heated metal oxide (HMOX) sensors as electrochemical, since the resistance changes as the surface charge is altered or as the bulk stoichiometry is changed. But HMOX devices primarily rely on electronic changes as opposed to electrochemical changes, i.e. electronic vs electrolytic conductivity. In any case, we will not consider the HMOX hydrogen sensor here and also not consider the limited applicability of liquid conductometric sensors further. Electrolytic conductivity can be used for sensing and is an important aspect/property of many electrolytes, including those used in  $H_2$  sensors.

## 3. Electrochemical $H_2$ Sensor Designs and Materials

The analytical performance of the electrochemical sensor is intimately tied to the structures and materials from which the sensor is made. It is often the major goal of research efforts to find the link between operating characteristics and the many kinetic factors, including mass transfer of the analyte to the electrode as well as the electrocatalytic activity of the electrode material. The geometry and dimensions of the sensor device have a profound effect on a  $H_2$  sensor's analytical performance, including the observed sensitivity, selectivity, response time, and signal stability. The materials are chosen for their specific chemical interactions, their fundamental electronic and electrochemical properties, and their stability, so as to precisely control sensory reaction thermodynamics and kinetics.

### 3.1. Membranes

A gas permeable membrane can be used to regulate the gas flow into the sensor, and it can aid selectivity, allowing only the analyte gas to pass as well as provide a barrier to prevent the leakage of the electrolyte from the interior of the sensor. Both porous and nonporous membranes can be used for hydrogen and some other gases. Hydrophobic porous membranes are used with aqueous electrolytes, since the pores are not wetted by the aqueous solution but allow the transport of dissolved gases to the electrode-electrolyte interface. The choice of membrane, its pore size, and its thickness can determine the sensitivity and response time of the sensor. For example, a low-concentration gas sensor with very high sensitivity uses a coarse, high-porosity hydrophobic membrane and less restricted capillary to allow more gas molecules to pass through per unit time to produce higher sensitivity. However, this design also allows more of the electrolyte's water molecules to escape out to the environment and the sensor can dry out faster. Depending on the electrolyte, dry out can change the electrolyte concentration, the solubility of the analyte, and the conductivity of the electrolyte, and these changes will often negatively affect the sensor signal/noise ratio and can lower sensitivity and response time.

Several types of porous and gas-permeable membranes exist and can be made of polymeric or inorganic materials. Most common are the commercially available very thin solid Teflon films, microporous Teflon films, or silicone membranes. Issues concerning the choice of membrane include permeability to the analyte of interest, the ability to prevent



**Table 1. Examples of Electrochemical H<sub>2</sub> Sensors Based on Liquid and Polymer Electrolytes**

gas	electrolyte	membrane	El'de mat'l	sens type	LOD [H <sub>2</sub> ]	upper range	ref
H <sub>2</sub> –air	6 N KOH or 5 N H <sub>2</sub> SO <sub>4</sub>	Teflon	Pt				23
H <sub>2</sub>	5 M H <sub>2</sub> SO <sub>4</sub>	Teflon	Pt/C			4000 ppm	45
H <sub>2</sub>	9 M H <sub>2</sub> SO <sub>4</sub>	PTFE	Au				57
H <sub>2</sub>	1 M H <sub>2</sub> SO <sub>4</sub>	Nafion	Pt–Ag/AgCl	A	<1%	16% ppm	58
H <sub>2</sub> –N <sub>2</sub>	1.0 M NaOH	PTFE	Pt/C	A	<0.1%	2%	59
H <sub>2</sub> –air	H <sub>2</sub> SO <sub>4</sub>	Teflon	Pt–Ag/AgCl	A	<0.2%	0.2–4%	60
H <sub>2</sub> –N <sub>2</sub>	H <sub>2</sub> SO <sub>4</sub>	Teflon	Pt–Ag/AgCl	A	<0.4%	1–100%	60
H <sub>2</sub> –air	Nafion	PTFE	Pt/C	A	<50 ppm	12000 ppm	43
H <sub>2</sub> –N <sub>2</sub> (CO <sub>2</sub> )	Nafion	ionic polymer	Pt			10%	61
H <sub>2</sub> –N <sub>2</sub>	Nafion		Pt	A	10 ppm	10%	52
H <sub>2</sub> –N <sub>2</sub>	0.5 M H <sub>2</sub> SO <sub>4</sub>	PTFE	Pt/C	A	<0.1%	2%	59
H <sub>2</sub> –argon	Nafion	Teflon	Pt/C	A	<10 ppm	4%	62
H <sub>2</sub> –argon	PVA/H <sub>3</sub> PO <sub>4</sub>	Teflon	Pd and Pt	A	<10 ppm		47
H <sub>2</sub>	Nafion/0.1 M H <sub>2</sub> SO <sub>4</sub>		Pt			5000 ppm	63
H <sub>2</sub> –air	Nafion		Pt	A,P	20 ppm	4000 ppm	64
H <sub>2</sub> –air	Nafion		Pt	P	30 ppm	1000 ppm	65
H <sub>2</sub>	Nafion	Teflon	Pt	A	<10 ppm	1000 ppm	48
H <sub>2</sub> –air	PBI/H <sub>3</sub> PO <sub>4</sub>		Pt/C–Ag/AgCl	P	<10 <sup>−4</sup> Pa	1 Pa	66

<sup>a</sup> PTFE, polytetrafluoroethylene; PVA, polyvinylalcohol; PBI, polybenzimidazole; A, amperometric; P, potentiometric; LOD, limit of detection.

electrolyte leakage, manufacturability, and the thickness and durability of the membrane. In a number of cases, the rate of mass transport through the membrane controls the limiting current and, hence, the sensitivity of the sensor. As seen from the data presented in Figure 3, an increase in membrane thickness decreases the sensor sensitivity. Ideally, the gas membrane must have a constant permeability to the target gaseous analyte during sensor operation over a wide temperature range and possess mechanical, chemical, and environmental stability. Electrochemical hydrogen sensors typically use membranes of Teflon (see Table 1). The expanded polytetrafluoroethylene (ePTFE) membrane is a chemically stable substance and has high gas permeability without permeation of aqueous electrolytes.

### 3.2. Electrolytes

The role of the electrolyte is to transport charge within the sensor, contact all electrodes effectively, solubilize the reactants and products for efficient transport, and be stable chemically and physically under all conditions of sensor operation. The electrolyte is an ionically conducting medium that ionically transports charge within the cell. For electrochemical gas sensor applications, the electrolyte solution needs to support both counter electrode and sensing electrode reactions, form a stable reference potential with the reference electrode, be compatible with the materials of construction, and be stable over long periods of time under various operating conditions. Examples of commonly used electrolytes in H<sub>2</sub> sensors are presented in Table 1. Most hydrogen sensors utilize H<sub>2</sub>SO<sub>4</sub> electrolytes.

In addition to inorganic materials as electrochemical hydrogen sensors, one can also use biological materials such as hydrogenases,<sup>67</sup> a class of enzymes that catalyze the interconversion among H<sub>2</sub>, protons (H<sup>+</sup>), and electrons. The enzymes can be found in many phylogenetically different microorganisms, including *T. roseopersicina*, *Allochroa vinosum*, *Clostridium pasteurianum*, and *Ralstonia eutropha*. The bio-H<sub>2</sub>-sensor's detection signal is generated in a flow cell in which gaseous H<sub>2</sub> is transported to an aqueous phase and oxidized by hydrogenase using benzyl viologen as an artificial electron acceptor. Reduced BV<sup>+</sup> is subsequently detected by chronoamperometry. The net current obtained is proportional to the H<sub>2</sub> concentration in the gas phase. This branch of amperometry using biomaterials

has addressed many sensing problems in medical applications, but this particular design has limited sensitivity and stability and will require additional research to achieve practicality in many of the known field applications for hydrogen sensing.

### 3.3. Electrodes

Many liquid electrolyte gas sensors use designs that are somewhat derived from modifications of the Clark electrode,<sup>68</sup> especially those that utilize metallized membranes for electrodes.<sup>23,28,42</sup> In the latter cells, the precious metal electrode is evaporated or sputtered directly onto the electrolyte facing side of a polymer membrane.<sup>28,42</sup> The common feature of the “Clark” type of gas sensor is an interface at the working electrode (WE or sensing electrode, SE) that facilitates rapid transport of the gas to the WE–electrolyte interface. Gas sensors with electrodes made as a back-side metallized porous membrane are not affected by evaporation of water from the electrolyte as much as those electrodes that are open to the analyte or air because the electrode is directly in contact with the bulk of the electrolyte solution. The mass transfer of analyte from the sample to the working electrode can be fast, but even faster in electrodes open to the air, resulting in short response times and high sensitivity.

Sensors employing fuel cell electrode technology or gas diffusion electrodes (GDEs) are also well studied.<sup>54,69</sup> These are generally composed of a sintered composite (e.g., powdered Teflon and noble metal black) with two or three similar gas diffusion electrodes separated by an aqueous electrolyte or an ion conducting membrane. The GDEs combine the following functions:<sup>54</sup>

- a catalytic function within the electrode structure for electrochemical reactions;
- electrons released in the anodic reaction or consumed in the cathodic reaction at the reaction sites have to be collected, i.e. the electrode composite must be electrically conductive;
- ions in the membrane must be transported toward the reaction sites, i.e. the electrode needs to house some electrolyte to have ionic conductivity;
- noncharged reactants have to be transported toward the reaction sites, primarily via pore diffusion inside the electrode structure.

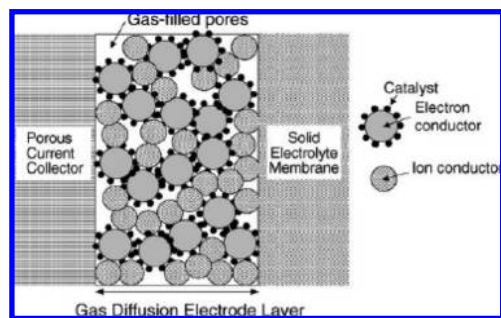


**Figure 7.** Schematic illustration of gas diffusion electrode (GDE). (Reprinted from ref 54, Copyright 2005, with permission from Elsevier.)

**Table 2.** Description of the Standard Gas Diffusion Electrodes (Reprinted from Ref 74, Copyright 2005, with Permission from Elsevier)

electrode	ETEK	SORAPECH2	SORAPECO2
platinum loading (mg/cm <sup>2</sup> )	0.5	0.2	0.35
NAFION (mg/cm <sup>2</sup> )	unknown	1	0.8
roughness factor	5	80	150
active layer (10 <sup>-6</sup> m)	10	5	5
diffusion layer (10 <sup>-6</sup> m)	250	250	250

Optimal electrode design requires a perfectly executed balance of the different functions. This is often achieved by preparing mixtures of ion conducting particles (made of the membrane material), particles of an electron conductor or metal, and catalytic particles that are the same as the metal or different. By using well-defined particle size distributions, one can adjust the electrode pore structure. This in turn offers the possibility to optimize the transport properties of the GDE with respect to the noncharged reactants. As a result, the catalytically active surface area of the electrode can be several orders of magnitude higher in comparison with standard electrodes, allowing species with relatively poor electroactivity to produce measurable currents. Figure 7 shows a schematic of a typical GDE.

Gas-diffusion electrodes (GDEs), manufactured similarly to fuel cell electrodes, have highly efficient three-phase boundaries,<sup>70</sup> where the reacting gas, metallic electrode, and electrolyte meet together. The design of GDE electrochemical sensors has been shown to provide fast responses, high sensitivities, and low detection limits.<sup>49,50</sup> The mechanism of transport is often modeled as a process consisting of diffusion through the air filled pores of the porous current collector, diffusion to the triple phase boundary, and electron transfer occurring just as the analyte reaches the three-phases where electrodes, ion-exchange membrane or electrolyte, and gas phase meet. The GDE was first deployed for reducing gases by Blurton.

The GDE was first deployed for reducing gases by Blurton et al.<sup>71</sup> with free electrolyte and also for H<sub>2</sub> sensors using a Nafion polymer electrolyte by La Conti et al.<sup>72</sup> In this work, a fuel cell can also be used as a gas sensor if the configuration is appropriate.

Descriptions of the most frequently encountered Pt-black gas-diffusion electrodes are given in Table 2. Platinum based metal nanoparticles of around 2–5 nm supported on high-surface-area carbon (40–50 nm particles) are often used for the fabrication of gas-diffusion electrodes,<sup>8,73</sup> as is typical in fuel cells. It is important to note that, for the last 20 years, the contents of Pt in GDEs, expressed in mass of Pt per unit of geometric area, have decreased more than 10 times from 5 mg Pt cm<sup>-2</sup> to 0.2–0.4 mg Pt cm<sup>-2</sup>.

The gas diffusion electrodes (GDEs) used in amperometric sensors are semihydrophobic with a very developed microporous structure.<sup>8,71,73</sup> Usually they are composed of two layers deposited on an appropriated support. A diffusion layer is prepared with a suspension of PTFE (for example DuPont TM 30) with high-surface-area carbon (Cabot XC-72, 250 m<sup>2</sup> g<sup>-1</sup>). The mixture is filtered on a support (a carbon cloth or a carbon paper or Teflon film that is totally hydrophobic). Onto the hydrophobic layer, the catalytic layer is deposited using several procedures.<sup>73,75</sup> The catalytic layer contains metal nanoparticles anchored on a carbon support and may incorporate Nafion (DuPont), which is a proton exchange material and, as such, an ionic conductor. The result is a matrix which has pores, electrolyte channels, electronic pathways, and electrocatalytic surfaces intermixed. The composite material is a good electronic conductor, porous to gases, and can conduct ions in and around the catalyst, which has a very high electroactive area. Because the electrochemical oxidation of hydrogen takes place only at the triple-phase boundary, where the Pt catalytic sites, electrolyte or Nafion, and H<sub>2</sub> meet in the AGS, the effective electrode surface area should be as large as possible.

The reference electrode, or RE, also presents challenges for electrochemical sensors and especially miniaturized sensors. A small, stable, and long-lived RE is needed. Silver/silver chloride (Ag/AgCl) has been used as a reference electrode in many electrochemical applications, but it maintains a fixed potential only when the chloride concentration is fixed, and its lifetime is limited because silver chloride can gradually dissolve in aqueous solutions. In general, the Pt–air electrode has been used widely for gas sensors and is often called a pseudoreference or quasi-reference electrode.<sup>71</sup>

### 3.3.1. Materials for Electrodes

The material of choice for the sensor's electrodes can be different for each function. The RE needs to establish a stable potential. The counter electrode, CE, or auxiliary electrode should be able to catalyze its half-cell reaction over a long time. And, of course, the (SE or WE) should be the ideal catalyst for its sensing reaction and be selective for it. All of the electrodes need to be stable and manufacturable, and provide stable and facile interfaces for the electrochemistry. Materials used as reference or sensing electrodes in H<sub>2</sub> electrochemical sensors are presented in Table 3.

In an electrochemical sensor, the working electrode is typically made from a noble metal, such as platinum or gold, that is capable of making a defined interface with the electrolyte in the cell and is in a porous structure to allow efficient diffusion of the gas phase to a large-area and reactive electrode–electrolyte interface. The noble metals generally exhibit excellent stability under polarized potentials that may be corrosive to other metals. The noble metals are also excellent catalysts for many analyte reactions. Carbons, including graphite and glassy carbon, are also popular materials for working electrodes. Using Pt/C composites and nanoscale materials in gas-diffusion electrodes maximizes the effective electrode surface area, and because carbon is conductive, the electrode can achieve an optimum combination of such properties as conductivity–porosity.<sup>43</sup> Carbon provides good electrical contact between the grains of the noble metal in the porous matrix. Using thick film technology, a few milligrams of a carbon slurry paste can be added along with Pt grains to make effective electrodes.



**Table 3. Reference and Sensing Electrode Materials Used in H<sub>2</sub> Electrochemical Sensors**

electrode material	electrode type <sup>a</sup>	examples	working temp	ref
Ag/Ag <sup>+</sup>	RE	(Ag/AgSO <sub>4</sub> ; Ag/AgCl)	RT	60, 66, 76
hydrated oxides	RE	(NiO; PbO <sub>2</sub> ; etc.)	RT	77, 78
Ag	SE	Ag-loaded epoxy resin	<100 °C	59, 79
Au	SE; RE		<500 °C	38, 48, 80–82
Pd	SE (WE)		>600 °C	47, 79, 88
Pt	SE; RE		>600 °C	78, 82–85
Pt/C	SE (WE)	Pt-carbon		43, 62, 86
Pt-alloy	SE (WE)	Pt–Au; Ag; Cu; Ni	>500 °C	87
transition metal				
hydrides	RE; CE	(ZrH <sub>x</sub> ; TiH <sub>x</sub> ; ThH <sub>x</sub> ; NbH <sub>x</sub> )		88–92
metal oxides	SE (WE)	ITO, ZnO, SnO <sub>2</sub> , CdO	up to 700 °C	91, 93–95
nanocomposites	SE	(Au/CuO; Au/Nb <sub>2</sub> O <sub>5</sub> ; Au/Ga <sub>2</sub> O <sub>3</sub> ; Au/Ta <sub>2</sub> O <sub>5</sub> )	up to 700 °C	80, 81, 96, 97

<sup>a</sup> RE, reference electrode; SE, sensing or working (WE) electrode; CE, counter electrode

### 3.3.2. Fabrication of Electrodes

From the analysis of the literature, there are many approaches which can be taken to create electrodes in electrochemical sensors. Opekar<sup>31</sup> underlines four of the most often used methods:

- Mechanical procedures. An electrode of a suitable shape and material, e.g. a fine mesh, can be pressed, under ambient or an elevated temperature, onto the surface of a membrane, or a wire can be tightly wound around a solid or polymer electrolyte tube. Screen printing is also a mechanical procedure for depositing material from an ink onto a surface.

- PVD (physical vapor deposition) and CVD (chemical vapor deposition) plating. This procedure permits formation of electrodes of various shapes on the surface of membranes and solid electrolytes, but the electrodes often have poor mechanical stability and are destroyed by changes in the membrane dimensions due to test medium humidity variations. However, vacuum evaporation (or sputtering) is one of the principal methods for preparation of planar sensors, with electrodes produced photolithographically on an inert support (glass, ceramics).

- Chemical deposition. A metal can be deposited from a solution, especially cases where the electrode is produced on the surface of membranes and solid electrolytes, by chemical reduction of a suitable metal compound. This approach was patented for platinum and gold electrodes but also can be used for other metals (e.g., Ni, Cu, Ag).

- Impregnation. The polymer or solid electrolyte membrane is immersed in a solution of a suitable compound of the metal to be deposited and is saturated with the solution; the saturation can be accelerated for Nafion by adding methanol to the solution. The membrane is then immersed, one or both sides, in a solution of a strong reductant and the metal deposits where the reductant is placed. The procedure can be repeated to obtain a thicker metal film.

In addition, the GDE of the fuel cell can be sprayed onto the substrate or vacuum filtered onto the substrate with subsequent curing to bond the electrode structure together. Of course, every method has both advantages and disadvantages and some detailed information is available in reviews.<sup>31</sup>

### 3.3.3. Mechanism of Electrode Reactions

The kinetics of the H<sub>2</sub> electro-oxidation on a Pt electrode in acid media is relatively fast.<sup>98–100</sup> Possible mechanisms of H<sub>2</sub> electro-oxidation on Pt have been considered.<sup>101</sup> Reports by Bagotsky et al.,<sup>99</sup> Harrison et al.,<sup>102</sup> and Gasteiger et al.<sup>100</sup> all agree that, for smooth Pt surfaces in acid media, the mechanism is a reversible direct discharge (in this case,

the reaction is not limited by adsorption). Pd has also shown high electrocatalytic activity for the hydrogen oxidation reaction (HOR).<sup>103</sup> Contrary to the case of Pt and Pd, the HOR on Au surfaces shows a relatively low activity.<sup>104</sup> Not much has ever been reported about the role of the exchange current density in the AGS. But, in order to establish a new steady state rapidly, i.e. a state where the net anodic or cathodic current is constant, the exchange current should be large compared to the sensor signals. Study of the exchange current can offer insight into sensor mechanism, response time, and other analytical performance parameters.

### 3.4. Bias Control of Selectivity and Sensitivity

It is necessary to note that the control of the sensing electrode potential is another effective way to change or optimize the performance of the sensor. Through selection of operating potential, we can provide conditions that thermodynamically favor either the oxidation reaction or the reduction reaction for a particular analyte. The applied potential between working and reference electrodes set by the potentiostat is critical for the observed sensitivity and the selectivity of the sensor.<sup>23,28,105</sup>

## 4. Practical Electrochemical H<sub>2</sub> Sensors with Liquid Electrolytes

The development of an amperometric sensor demonstrates, by example, many of the important considerations in the fabrication of a practical hydrogen sensor.<sup>60</sup> As illustrated in Figure 8, three sensor designs address three issues present in liquid electrolyte hydrogen sensors generalizable to all AGSs.

In device I, the WE, RE, and CE were Pt electrodes deposited onto the same side of a 1.5 cm diameter Teflon membrane. The Teflon membrane with Pt electrodes was mounted onto a polypropylene cell body and sealed. The backside of the cell body contained a reservoir into which 0.5 mL of 30% (w/w) H<sub>2</sub>SO<sub>4</sub> electrolyte was added. The electrolyte was in direct contact with the electrodes. Device II was identical to device I except that a 2 mil (50 μm) thick semipermeable FEP membrane (Type 200A, DuPont, Circleville, OH) was mounted over the gas inlet hole. And device III is identical to device II except that an alternative RE is inserted.

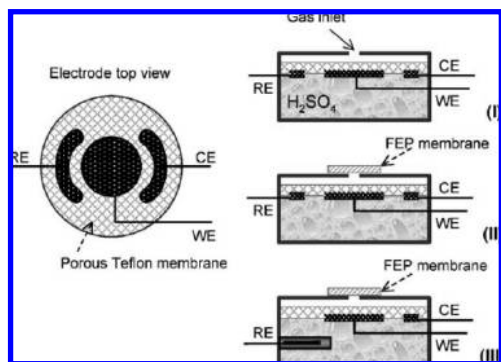


**Figure 8.** Schematic diagram of the AGS. (Left) Orientation of the WE, CE, and RE on a porous Teflon membrane. This electrode structure was mounted onto polypropylene cells. (Right, top) Device I simulated a commercial sensor design. (Right, middle) Device II incorporated a semipermeable FEP membrane. (Right, bottom) Device III incorporated a semipermeable FEP membrane and an alternative and stable RE. (Reprinted from ref 60, Copyright 2005, with permission from Elsevier.)

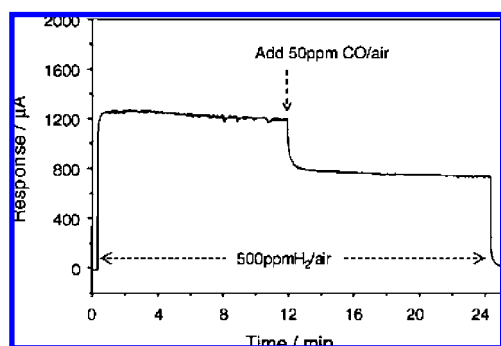


**Figure 9.** Response of device I to 500 ppm H<sub>2</sub>-air for 24 min. At 12 min, the gas mixture was changed from 500 ppm H<sub>2</sub>-air to 500 ppm H<sub>2</sub> with 50 ppm CO in air and finally to zero filtered air at 24 min. (Reprinted from ref 60, Copyright 2005, with permission from Elsevier.)

#### 4.1. Details of Electrode and Sensor Fabrication

Electrodes were fabricated from a suspension prepared with 60 mg of platinum black (Englehard, fuel cell grade Pt black), 400 L of Teflon suspension (Type 30, DuPont, Circleville, OH), and 1600 L of 18 M DI water prepared with a commercial water purification system (Model D7381, Barnstead Thermolyne Corp., Dubuque, IA) using a well-known procedure.<sup>105</sup> Electrode structures were fabricated directly on porous Teflon membrane sheets as the supporting material (Type G110, Northern Performance, Wayne, NJ) using a vacuum filtration apparatus with a precut die that outlined the electrode shapes and positions. Three individual electrodes, which serve as the WE, the counter electrode (CE), and the RE, were simultaneously deposited on the same side of the Teflon membrane in a planar geometry, as illustrated in Figure 8. Once formed, the electrode-membrane structure was sintered at 310 °C for 90 min and had a platinum black loading of about 7 mg/cm<sup>2</sup>.

The results, obtained with sensors I, II, and III, clearly demonstrate the issues resolved by each unique sensor design. Sensor design I has a response to H<sub>2</sub> (see Figure 9) that illustrates that using a standard configuration (device I) does not provide a stable or selective hydrogen detector. The Pt WE is sensitive to both CO and H<sub>2</sub>,<sup>106-108</sup> and as a result the presence of CO interferes with the H<sub>2</sub> measurement. For example, as is shown in Figure 9, the H<sub>2</sub> signal was dramatically affected by low concentrations of CO. Upon

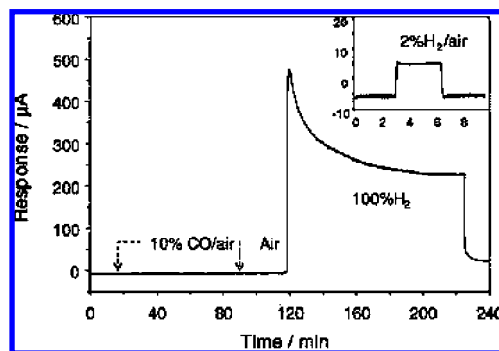


**Figure 10.** Response of device II to CO and hydrogen in air and then to zero filtered air. (Reprinted from ref 60, Copyright 2005, with permission from Elsevier.)

exposure to only 50 ppm of CO, the signal magnitude dropped by nearly 33% while the hydrogen concentration was kept constant.

Embedding a solid FEP membrane (device II), to prevent CO and other gases from reaching the working electrode, makes the sensor very selective to H<sub>2</sub> gas. Hydrogen has a much higher permeability through polymeric films such as FEP Teflon than CO and other gases.<sup>109-115</sup> This modification fixed the first problem of the traditional amperometric H<sub>2</sub> sensor, its selectivity, and it also reduced the large amount of H<sub>2</sub> getting into the sensor. Device II exhibited a response to 100% H<sub>2</sub> and 2% H<sub>2</sub> in air and no detectable response to 10% CO over a 10 min exposure (Figure 10). So, it is seen that the FEP membrane was effective at improvement of selectivity.

However, just simply embedding an additional membrane does not resolve a second important problem of hydrogen sensors with Pt electrodes, i.e. related to diffusion and adsorption of hydrogen molecules on the Pt-air RE. This results in a sizable shift in the thermodynamic potential of the reference electrode. The shift in the RE potential immediately translates into a shift in the thermodynamic potential of the working electrode because the bias (e.g., the potential difference between the WE and RE) is held constant by the potentiostat circuit. The potential shift of the RE can be observed at even moderate hydrogen concentrations and is a reason for the unstable hydrogen signal from Design I and II sensors. As a result, device II, similar to device I, showed dramatic decreases in signal magnitude during extended exposures at high H<sub>2</sub> concentration (Figure 10 above). A measurable change in the reference potential was observed almost immediately following the hydrogen exposure. Over time, the magnitude of this drift can become quite large (more than 150 mV). Because of the unstable signals, a reliable hydrogen calibration curve was limited to concentrations less than 3% H<sub>2</sub> with sensor designs I and II (Figure 11).

This second deficiency of the design, the hydrogen-induced potential drift of the RE, was eliminated by the replacement of the Pt-based RE with an RE not sensitive to hydrogen gas, such as the Ag/AgCl electrode. This change led to device III of Figure 8 with an Ag/AgCl RE and the performance shown in Figure 11. Device III was identical to device II but incorporated the alternative RE by mounting the Nafion-coated Ag/AgCl wire into the bulk electrolyte through a hole in the side of the sensor body.

The Ag/AgCl reference electrodes were prepared by modification of an electrodeless chloridization method.<sup>116</sup> The chloridization of Ag wires was carried out for 24 h in a 1 M

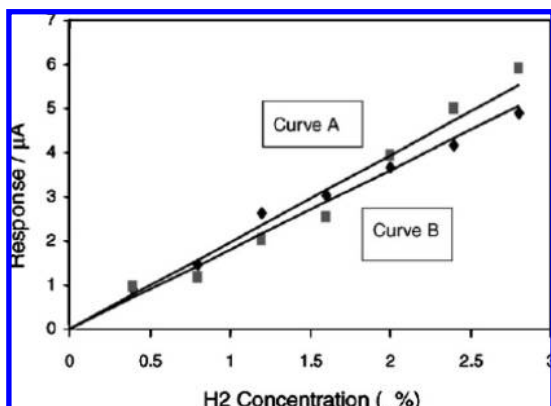


**Figure 11.** Hydrogen calibration curves for device II. The CO concentration in curve A was 0 ppm and was maintained at 1000 ppm in curve B. (Reprinted from ref 60, Copyright 2005, with permission from Elsevier.)

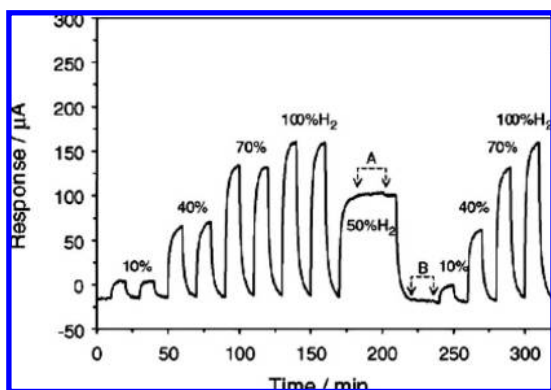


**Figure 12.** Response of device III to various concentrations of H<sub>2</sub> and CO mixtures in air. In region A, the gas mixtures were 50% H<sub>2</sub>–air with 0.5, 1, 2.5% CO (each for 15 min). In region B, the gas mixture was 5% CO–air. (Reprinted from ref 60, Copyright 2005, with permission from Elsevier.)

FeCl<sub>3</sub>–0.1 M HCl solution. The wires were rinsed with DI water and put in a saturated AgCl solution for 24 h to remove traces of FeCl<sub>3</sub>. Finally, the wires were dried at 100 °C overnight. A uniform gray black layer of AgCl developed on the surface of the Ag wire. The chloridized wires were dipped in a 5% Nafion 117 solution (Aldrich, Milwaukee, WI) and allowed to dry at room temperature. Immersion of the wires in the Nafion solution and air-drying was repeated several times to make a uniform Nafion coating on the wires.

Testing has shown that design III sensors exhibited a reversible, drift-free response even at high levels of H<sub>2</sub> with negligible cross-sensitivity to CO (see Figure 12). The steady-state signal remained constant for more than a 2 h continuous exposure to 100% H<sub>2</sub>, and no detectable interfering CO responses were observed for device III as gas mixtures of 0.5–2.5% CO + 50% H<sub>2</sub>/air were introduced. The sensor responses to H<sub>2</sub> before and after CO (5%) exposures were the same. It is noted that device III also showed no detectable responses to 500 ppm of NH<sub>3</sub> or 500 ppm of H<sub>2</sub>S in air when exposed for over 10 min to these potential interferants.

The AgCl electrode had to be designed specifically for this amperometric sensor.<sup>60</sup> While the Ag/AgCl electrode is a well-known standard reference electrode,<sup>117</sup> the basic design of the Ag/AgCl RE is unstable in many electrolytes. The AgCl layer may dissolve in an electrolyte such as sulfuric acid, causing the Ag/AgCl RE potential to change as the

chloride layer is dissolved. In addition, free chloride ions in the electrolyte may form complexes with the platinum particles on the WE and CE. This can have deleterious effects on the chemical stability of the electrodes and adversely affect the sensor performance. Nafion is a cation exchange membrane that allows only small cations such as protons in the electrolyte to move freely from the bulk solution to the Ag/AgCl wire surface. Anions such as Cl<sup>-</sup> will not readily diffuse into the electrolyte due to the electric repulsion (Donnan exclusion) within the positively charged Nafion ion exchange layer. The protective Nafion coating both minimizes the dissolution of chloride ions into the bulk solution and, at the same time, maintains ionic contact between the RE and the bulk solution. In addition, the geometric placement of this Nafion-coated Ag/AgCl RE is further from the WE than the RE in device II, and this also minimizes the chance of significant hydrogen levels from reaching the RE. The solid Teflon membrane is effective at providing differential selectivity, but it slows the response time of the sensor from 5–90% signal to a few minutes from a few seconds.

## 4.2. Design of Electrochemical Sensors for Field Applications

The physical size, geometry, selection of various components, and construction of an electrochemical H<sub>2</sub> sensor usually depends on its intended use as well as on the manufacturing processes and materials used in construction. There are significant variations in sensor design. However, the main characteristics and requirements for H<sub>2</sub> electrochemical sensors applications share many similarities with each other and with other electrochemical sensors.<sup>118</sup>

### 4.2.1. Temperature

Electrochemical sensors are quite sensitive to temperature. In general, when the temperature is above 25 °C, the sensor will read higher; when it is below 25 °C, it will read lower. The temperature effect is typically 0.5% to 1.0% per degree centigrade, depending on the manufacturer and type of sensor. In general, the lowest temperature at which a sensor can be expected to function properly over long periods of time is 0 °C, but acid electrolytes do not freeze and allow operation to about –40 °C. The sensors are typically internally temperature-compensated. For this purpose, electrochemical H<sub>2</sub> sensors should incorporate a sensitive temperature sensor, which the electronics use to compensate for temperature variations. However, it is better to keep the sample temperature as stable as possible or, for maximum accuracy, calibrate and operate the sensor at the same temperature.

### 4.2.2. Humidity

Unlike many solid-state or semiconductor devices, electrochemical H<sub>2</sub> sensors with aqueous electrolytes are not affected directly by humidity. However, continuous operation below 15% or above 90% relative humidity can change the water content of the electrolyte affecting the signal from the sensor. This process often occurs very slowly and depends upon the temperature, the electrolyte, and the vapor barrier. Under high-humidity conditions, prolonged exposure can cause excessive water to build up and create leakage in some sensor designs. Under low-humidity conditions, the sensor



can dry out. Under dry conditions, the acid content of the electrolyte can rise, causing crystallization, or allowing the acid to attack the seals. In general, high-temperature and low-humidity conditions are most likely to result in a shorter lifetime for the sensor. In many workplace situations, the RH varies cyclically with the season and the sensitivity of the sensor can be seen to follow the seasons and last for many years.

#### 4.2.3. Pressure

The thermodynamics of electrochemical H<sub>2</sub> sensors are minimally affected by pressure changes. However, pressure changes do change the concentration (mol/cc) of the analyte, and this is reflected linearly in the sensor signal. Electrochemical sensors are minimally affected by pressures within the normal range of ambient pressures  $\pm 10\%$  and should be calibrated and operated at the same pressure for the best accuracy. It is important to keep the entire sensor within the same pressure, since rapid differential pressure changes within the sensor can cause damage to the sensor's diffusion membrane. Sudden changes in pressure can cause more gas to be forced into the sensor, producing a current transient. These transients rapidly decay to zero as the normal diffusion conditions are re-established. Some transients could trigger false alarms.

#### 4.2.4. Calibration

For electrochemical sensors used to monitor H<sub>2</sub>, stable cylinders of calibration gases in the concentration range of interest as well as other, less convenient chemical generation systems (e.g., permeation tubes or electrochemical generators) may be used for calibration. The frequency of calibration cannot be prescribed exactly for all sensors and varies widely with design. The best accuracy can be obtained with more frequent calibration, and typical industrial applications use monthly to yearly calibration. Manufacturer's instructions or user experience is the best guidance for frequency of calibration.

The environmental conditions (temperature, relative humidity, barometric pressure) of the monitor at the time of calibration should be as near as possible to those that will be encountered during use. Of these three, temperature is most important because changes in temperature are most often encountered in the field and can cause readings to change. Even with the temperature compensating circuitry employed in most sensors, the time required for equilibrium to be reached can vary. If it is not possible to calibrate at the working temperature, the user must allow sufficient time for field equilibration of temperature. Changes in barometric pressure are usually less significant than temperature changes, and so are of less concern to the user.

#### 4.2.5. Potential Failure Mechanisms

**4.2.5.1. Blocking Mechanisms.** Blocking is a condition which causes the sensor to function poorly or not at all until the condition is removed. Normally the block does not damage the sensor permanently as a poison would. Some of the most common blocking mechanisms for electrochemical cells are as follows:

**Freezing the Electrolyte.** As the temperatures of the cell decreases, the chemical reaction which the user sees as a signal decreases. At some point, depending upon the

electrolyte, the cell current stops. Usually, upon returning to a normal temperature, the cell will reactivate.

**Filter or Membrane Clogging.** If the cell's diffusion barrier becomes clogged or coated, the normal supply of analyte gas may be cut off. Sensors used in front of air inlets, in front of exhaust fans, or in dusty areas are can be clogged or partially clogged. A dust filter should be used, and it should be cleaned regularly to prevent the cell's gas supply from being blocked. In a sample draw system, pump failure will produce the same effect as a clog. As one can imagine, any blockage of the analyte gas will stop the signal.

**Vapor condensation** on the sensor diffusion barrier can also effectively cut off the signal gas. This is a form of sensor clogging. If the sensor temperature is lower than the atmospheric temperature and the RH is high, it is likely that condensation will occur. To prevent this, the cell may need to be warmed or the air being circulated to the cell may need to be dried.

**4.2.5.2. Poisoning Mechanisms.** A poison blocks and/or degrades the sensor's operation on a temporary or permanent basis. Prolonged exposure to a poison can eliminate the sensor response. Most sensors are not directly poisoned by a gas or vapor, but they may be poisoned indirectly. Common poisons include the following:

**Solvent Vapors.** High concentrations of solvent vapors which can attack the plastic housing or filters. The most common solvents which can cause problems (depending upon the construction of the sensor) are alcohols, ketones, phenols, pyridine, amines, or chlorinated solvents. Sensors used in these atmospheres may have a shorter life depending upon design. Chlorine containing compounds can sometimes corrode electrodes or adsorb at catalytic interfaces to change reaction sensitivity.

**High Temperatures.** Continuous operation at high temperatures (usually above 40 °C) in addition to reactive compounds (e.g., amines can react with acid electrolytes) will accelerate failure mechanisms including dry out and poisoning.

#### 4.2.6. Sensor Life

The life expectancy of an electrochemical H<sub>2</sub> sensor depends on several factors, including the total amount of gas exposed to the sensor during its life, as well as other environmental conditions, such as poisons, temperature, pressure, and humidity. Exposure to a signal producing gas can degrade catalytic response over time, but typically the sensor is designed with excess catalyst to maintain a long useful sensor lifetime. Low humidity, high temperatures, and exposure to poisons can combine to shorten a sensor's life. Normal life expectancy from modern design electrochemical sensors may be five years or more from the date of manufacture. Some manufacturer's recommend that the electrochemical cells be stored with a shorting clip to extend life during nonuse. Others recommend keeping sensors in a refrigerator rather than storing them at ambient temperature. Sensor's with in-board filters can last beyond the lifetime of the filter, and interference signals can change with filter degradation. Exposure to gases being removed by the filter shortens its effective life.

## 5. Amperometric and Potentiometric H<sub>2</sub> Sensors with Polymer Electrolytes

### 5.1. Advantages/Limitations of Polymer Electrolyte H<sub>2</sub> Sensors

One of the approaches to design a room temperature H<sub>2</sub> sensor is the employment of solid polymer electrolytes (SPEs).<sup>20,54,119,120</sup> Bobacka<sup>121</sup> underlined the following reasons to explain the utility of using conducting polymers in electrochemical sensors: (i) conducting polymers can form an Ohmic contact to materials with high work function, such as carbon, gold, and platinum; (ii) conducting polymers can be conveniently electrodeposited on the electronic conductor by electrochemical polymerization of a large variety of monomers; (iii) several conducting polymers are soluble and can therefore be deposited from solution; (iv) conducting polymers are often materials with mixed electronic and ionic conductivity, which means that they can transduce an ionic signal into an electronic one in the solid state. These multifunctional properties are advantageous for ion-to-electron transduction solid state devices.

Solid polymer electrolytes became important during the mid-1970s because of the inefficiencies and maintenance requirements of liquid electrolytes. Originally, a solid polymer electrolyte (SPE) was described as a solid plastic sheet of perfluorinated sulfuric acid polymer that, when saturated with water, became an excellent ionic conductor. Ionic polymers in contact with a conductive medium such as a metal allow electrochemical reactions at this interface. Early SPEs, e.g. Nafion, were not electronic conductors. Nafion, a typical solid polymer electrolyte, is a hydrated copolymer of polytetrafluoroethylene (PTFE) and polysulfonated vinyl ether containing pendant sulfonic acid groups (Dupont) and is a cation-exchanger containing hydrophilic SO<sub>3</sub><sup>-</sup> radicals firmly bound to the hydrocarbon backbone, whose charge is compensated by counterions (mostly H<sup>+</sup>). The counterions are dissociated and solubilized by water present within the polymer structure and give rise to the ionic (proton) conductivity of the polymer. The water required for proton solubility is bound in the hydration mantles of the ions present, and thus, the polymer is a solid which contains no macroscopic liquid phase unless excess water is present.<sup>31</sup>

Nafion has good proton conductivity, high gas permeability, outstanding chemical stability, and good mechanical strength, and it has been widely used in fuel-cell and sensor applications. However, the geometric dimensions of Nafion and its electrical properties (primarily its ionic conductivity) are strongly dependent on the amount of water contained in the polymer. The maximum water content, corresponding to 22 water molecules per single sulfo group of the polymer, is attained by boiling Nafion in water, and this number decreases to 14 for the polymer in contact with a gaseous phase saturated with water vapor; the water content fluctuates with the relative humidity (RH) of the surrounding medium.<sup>122</sup> In general, perfluorated polymer membranes show high ionic conductivities at high water vapor pressure.<sup>123</sup> Nafion electrolyte gas sensors, because Nafion conductivity is a function of RH, typically produce a gas response that depends on the RH.<sup>64,124–126</sup> The RH response is not desired for an ambient air sensor wherein the RH can change over wide limits and typically is either eliminated or compensated.

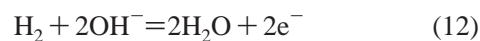
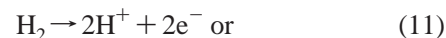
Nafion and polymer electrolytes such as PBI (sulfonated polybenzimidazole), S-PEEK (sulfonated polyether ether

ketone),<sup>54,89,127–129</sup> and PVA/H<sub>3</sub>PO<sub>4</sub> can be used in H<sub>2</sub> sensors.<sup>47,130</sup> Some of these solid polymer electrolytes have excellent mechanical and thermal properties and good protonic conductivity even in dry atmospheres.<sup>74,127</sup> The remarkable properties of these polymers lie in the combination of the high hydrophobicity of the perfluorinated polymer backbone and the high hydrophilicity of the sulfonic acid branch. The hydrophilic branches act as a plasticizer, and the backbone retains strong mechanical properties.<sup>92</sup> More detailed information about polymers used in electrochemical gas sensors can be found in various reports in the literature.<sup>21,92,131–135</sup>

In some cases, hydrogels or an electrolyte inside a porous matrix are used to replace free liquid electrolytes in order to raise viscosity, lower evaporation rates, and resist leakage of the electrolyte from sensor devices. The polymers or hydrogels can prevent the evaporation of electrolyte during sensor fabrication, especially for microsensor devices where very small amounts of electrolyte are used. Using polymer electrolytes provides opportunities for the design of planar sensors and the applications of standard microelectronic fabrication technologies.<sup>21</sup> Polymers allow decreasing essentially both the size and weight of electrochemical sensors. In addition, polymer electrolytes allow a larger range of operating temperatures for the electrochemical sensor. As research has shown, polymer-based H<sub>2</sub> sensors successfully operate in the temperature range RT–100 °C,<sup>44,62</sup> and compared to liquid electrolytes, solid polymer electrolytes can be used as separators in electrochemical cells, do not dissolve impurities from the gas as easily, and permit the construction of miniaturized devices that are leak proof to help avoid premature sensor failure.

### 5.2. Response Characteristics of Polymer H<sub>2</sub> Sensors

The electrode reaction, i.e., electron-transfer reaction at the WE, is part of a mechanism of response that is similar to all AGS technologies and has several steps, including gas diffusion to the electrode–electrolyte interface, dissolution of the analyte gas, adsorption of the analyte onto the surface, electroreduction at the triple phase boundary, and desorption of products from the electrode surface.<sup>23</sup> Similar reactions in air are proposed for anode and cathode, respectively:



These reactions are the idealized version, and the actual electrode reaction at the electrode surface is dependent on the nature of the electrode material, the electrolyte solution, the thermodynamic potential, the interface of the electrode–electrolyte, and, of course, the analyte, which in this case is hydrogen. If the products of the reaction are sensor poisons, the sensor lifetime or response characteristics may be severely limited, but in this case, hydrogen produces water and is a very “green” system and makes the choice of materials and methods for the electroanalytical processes simple.

Metallization of the polymer, i.e., how the electrode is deposited, is a most important process in the manufacturing of polymer sensors. The Nafion surface has to be metallized by noble metals to create reference, counter, and sensing electrodes. A laminated structure or one with intimate contact

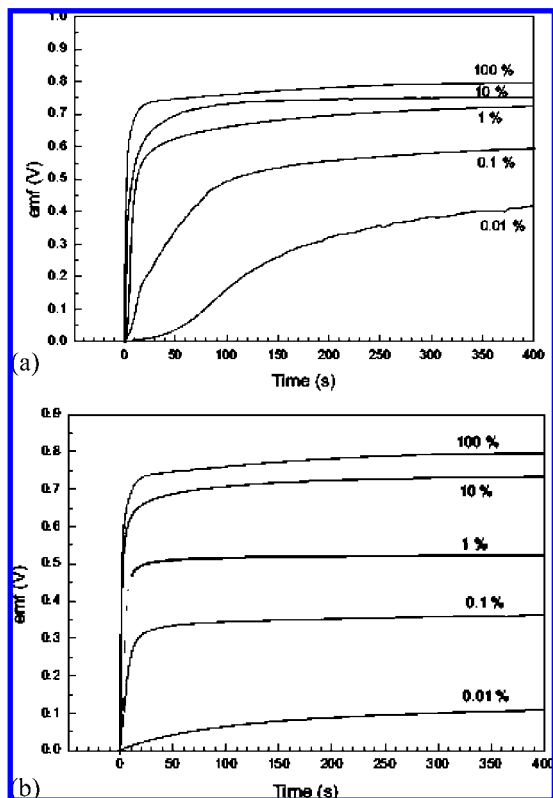


**Figure 13.** Response time of the sensor with (a) Ag and (b) Pd reference electrodes to various concentrations of hydrogen in nitrogen: (a) for short exposure times. The sensor was flushed with air prior to the introduction of each new hydrogen gas mixture. (Reprinted from ref 79, Copyright 2004, with permission from Elsevier.)

of electrode and electrolyte is required. This contact between the two solids, i.e., the membrane and catalytic metal, with a provision for gaseous contact, is a very critical factor in obtaining performance. The Nafion itself must also be cleaned by leaching/cleaning with ethanol for several hours, by boiling in nitric or perchloric acid, or sometimes by mechanical abrasion to obtain optimal performance.<sup>31</sup>

Various noble metals, including Ag, Pd, and Pt, are typical electrode materials. However, Pt and Pd electrodes seem to have better stability, reliability, and rate of response.<sup>79</sup> The performance is compared in Figure 13, for H<sub>2</sub> sensors made with the hydronium Nafion system.

Figure 13 shows that this potentiometric H<sub>2</sub> sensor with Ag electrodes does not reach equilibrium at very low hydrogen gas concentrations even after 1 h. The sensor response with Pd electrodes is extremely rapid for all hydrogen concentrations from 1 to 100%. The response time is typically less than 10 s to achieve a signal level of 90%, and additional research on this system has indicated that, with Pt electrodes, the response time is even faster.<sup>136</sup>

The response time seems to be a function of the H<sub>2</sub> concentration and is observed to be longer as the concentration is lowered. This could be due to the presence of adsorbed O<sub>2</sub> on the WE surface, which has to be removed by the reaction with the sparsely available hydrogen in the system, and only after this process is satisfied, can one observe the hydrogen equilibrium at the palladium electrode.

The same effect of H<sub>2</sub> concentration influence on response time was observed for amperometric type sensors as well. Research has shown that, for the amperometric polymer H<sub>2</sub> sensor, both response and recovery times decrease with

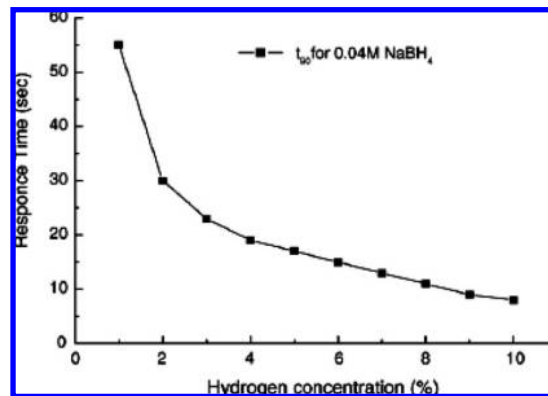


**Figure 14.** Response time vs hydrogen concentration (1–10%) for a Pt Nafion electrode prepared from 0.01 M Pt(NH<sub>3</sub>)<sub>4</sub>Cl<sub>2</sub> and 0.04 M NaBH<sub>4</sub>. (Reprinted from ref 44, Copyright 2006, with permission from Elsevier.)

increasing hydrogen concentration.<sup>44</sup> At higher concentrations, a higher number of hydrogen gas molecules can reach the electrode surface, which promotes rapid achievement of steady-state conditions. In Figure 14, the response time ( $t_{90}$ ) versus H<sub>2</sub> concentration in the range 1–10% for a Pt/Nafion sensor illustrates a 6-fold decrease in response time, but the recovery time was always a few seconds.<sup>44</sup>

The observed asymmetry in response and recovery times is due to the fact that the two reactions, i.e. the reactions responsible for rise and decay, are different and not symmetrical. The response reaction has to do with the hydrogen reacting with the electrode surface and setting up a steady-state surface concentration. In the reverse reaction, oxygen from the air must remove the hydrogen and re-establish the electrode's surface condition in air. The response time is also complicated by mass transport and the potential interference of coreactants. Mass transport to the sensor and through the membrane pores can be slow or fast relative to the surface reactions. Further, for a Nafion sensor, the RH of the sample affects the water activity in the electrolyte and can change the conductivity,<sup>43</sup> thereby affecting the response of the system and the establishment of steady state. Therefore, the sensor system design (mass transport) as well as the fundamental electrochemical thermodynamics and kinetics needs to be considered in order to understand sensor performance characteristics. (See Figure 3, part 2.1).

In some structures, the metal electrode is deposited directly onto the polymer electrolyte. Any one of several methods can be used for polymer/electrolyte metallization (see above discussions in section 3.3.2) during H<sub>2</sub> sensor fabrication, e.g., mechanical, electrochemical, and chemical reduction processes.<sup>137</sup> Each method produces a different quality electrode and electrode–electrolyte interface and thereby affects the analytical performance of the resulting sensor. Potentiometric H<sub>2</sub> sensors prepared by sputtering, electroless plating, and Pt powder molding have been compared.<sup>138</sup> The sputtered electrode had the highest catalytic activity, and the sensitivity of the sensor was 16 times higher than that prepared by the molding method.<sup>138</sup> The sensitivity of the sensor was about 4  $\mu$ A/100 ppm, with a linear output from 0 to 10<sup>4</sup> ppm. The sensors with electroless plating electrodes were unstable.

The most efficient method for electrode preparation is believed to be a chemical reduction process,<sup>135</sup> which can be divided into two types, the Takenata–Torikai method<sup>139</sup> and the impregnation–reduction method,<sup>140</sup> and both meth-



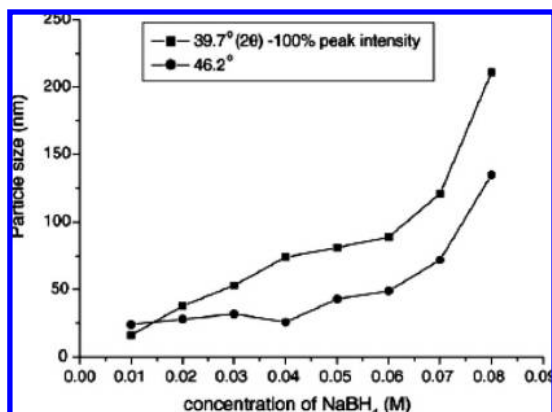


**Figure 15.** Particle size effect on Pt electrode preparation using different concentrations of the reducing agent NaBH<sub>4</sub>. (Reprinted from ref 44, Copyright 2006, with permission from Elsevier.)

ods have a low investment and production cost. Chemical reduction produces mechanically stable electrodes with good interfacial contact.<sup>140</sup> The control of the reductant concentration provides control of the size of the resulting metal particles and their average grain size.<sup>44</sup> As a result, one obtains possibilities to optimize the H<sub>2</sub> sensor electrode performance (Figure 15).

The average particle diameter increases with increasing reductant concentration (Figure 15). The increase in grain size is believed to be due to higher nucleation growth with fast reduction of the [Pt(NH<sub>3</sub>)<sub>4</sub>]<sup>2+</sup> in the electrode. The optimum particle size of 74 nm with good interparticle connections was found at 0.04 M concentration of NaBH<sub>4</sub>,<sup>44</sup> and this may correspond to the optimum electrochemical sensor performance. Smaller particles with enhanced surface area can be expected to have high electrocatalytic activity but were isolated from each other, resulting in an interruption of the electrical contact. In contrast, a Pd layer deposited at high concentrations showed good electronic contact, but as one may expect, when the particles were grown to micrometer size, the surface area and the electrocatalytic activity decreased.

Some polymer amperometric H<sub>2</sub> sensors discussed earlier (Figure 2, part 2.1) used a microporous PTFE as a gas permeable diffusion membrane and Pt/Ru mesh as a current collector.<sup>43</sup> The sensor was prepared with a Pt/Ru mesh that was placed onto the PTFE membrane, and its upper side was coated with a thin layer of the Pt/C catalyst mixture. Then the Nafion-117 membrane was placed onto the thin layer and the other side of the membrane was coated with a thin layer of the Pt/C catalyst mixture divided into two parts of different surface areas by an insulator. Afterward, two Pt/Ru meshes were placed onto the two parts of the thin Pt/C catalyst layer, making a CE and RE, respectively. Finally, the assembly was placed in a hot-press at 110 °C and kept in a nitrogen atmosphere for 10 min under a pressure of 40 kg/cm<sup>2</sup>. The diameter of the sensor with 3.0 mg/cm<sup>2</sup> Pt loading was 15 mm, making the overall PEM (polymer-electrode-membrane) structure small and suitable for small portable H<sub>2</sub> sensor applications.

The performance of the assembled H<sub>2</sub> sensors illustrates a useful sensitivity, stable sensing current, short response and recovery time, and long-term stability (Figure 16).<sup>43</sup> For a step change of the hydrogen concentration, the *t*<sub>90</sub> response time (time required to reach 90% of the steady-state current) of the sensor is about 20–50 s, suitable for most monitoring applications.<sup>43</sup>

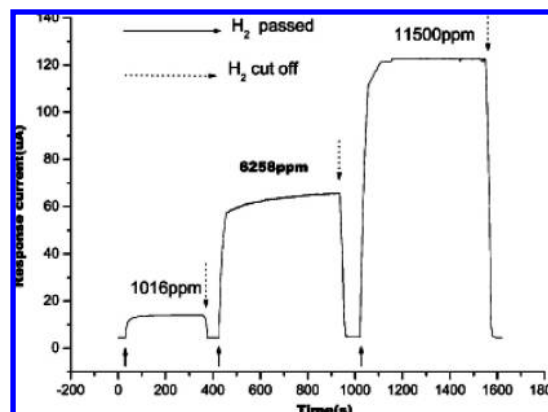


**Figure 16.** Response curves of the sensor for various concentrations of hydrogen. (Reprinted from ref 43, Copyright 2005, with permission from Elsevier.)

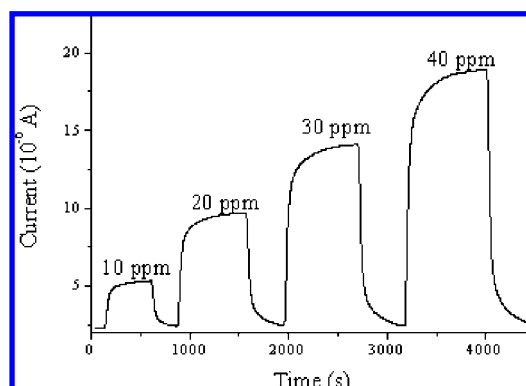


**Figure 17.** Response of the Pd/PVA-H<sub>3</sub>PO<sub>4</sub>/Pt-based sensor for various concentrations of H<sub>2</sub> in air. (Reprinted from ref 47, Copyright 2003, with kind permission from Springer Science+Business Media.)

The response of many polymer H<sub>2</sub> sensors is sensitive enough to detect below 10 ppm and perhaps even 1 ppm with the appropriate electronics and controlled exposures (Figure 17).<sup>47,52</sup> The results (Figure 17) were obtained using a PVA/H<sub>3</sub>PO<sub>4</sub> electrolyte that was prepared by casting the structure onto a Teflon sheet.<sup>47,130</sup> The electrolyte film was fixed to a supporting ring and coated with palladium as an anode on the sensing side and platinum as a cathode on the counter electrode side. The electrolyte thickness was about 2 mm. The housing assembly for the sensor was made from polycarbonate. The schematic diagram of this sensor is shown in Figure 5. The palladium anode was deposited by vacuum vapor deposition. The thickness of the anode film in the sensor was of the order of 1000 Å. The cathode on the counter electrode side of the sensor was platinum supported on carbon prepared by screen-printing. Before coating, 20–25% of a Teflon emulsion was added to the mixture. The electrode was sintered at 100 °C under vacuum. Two gold-coated nickel grids were used as current collectors on both sides.

Pt was chosen as cathode material because of the lower overpotential for oxygen reduction and lesser solubility for hydrogen. Pd is not a suitable material for the cathode, since the cathodic overpotential for oxygen reduction at Pd is high and it does not reach a diffusion controlled electrode process because of the high solubility of hydrogen in palladium. Pd also exhibits a decrease in catalytic activity at the cathode due to the oxide formation on the air side. However, as an anode, Pd can be effective, since the high solubility, large

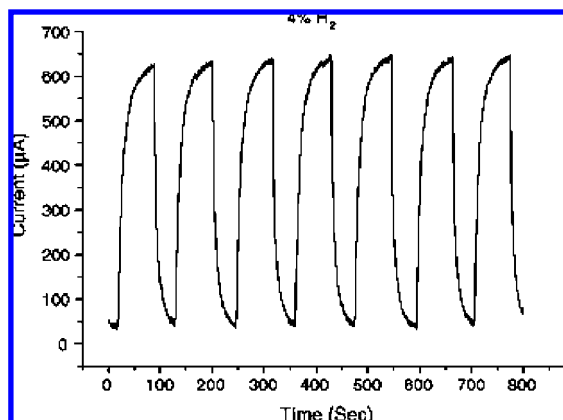


**Figure 18.** Cyclic behavior of 4% H<sub>2</sub> exposure to the sensor Pt Nafion WE with an area of 2 cm<sup>2</sup> made from 0.01 M Pt(NH<sub>3</sub>)<sub>4</sub>Cl<sub>2</sub> and reduced with 0.04 M NaBH<sub>4</sub> in a 1 min time interval. (Reprinted from ref 44, Copyright 2006, with permission from Elsevier.)

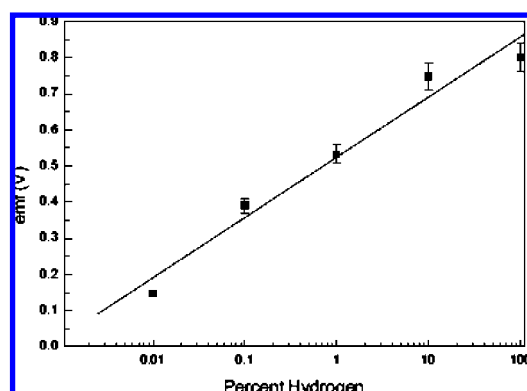


**Figure 19.** Equilibrium emf of a Pd/Nafion-based sensor vs the logarithm of the hydrogen partial pressure for hydrogen–air gas mixtures. (Reprinted from ref 79, Copyright 2004, with permission from Elsevier.)

sticking coefficient, and fast diffusion coefficient for hydrogen are advantageous for sensing a low concentration of hydrogen in argon or another gas. The low overpotential for hydrogen oxidation on the Pd film anode was also found to provide sufficient catalytic oxidation rates to make the above sensor function well.

While many measurements of the rate of response are limited by the apparatus, in general, the rate of response of the polymer hydrogen sensor is at least a minute to 90% signal. For example,<sup>44,52</sup> Figure 17 shows cyclic exposure of the Pt Nafion sensor element to 4% hydrogen and no hydrogen.<sup>44</sup> Results (Figure 18) can be used to calculate the measurement precision during cyclic exposures. Also, short-term drift and long-term drift under laboratory conditions (downward drift in the output current) was reported to be about 2% of signal per day.

The potentiometric response of a polymer sensor is given in Figure 19, and, as is typical for potentiometric sensors, H<sub>2</sub> can be detected over many orders of magnitude in concentration. The EMF dependence on the logarithm of the hydrogen partial pressure is very close to linear but is non-Nernstian. A nonlinear least-squares fit (NLLSF) of the data yielded a slope of 166 mV, well above the value predicted by the Nernst equation. If the data for 0.01% hydrogen is discarded, the value of the resultant slope is 145 mV and still significantly greater than the expected theoretical value. The reasons for the non-Nernstian behavior of this sensor to hydrogen–air mixtures are not clear. The fast, linear,

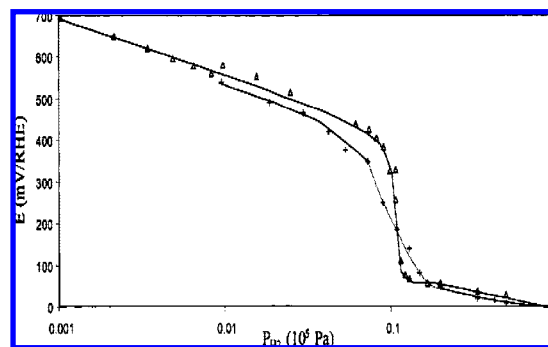


**Figure 20.** Potentiometric response of the Pt electrode (E-TEK) in PBI-H<sub>3</sub>PO<sub>4</sub> electrolyte sensors to various H<sub>2</sub> partial pressures in dry air: experimental response ( $\Delta$ ); curve of the mixed potential mode (+). (Reprinted from ref 66, Copyright 2001, with permission from Elsevier.)

reproducible, and large, stable output of the sensor makes it very useful for detection of hydrogen leaks in air. The sensor performance thus suggests that it can be incorporated into a fuel cell or into other hydrogen process applications to detect explosive levels of hydrogen gas.

However, it would be most advantageous if the sensor would respond over the entire range of 0–100% hydrogen. The linearity of the semilog plot for the potentiometric H<sub>2</sub> sensor (Figure 19) is observed in the range 0.1–10%, and outside this range, there appears to be what is often called a mixed potential.<sup>66</sup> Over a wide range of hydrogen partial pressures, gas diffusion electrodes usually exhibit a sigmoidal response (Figure 20) on the semilog plot.

Calculations show that, in ambient air, the hydrogen sensor sensitivity (defined as the slope of the  $E$  versus  $\log(P(\text{H}_2))$  curve) is always higher than that given by the Nernst equation and the potential is influenced by electrode morphology.<sup>141</sup> The electrodes deposited on Nafion exhibit a non-Nernstian open-circuit voltage<sup>63</sup> that is characteristic of a mixed potential resulting from at least two simultaneous electrode reactions, e.g., the hydrogen oxidation reaction (HOR) and the oxygen reduction reaction (ORR).<sup>141</sup> According to this model:

- For low hydrogen partial pressure, the sensor potential varies linearly with the logarithm of the hydrogen partial pressure and the sensitivity, deduced from the ORR Tafel slope, and is of the order of 120 mV/decade.
- For high hydrogen partial pressure, the sensor potential varies linearly with the logarithm of the hydrogen partial pressure and the sensitivity is in agreement with the Nernst equation (30 mV/decade at room temperature).
- The abrupt change of potential between these two zones can be explained by mass transport limitations of both HOR and ORR reactions.

While some have suggested that these characteristics reduce the utility of Pt potentiometric hydrogen sensors,<sup>74</sup> there is hardly another metal better suited for the hydrogen oxidation reaction. The ideal metal would have the response for the hydrogen reaction only; this is the challenge of selectivity.

### 5.3. Methods to Improve H<sub>2</sub> Sensor Performance

One can always improve on sensor performance in a given application. There are five general areas to improve sensors: (1) sensitivity, signal-to-noise ratio, and limit of detection, (2) selectivity, (3) response time, (4) stability for short and

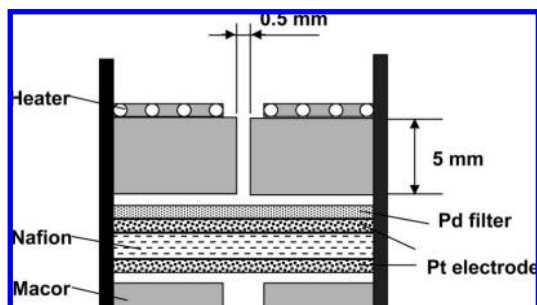


**Figure 21.** Schematic diagram of the cell construction showing top and side views of the sensor DHS-IV with the heating element on top. (Adapted from ref 61, Copyright 2008, with permission from Elsevier.)

long-term performance, including lifetime, and (5) logistical or applications specific properties such as cost, size, weight, power requirements, ruggedness, and packaging. Sometimes, improvements can come from packaging or software and include pumps or membranes to improve sensitivity and selectivity or even algorithms to predict steady-state values for improved response time. But overall, most electrochemical  $H_2$  sensors are not perfect for all applications, and fundamental improvements to the sensor are always desired.

Control and improvement in amperometric sensors can be enhanced by physical optimization of the sensor package; for example, a diffusion hole can control the concentration range for  $H_2$  sensitivity.<sup>44</sup> This diffusion hole type amperometric limiting current sensor have a linear current with  $P_{H_2}$ ,<sup>26,142</sup> and small changes in the hydrogen partial pressure may be measured with high accuracy.<sup>44,143</sup>

Several engineering designs targeted toward optimization of the  $H_2$  sensor have also been suggested. A schematic diagram of the  $H_2$  sensor designed by Sakthivel and Weppner<sup>61</sup> is shown in Figure 21.

The decrease of the inlet diameter to 0.5 mm at a length of 5 mm, i.e. a length to diameter ratio or L/D of 10, improved selectivity to  $H_2$  with respect to  $CO_2$ . This same idea was used in a prefilter to gain selectivity for CO over  $H_2$  using a prefilter to remove hydrogen.<sup>23</sup> Since hydrogen diffuses much faster than other gases, this diffusion barrier would allow a significant (approximately factor of 4 over air) advantage to hydrogen over other gases. Further, catalytic electrode poisoning by  $CO_2$  gas mixtures along with  $H_2$  could be eliminated with a Pd diffusion barrier on the top of the sensing Pt electrode.<sup>61</sup> The result is that the amperometric  $H_2$  sensor performance was improved in environments containing high concentrations of  $CO_2$  (Figure 22).

Additional improvements in this sensor include a screen printed Pt heater to compensate for any temperature variation within the diffusion hole in the sensor chamber. The heater further keeps the gas mixture and sensor measurements at constant temperature. The decrease of space between the Pd barrier and the diffusion hole avoids the excessive condensation water vapor from the reactor samples.

The membrane can also be optimized to improve sensor performance. Ion implantation of the ePTFE membrane is an effective way to improve  $H_2$  selectivity.<sup>57</sup> Implantation of the PTFE membrane with various kinds of ions ( $N^+$ ,  $N_2^+$ ,  $O^+$ , and  $O_2^+$ ;  $1 \times 10^{15}$  ions/cm<sup>2</sup>) decreases the detection current for the interference gases such as  $H_2S$ ,  $SO_2$ ,  $NO$ , and  $NO_2$  relative to  $H_2$ . It was proposed that structure modification of ePTFE under ion implantation (Figure 23) can provide a high rate of  $H_2$  permeation when compared with permeation

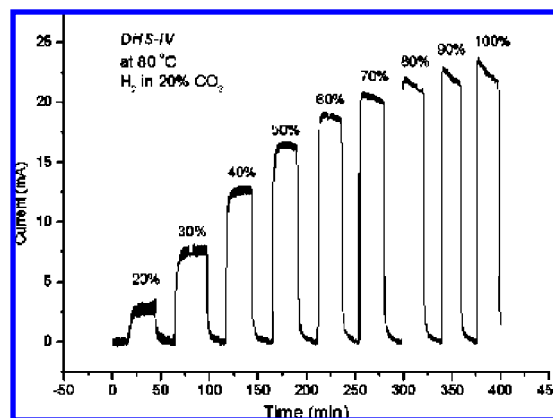


**Figure 22.** Typical step response of design DHS-IV up to 100%  $H_2$  in Ar + 20%  $CO_2$  measured at 80 °C. (Reprinted from ref 61, Copyright 2008, with permission from Elsevier.)

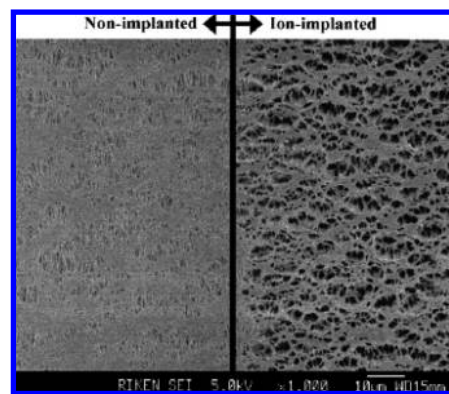


**Figure 23.** SEM images of a nonimplanted ePTFE membrane and one  $N^+$ -implanted with  $5 \times 10^{15}$  ions/cm<sup>2</sup>. (Reprinted from ref 57, Copyright 2007, with permission from Elsevier.)

for other gases ( $H_2S$ ,  $SO_2$ ,  $NO$ , and  $NO_2$ ). It is known that the chemical bonding structural change of ePTFE, especially the pore surfaces, influences the interactions between gas molecules and polymer surface, which induces a change in the permeability unique to each gas.

The required operating temperatures can add complexity to a gas sensor system. For example, sensors using Nafion 117 often do not reach a steady state at temperatures in excess of about 50 °C.<sup>144</sup> This instability is caused by the rapid and continuous drying of the membrane in gas streams that affect the membrane's conductivity. Nafion is a hygroscopic polymer, and changes in the water content cause the membrane to physically swell.<sup>145</sup> This swelling alters the size and shape of the membrane and thereby changes the rate of proton diffusion; that is, proton diffusion is the charge-carrier mechanism within the polymer. Therefore, a changeable very dry or very wet atmosphere provides a difficult working environment for Nafion-based  $H_2$  sensors. Even Nafion in contact with a water phase to maintain the water content constant is sometimes not sufficient to remove the signal dependence on RH, since local chemical and physical effects at the sample–electrode interface can dominate the response<sup>31</sup> and the rate of water exchange in the Nafion itself can change.<sup>146</sup>

New polymers that are fast proton conducting membranes, based on hybrid inorganic–organic phosphosilicate polymers prepared from orthophosphoric acid, dichlorodimethylsilane, and tetraethoxysilane, have been synthesized.<sup>144</sup> Membranes are amorphous, translucent, and flexible. The proton con-

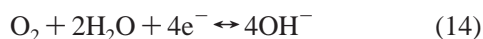


ductivity increased with rising temperature following an Arrhenius behavior and an activation energy of 20 kJ/mol. Under dry conditions at 120 °C, the conductivity was 1.6 S/m. A potentiometric gas sensor with a  $\text{TiH}_x$  reference electrode and a Pt sensing electrode exhibited a fast, stable, and reproducible response to dry  $\text{H}_2$  and  $\text{O}_2$  gases at temperatures above 100 °C.

Operation at high temperature might be at least one way to resolve the RH response of polymer  $\text{H}_2$  sensors. However, at higher temperatures, any degradation mechanism will be enhanced, and this can cause drift. The new hybrid-inorganic-polymer-electrolyte sensors did exhibit drift,<sup>144</sup> which results in a need for frequent calibration. The hybrid-polymers appeared to be stable up to 400 °C, but the membrane slowly degrades, as was revealed by the thermal analysis.<sup>144</sup>

Another polymer,  $\text{H}_3\text{PO}_4$ -doped polybenzimidazole (PBI), has sufficiently high proton conductivity in dry air for sensor applications.<sup>74,127</sup> Experiments<sup>66</sup> have confirmed operation in RH of only 10–30%, and this is about the same as the performance of the PVA/ $\text{H}_3\text{PO}_4$  polymer electrolyte.<sup>47</sup>

Pt/air electrodes designed with a PVC polymer composite have much better stability in comparison with electrodes made from Nafion/metal composites. Pt/air or Au/air electrodes are very often used as pseudo-reference electrodes in amperometric gas sensors.<sup>9</sup> These electrodes are not reversible electrodes, but their potential is reported to be sufficiently stable for use over a long time in gas sensors.<sup>147</sup> The Pt/air electrode potential is a mixed potential determined by oxygen reduction:<sup>148</sup>



According to reactions 13 and 14, the electrode potential depends on the activity of water. In aqueous solutions, the effect of the water activity is not considered to change, as the water is actually at a 55 M concentration and small changes produced by reactions have little or no effect on its activity. This does not hold for solid-state sensor systems with solid-state electrolytes. These systems contain no macroscopic water phase, and the concentration of water in the solid-state electrolyte is determined entirely by the relative humidity (water fugacity) of the surrounding gaseous environment and by the partition coefficient (equilibrium constant) for water between the gas phase and the solid state electrolyte phase. Therefore, the electrode potential in such a sensor is influenced by a change in the relative humidity (RH) of the test gas. Measurements show that the potential changes with RH are less for the hydrophobic PVC composite RE than for the hydrophilic Nafion composite RE.<sup>149</sup> Quantitatively, over a 30–70% RH range, the potential of the Pt-PVC/air RE changes by only a few millivolts as opposed to by tens of millivolts for the Pt-Nafion RE. For this reason, the Pt-PVC/air RE is preferable to the Pt-Nafion electrode for sensors that operate in environments with variable humidity.

## 6. Solid Electrolyte $\text{H}_2$ Sensors

Solid electrolyte electrochemical sensors function much like their liquid and polymer electrolyte counterparts except that the mobility of ions in crystalline or polychryalline solids is typically much lower than that in liquids. This often requires solid electrolyte sensors to operate at higher tem-

**Table 4. Solid Electrolytes Used in Electrochemical Solid Electrolyte  $\text{H}_2$  Gas Sensors**

solid electrolyte	temp of stability	type of gas sensor <sup>a</sup>	ref
$\text{HUO}_2\text{PO}_4 \cdot 4\text{H}_2\text{O}$	<100 °C	P; C	33, 157
$\text{Sb}_2\text{O}_5 \cdot 4\text{H}_2\text{O}$	<100 °C	P; A	82, 158, 159
$\text{Sb}_2\text{O}_5 \cdot \text{H}_2\text{O} - \text{H}_3\text{PO}_4$	<100 °C	P	76
$\text{Zr}(\text{HPO}_4)_2 \cdot n\text{H}_2\text{O}$	<350 °C	P; A	89, 158, 160, 161
$\text{H}_4\text{SiW}_{12}\text{O}_{40} \cdot n\text{H}_2\text{O}$	100 °C	P	78
$\text{Me}_x\text{H}_{3-x}\text{PW}_{12}\text{O}_{40} \cdot n\text{H}_2\text{O}$	100 °C	P	78
$(\text{NH}_4)_2\text{HPW}_{12}\text{O}_{40} \cdot n\text{H}_2\text{O}$	100 °C	P	162
hydronium NASICON	100 °C	P	79, 80, 85, 136
$5\text{P}_2\text{O}_5 \cdot 95\text{SiO}_2$ glass		P	163
$\text{Na}_3\text{PO}_4$	>600 °C	P	164
$\text{K}_3\text{PO}_4$	>600 °C	P	164
$\text{In}^{3+}$ -doped $\text{SnP}_2\text{O}_7$			86
YSZ	>1000 °C		87, 93, 165–167
$\alpha\text{-Al}_2\text{O}_3/\text{Mg}$	>1500 °C		168
$\text{Ce}_{0.8}\text{Gd}_{0.2}\text{O}_{1.9}$	>1000 °C	P	169
Perovskites			
$\text{SrCeO}_3$	>1000 °C	P	90, 164, 170
$\text{SrCeO}_3/\text{Yb}$	>1000 °C	C; P	171–175
$\text{CaZrO}_3$	>1000 °C	P	83, 164, 176, 177
( $\text{CaZrO}_3/\text{In}$ )		P	164, 178
$\text{BaCeO}_3$	>1000 °C	P	164, 179
$\text{BaCe}_{0.8}\text{Gd}_{0.2}\text{O}_3$	>1000 °C	P	180–183
$\text{BaZr}_{0.4}\text{Ce}_{0.4}\text{In}_{0.2}\text{O}_3$	>1000 °C		185
$\text{Ba}_3\text{Ca}_{1.18}\text{Nb}_{1.82}\text{O}_{9-\delta}$	>1000 °C	P	185
$\text{KCa}_2\text{Nb}_3\text{O}_{10}$	>1000 °C	P	84

<sup>a</sup> P, potentiometric; A, amperometric; C, conductometric; NASICON,  $\text{Na}_3\text{Zr}_2\text{Si}_2\text{PO}_{12}$ .

perature in order to have high concentrations of mobile ions in the bulk solid phase.<sup>89</sup> The solid state ions participate in the electrode reactions involving gaseous components and electrons, and the electrodes act as a catalyst for the electrode reactions, very similar to their liquid electrolyte sensor counterparts.

### 6.1. Solid Electrolytes Used in $\text{H}_2$ Sensors

The majority of electrochemical  $\text{H}_2$  sensors are based on proton conductors.<sup>150</sup> Among a number of fast proton conductors reported during the past two decades, polymer membranes such as Nafion are well-known to show high conductivities, e.g.  $\sim 10^{-2}$  S/cm below 100 °C.<sup>151</sup> By comparison, solid electrolyte proton conductors have attracted significant interest because of their chemical and physical durability, especially at elevated temperatures, thus their ability to extend the application of electrochemical hydrogen sensor systems.<sup>80,82,152–155</sup> There are quite a large number of solid-state materials that can potentially meet the requirements for application in solid electrolyte  $\text{H}_2$  sensors.<sup>156</sup> Similar to liquid systems, solid-state electrochemical cells for hydrogen sensing are typically constructed by combining a membrane of solid electrolyte (proton conductor) with a pair of electrodes (electronic conductors). As typical of all electrochemical systems, the interface of solid electrolyte and electrode plays a most important role in determining the gas sensor's analytical characteristics. A list of solid electrolytes that have been tested as materials for  $\text{H}_2$  sensors is presented in Table 4.

Each solid material has its own range of temperatures over which it possesses the required proton conductivity and is stable. The proton mobility is a function of temperature (Figure 24 illustrates this for some solids vs liquids and polymers), and each material has an optimum temperature or temperature range for operation. For example, the working

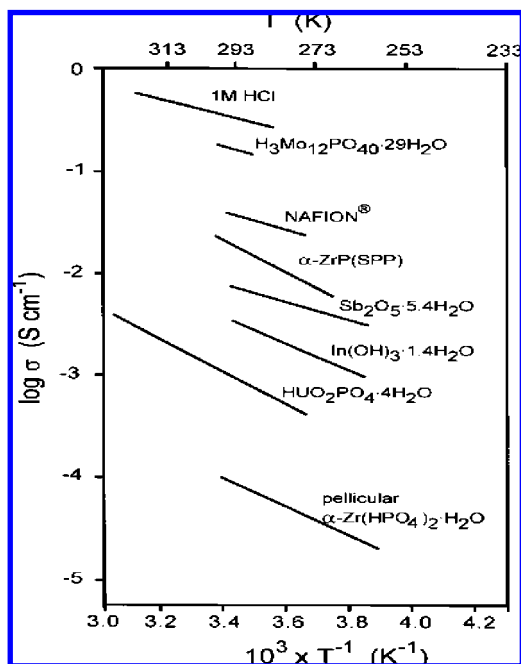


**Figure 24.** Conductivity as a function of temperature for some proton conductors. (Reprinted from ref 89, Copyright 2001, with permission from Elsevier.)

temperature range of the BaCeO<sub>3</sub>-based sensor, due to the high protonic conductivity of BaCeO<sub>3</sub>, varies from 200 to 900 °C.<sup>179</sup> Also, the electrical conductivity measurements of BaZrO<sub>3</sub>/Y showed predominantly proton conduction at temperatures below 500 °C, which is suitable for hydrogen sensor operation.<sup>186</sup> Many of these materials compare favorably to Nafion and should be suitable for H<sub>2</sub> sensing applications.

## 6.2. Solid Electrolyte H<sub>2</sub> Sensors: Fundamentals of Operation

Most of the H<sub>2</sub> sensors that use solid electrolytes are operated potentiometrically. The simplest scheme for such a sensor is represented in Figure 25. The voltage produced is from the concentration dependence of the chemical potential, which at equilibrium is represented by the Nernst equation.

Basically, such a potentiometric (Nernst-type) sensor is often called a concentration cell, where the gas activity at the sensing electrode can be obtained from the open circuit potential  $E$  (EMF), if a well defined, constant gas activity at the reference electrode is established. This cell potential (or open circuit potential) is related to the concentration (activity or fugacity) of the active species at the sensing electrode according to the Nernst equation:

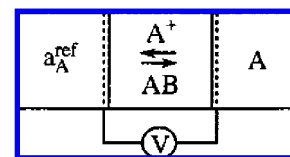


**Figure 25.** Diagram illustrating the potentiometric sensor mechanism: A is the analyte with variable activity/concentration,  $a_A^{\text{ref}}$  is the constant activity of analyte A on the reference side of the solid electrolyte membrane, AB is a solid electrolyte membrane (A<sup>+</sup> ion conductor), and the electrodes facilitate the reaction  $A^+ + e^- = A$ ; when the activity of A is different on each side of the membrane, a potential,  $V$ , is observed.

$$E = \frac{RT}{nF} \ln \frac{P_X}{P_{\text{ref}}} \quad (15)$$

with  $R$  the gas constant,  $F$  the Faraday constant,  $T$  the temperature (K),  $P_X$  the partial gas pressure in the sample gas mixture,  $P_{\text{ref}}$  the reference partial pressure, and  $n$  the number of electrons involved in the basic electrochemical reaction of the sensor ( $n = 2$  for hydrogen and  $n = 4$  for oxygen). The sensing electrode potential usually is a function of the logarithm of the H<sub>2</sub> concentration in air.

Configurations for potentiometric hydrogen sensors have been reported.<sup>33,187</sup> There are typical advantages and limitations in using the solid electrolytes. Water can often interfere because water can affect the activity of the proton through well-known reactions such as  $H_2O = H^+ + OH^-$  and these reactions can be accelerated at high temperature. Further, oxides can be formed, and so the presence or absence of oxygen often affects certain solid electrolytes. Finally, poisoning by strongly adsorbed species such as CO or CO<sub>2</sub> can affect the electrode or electrolyte performance and thereby affect observed sensor operating characteristics. Therefore, solid electrolyte sensors must be characterized for each application to ensure performance, and the choice of materials for electrodes and the electrolyte are extremely important to the development of the desired analytical characteristics. A review of H<sub>2</sub> sensor performance in different applications is summarized in Table 5.

Each application has forced the development of a different sensor using different electrodes and solid electrolytes, filters, and/or various constructions. There is not yet a universal electrochemical H<sub>2</sub> sensor for all applications and it is still required to optimize the design of each sensor to obtain the needed analytical performance; for example, to eliminate the need for a standard reference concentration of hydrogen, a sensor with an internal reference has been designed,<sup>83</sup> as illustrated in Figure 26.

This design cleverly employs electrochemical pumping of hydrogen by means of electrolysis of water vapor in the atmosphere to create a constant activity for H<sub>2</sub> in the sensor reference compartment. The water vapor partial pressure

**Table 5. Summary of Publications on Performance of Electrochemical H<sub>2</sub> Sensors Designed for Different Applications**

field of application	ref
H <sub>2</sub> in N <sub>2</sub> (Ar)	59, 62, 80, 95
H <sub>2</sub> in air	43, 60, 87, 91, 93, 132, 188
H <sub>2</sub> with presence of CO and CO <sub>2</sub>	60, 61, 91
H <sub>2</sub> in wet atmosphere	43, 61, 64, 83, 90, 157, 170, 176, 177, 179, 189
H <sub>2</sub> in dry atmosphere	47, 66, 76, 91, 144
H <sub>2</sub> in water	148, 190, 191
H <sub>2</sub> in molten metals	168, 171, 178, 192, 193
sensors for RT	33, 76, 78, 82, 89, 156–159, 163, 194
high-temperature sensors	91, 93–95, 167, 169, 188, 195
operation without a standard reference gas	83, 163

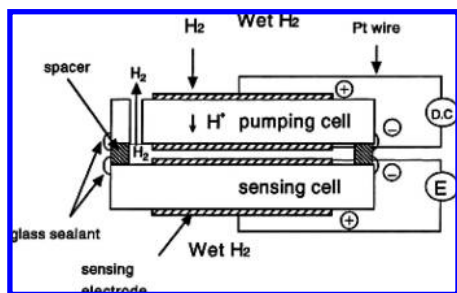


**Figure 26.** Example of an H<sub>2</sub> sensor with an electrochemically supplied hydrogen standard. (Reprinted from ref 83, Copyright 2001, with permission from Elsevier.)

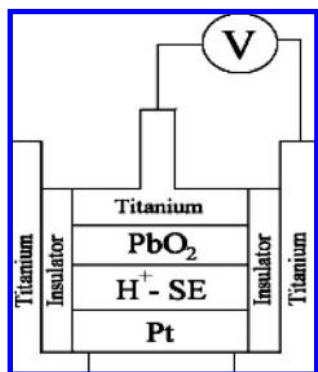


**Figure 27.** Solid electrolyte electrochemical cell used for H<sub>2</sub> sensing. (Reprinted from ref 78, Copyright 2005, with permission from Elsevier.)

could be determined from the EMF of the pumping cell using the pumped hydrogen as a standard gas. Combining the pumping and sensing function, the partial pressure of H<sub>2</sub> can be automatically controlled, and one can make a hydrogen pressure regulator, in principle. This concept actually combines the idea of potentiometry and amperometry in a single device and results in taking advantage of Faraday current and Nernstian potentials for a sensor that has automatic compensation features.

### 6.3. Low-Temperature Solid Electrolyte H<sub>2</sub> Sensors

There are advantages in working at low temperature because materials are more stable and corrosion reactions much slower. The compounds H<sub>2</sub>UO<sub>2</sub>PO<sub>4</sub>·4H<sub>2</sub>O<sup>33,157</sup> and Sb<sub>2</sub>O<sub>5</sub>·4H<sub>2</sub>O<sup>158,159</sup> were two of the earliest low-temperature solid electrolytes tested in protonic conductor H<sub>2</sub> sensors. Compounds such as H<sub>4</sub>SiW<sub>12</sub>O<sub>40</sub>·28H<sub>2</sub>O, H<sub>3</sub>PW<sub>12</sub>O<sub>40</sub>·29H<sub>2</sub>O, HSbP<sub>2</sub>O<sub>8</sub>·10H<sub>2</sub>O, and H<sub>3</sub>Mo<sub>12</sub>PO<sub>40</sub>·29H<sub>2</sub>O also can be included in the category of low-temperature solid electrolytes with sufficient proton conductivity.<sup>89</sup> These heteropoly compounds are electrocatalytically active in reactions involving hydrogen<sup>78</sup> and can be used in the design of H<sub>2</sub> sensors. Reports have shown solid-state sensors for hydrogen concentrations from 10<sup>-2</sup> to 5 vol % in inert gases and air without the need for maintaining constant temperature.<sup>78</sup> Operation over the ambient temperature range from -60 to +60 °C has been reported.<sup>78</sup> The design and performance of this solid electrolyte cell is shown in Figures 27 and 28. Although the sensor response and recovery rate decreased with a decrease in temperature, the concentration dependence remained virtually unchanged over all operating temperatures (Figure 28), an important advantage in ambient sensors.

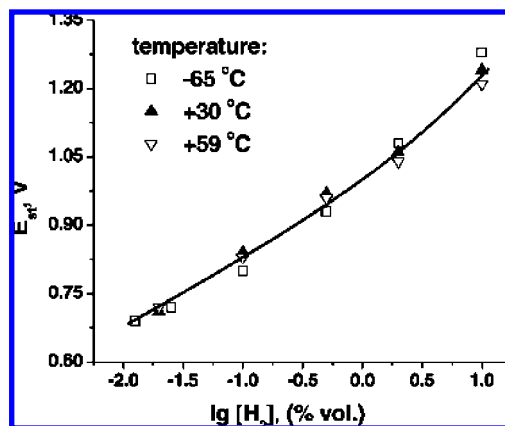


**Figure 28.** H<sub>2</sub> concentration vs the absolute EMF in air at different temperatures. (Reprinted from ref 78, Copyright 2005, with permission from Elsevier.)

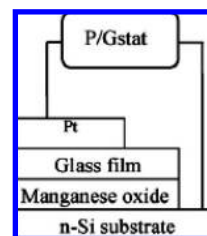


**Figure 29.** Schematic diagram of the H<sub>2</sub> gas sensor designed with P<sub>2</sub>O<sub>5</sub>-SiO<sub>2</sub> glass. (Reprinted from ref 163, Copyright 2006, with permission from Elsevier.)

The search for lower temperature solid ionic conductors has likewise led to potentiometric hydrogen sensors that can work near room temperature. A P<sub>2</sub>O<sub>5</sub>-SiO<sub>2</sub> glass has high conductivity, e.g. ~10<sup>-2</sup> S/cm at room temperature,<sup>163</sup> and very good chemical and thermal stability as well as a potentially low fabrication cost.<sup>189</sup> Nogami et al.<sup>163</sup> reported about a thin film potentiometric H<sub>2</sub> sensor with this same glass that does not require the use of reference gas (Figure 29).

As might be anticipated, the hydrogen sensor was extremely sensitive to water vapor.<sup>189</sup> This RH effect is generally applicable and is found in solid electrolyte room temperature protonic conductors such as uranylphosphate,<sup>157</sup> zirconium phosphate,<sup>160,161</sup> P<sub>2</sub>O<sub>5</sub>-SiO<sub>2</sub> glass,<sup>189</sup> and antimonic acid.<sup>159</sup> In this regard, they operate like the polymer sensors described above and are generally applied only in a gas with defined or constant RH (as a rule at the highest RH) because the conductivity of these solid electrolytes strongly depends on the relative humidity of the ambient. Quantitative investigation of the RH effects on the conductivity of HSbP<sub>2</sub>O<sub>8</sub>·H<sub>2</sub>O have measured a more than 4 orders of magnitude change in conductance with RH varying from 0 to 100%.<sup>196</sup> For the P<sub>2</sub>O<sub>5</sub>-SiO<sub>2</sub> glass, it is possible to work only in humid atmosphere with an RH of 50% or more at room temperature.<sup>189</sup>

Potentiometric hydrogen sensors designed using a NASICON solid electrolyte similarly exhibited a strong RH effect, and this makes it difficult to work in a dry atmosphere.<sup>85</sup> Figure 30 illustrates the large, orders of magnitude changes that can occur in the sensor signal with RH changes. This electrolyte (a bonded hydronium NASICON) was produced by the two-stage process of powder ion-exchange followed by a bonding and pressing method. Engelhard platinum paste A-4338 with a modified curing procedure was used as the



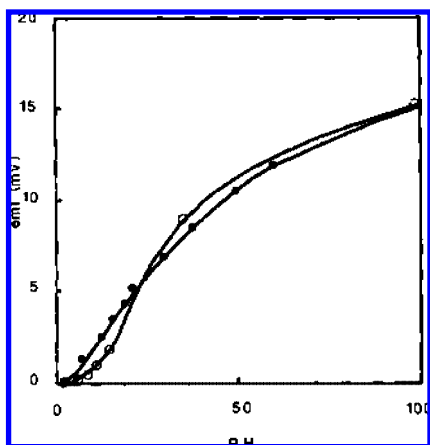


**Figure 30.** Pt/NASICON/Pt-based sensor EMF versus cell relative humidity. (Reprinted from ref 85, Copyright 1991, with permission from Elsevier.)

electrode material for both the anode and cathode. Measurements of EMF were made at constant hydrogen concentration with a Hewlett-Packard digital voltmeter with input impedance  $> 10^{12} \Omega$  for accurate potential determination.

The RH dependence of room temperature solid electrolytes can have serious deleterious effects on sensor performance. In spite of the fact that heteropoly compounds, such as the ammonium salts of phosphotungstic acid, are very stable to environmental oscillations of RH and temperature, at low RH, the conductivity of the salt and hence the sensor signal are reported to change significantly. Moreover, such salts are able to be reduced if they are in very high hydrogen concentration for extended periods of time, and this is evidenced by the appearance of electronic conductivity in the material.

Solutions to the problems with low-temperature heteropoly compound solid electrolytes have led to the development of composite structures. For example, a four-layer cell containing two solid electrolytes has been constructed.<sup>78</sup> In this structure, Pt directly contacts the ammonium salt of phosphotungstic acid, and the rate of the hydrogen exchange reaction is rapid at this electrode. Lead dioxide is in contact with silicotungstic acid such that it is not rapidly reduced chemically on exposure to hydrogen. The entire cell only produces a signal when hydrogen is present, due to the asymmetry of the electrode/electrolyte.

Other investigators<sup>76</sup> have suggested that composites based on hydrated antimony pentoxide and phosphoric acid are less sensitive to humidity in comparison with other known protonic electrolytes.<sup>157,159,160</sup> DTA (differential thermal analysis) experiments demonstrate that these composite materials retain water better than the initial pure  $\text{Sb}_2\text{O}_5 \cdot x\text{H}_2\text{O}$  material. The conductivity of the electrolyte  $\text{Sb}_2\text{O}_5 \cdot \text{H}_2\text{O} - \text{H}_3\text{PO}_4$  does not greatly depend on the relative humidity in the midrange RH (20–80%RH). Hence, an  $\text{H}_2$  sensitive element with this electrolyte should operate without RH drift under conditions where the humidity varies throughout the midrange of RH, and experiments confirm this prediction (20–95%RH produces a 15 mV EMF change at constant  $\text{H}_2$  concentration). Sensors, based on hydrated antimony pentoxide and phosphoric acid, were also found not to degrade with long-term storage (4 years) under ambient conditions.<sup>76</sup> This successful sensor consisted of an Ag or Ag/(Ag +  $\text{Ag}_2\text{SO}_4$ ) RE, the solid composite electrolyte, and a Pt or Pd  $\text{H}_2$  sensitive electrode. The sensor detection limit was in the low-ppm range (10 ppm), and the EMF of the

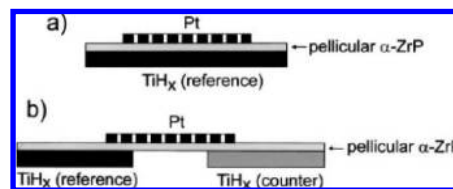
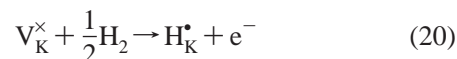


**Figure 31.** Schematic representation of sensors using pellicular zirconium phosphate as a proton conductor and titanium hydride as a reference electrode: (a) potentiometric sensor, (b) three-electrode amperometric sensor. (Reprinted from ref 89, Copyright 2001, with permission from Elsevier.)

sensor varied logarithmically with  $\text{H}_2$  concentration for hydrogen partial pressures in the range 100–2000 ppm. The slope of the EMF vs  $\log(\text{pH}_2)$  plot was 170 and 200 mV for Pt and Pd, respectively, which exceeds the Nernst value, presumably due to the formation of a mixed potential in air. Moreover, the sensor's characteristics did not appear to depend on the temperature within the range 286–303 K.

It has been suggested that many problems of low-temperature solid electrolyte  $\text{H}_2$  sensors could be resolved by using pellicular zirconium phosphates.<sup>89,161</sup> These compounds are sufficiently good proton conductors, have thermal stability up to 350 °C, and can be directly deposited over the reference electrode as a very thin skin. A potentiometric and amperometric sensor design with this material is illustrated in Figure 31. Limitation of this electrolyte includes the relatively low chemical and mechanical stability.<sup>92</sup>

Additional low-temperature proton conductors have been found that are based on layered perovskite oxides.<sup>197–199</sup> These compounds do not take up any measurable amount of water. An example of a layered perovskite D-J type oxide is  $\text{ACa}_2\text{Nb}_3\text{O}_{10}$ , where A is an alkali metal. In these niobates, the A atom is sandwiched between  $\text{Ca}_2\text{Nb}_3\text{O}_{10}$  perovskite slabs composed of corner-sharing  $\text{NbO}_6$  octahedral and Ca ions. The electrical conductivity has been explained to be due to the migration of alkali metal ions in interlayer conduction paths.<sup>200</sup> However, when the compound is exposed to hydrogen, a large increase in the ionic conductivity is observed. This is attributed to the added mobility of protons. For example, 2D-layered  $\text{KCa}_2\text{Nb}_3\text{O}_{10}$  exhibits an electrical conductivity of  $3.2 \times 10^{-4} \text{ S/cm}$  with activation energy of 0.25 eV at 45 °C in an  $\text{H}_2$  atmosphere.<sup>201</sup> Proton conductivity in  $\text{H}_2$  is commonly understood by assuming point defects according to the specific defect equations for  $\text{KCa}_2\text{Nb}_3\text{O}_{10}$  under hydrogen atmosphere, as follows:



where  $\text{V}_\text{O}^{\bullet\bullet}$ ,  $\text{O}_\text{O}^\times$ ,  $\text{e}^-$ ,  $\text{h}^\bullet$ ,  $\text{H}_\text{i}^\bullet$ ,  $\text{OH}_\text{O}^\bullet$ ,  $\text{H}_\text{K}^\bullet$ , and  $\text{H}_\text{i}^\bullet$  represent oxygen vacancy, lattice oxygen, excess electrons, holes, protons, protons attached to lattice oxygen, protons at a vacant K site in the lattice, and interstitial protons, respectively. The proton conductivity mechanism in acceptor-doped 3D perovskite oxides due to the migration of hydroxyl ions or protons has been described in detail.<sup>67</sup> The  $\text{KCa}_2\text{Nb}_3\text{O}_{10}$  layered perovs-

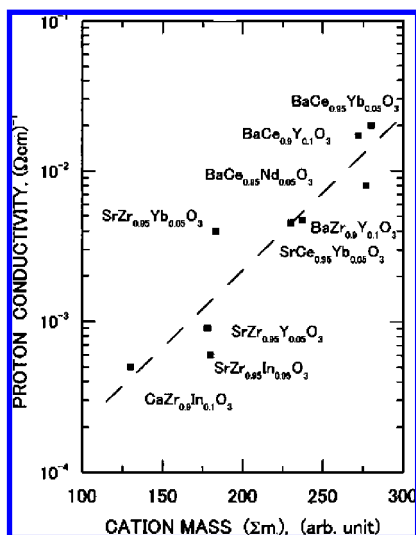


**Figure 32.** Total mass of constituent atoms in a unit cell versus the  $H^+$  ion conductivity at 600 °C for several perovskite-type proton conductors. A least-squares line is drawn through the data. (Reprinted from ref 210, Copyright 2005, with permission from Elsevier.)

kite contains neither oxygen vacancies nor structural protons nor water, but yet behaves as an electrolyte.

Amperometric type  $H_2$  sensors using  $KCa_2Nb_3O_{10}$  have been described.<sup>84</sup> The sensors were able to work in the temperature range of RT–65 °C. The sensitivity of this type of sensor is highly influenced by the electrode particle size and the operating temperature. The optimum particle size of 300–500 nm and a Pt loading of 1.85 mg/cm<sup>2</sup> were found to have high catalytic activity and be useful for  $H_2$  detection. The best operating temperature for the sensor appeared to be about 45 °C with respect to long-term stability, and at this temperature, the sensor exhibited reproducible results in 1–8%  $H_2$ .

#### 6.4. Performance of Mixed-Potential $H_2$ Sensors

Most of the high-temperature solid electrolyte  $H_2$  sensors are designed as potentiometric sensors. In most of the sensor systems, the potential is the result of several simultaneous reactions taking place, and this is called a mixed-potential system.<sup>93,95,165,166,169,187,222–228</sup>

The YSZ and many perovskite materials are compounds with mixed conductivity.<sup>205</sup> Therefore, sensors made from these materials will have at least the electrochemical reactions (eqs 2 and 3) taking place simultaneously on the sensing electrode. The non-Nernstian response of these sensors has usually been observed at relatively low temperature (e.g., 350–600 °C) and explained by invoking a mixed potential, which appears at the sensing electrode due to the simultaneous occurrence of the cathodic reduction of oxygen and the anodic oxidation of the reducing gas.<sup>88,222,223</sup> This phenomenon has led to the proposed use of zirconia-based potentiometric sensors for reducing gases and some basic explanations of the mechanism of mixed potential gas sensors.<sup>94,188,229,230</sup>

A typical representation of a mixed-potential device is shown in Figure 33. In this case both electrodes, with each forming a different electrolyte–electrode interface, are exposed to the analyte gas, usually a mixture containing oxygen and an oxidizable or reducible gas that is the target analyte (e.g., sometimes hydrogen).

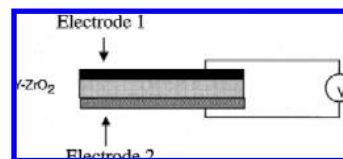
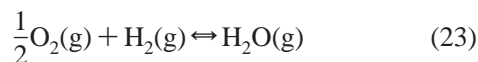
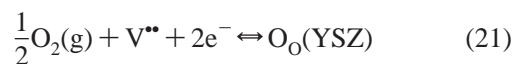


**Figure 33.** Schematic illustration of a mixed potential sensor fabricated from yttrium stabilized zirconia. Both electrode materials are exposed to a gas mixture containing an oxidizable or reducible gas and oxygen. (Reprinted from ref 230, Copyright 2000, with permission from Elsevier.)

The mixed potential at an electrode is established by the competing reactions of oxygen reduction (oxidation) and analyte ( $CO$ ,  $H_2$ , or hydrocarbon) oxidation (reduction). Equations 21–23 illustrate this for  $H_2$ , and reaction 23 can take place in the gas phase or on the surface of the electrodes with the participation of adsorbed species.



In these equations,  $V^{**}$  is an oxygen vacancy and  $O_O$  is a lattice oxygen in the electrolyte. The potential of the electrode is achieved at equal current exchange densities of the reactions (eqs 21 and 23). The device response voltage is the difference in the mixed potential attained at each electrode. Depending on the rates of the two reactions, a nonequilibrium potential that is more negative than that predicted by the Nernst equation develops under oxygen rich conditions (i.e., more oxygen present than would be required for stoichiometry). Experiments show that the sensor response may vary from a logarithmic potential dependence on gas concentration to a linear concentration–potential dependence with elevated sensitivities at low concentrations.<sup>230</sup> This mixed potential, being dependent on catalytic kinetic parameters, is expected to be a strong function of the electrode material.<sup>88</sup> Further, it should be a function of the electrode geometry and structure, since catalytic activity is very sensitive to material composition, structure, and geometry. For optimal sensor operation in a mixed-potential mode the material of the measuring electrode should exhibit a low catalytic activity for the combustion of the oxidizable gas to be detected. In contrast, at the catalytically active electrode, hydrogen can be adsorbed and then oxidized electrochemically with oxygen ions. These oxygen ions are delivered from the solid electrolyte, as indicated by eqs 21 and 22.

The sensor configurations reported in the literature either measure the potential between two different electrodes exposed to the same gas<sup>94</sup> or measure the potential of one electrode with respect to an air reference.<sup>93,96,169,231</sup> Important sensor parameters such as sensitivity, selectivity, and long-term stability are correlated mainly with the performance of the materials in the mixed potential electrode. During the past decade, many efforts have been made to understand the electrode processes and the interdependence between electrode defect chemistry and the mixed potential behavior.<sup>81,94,188</sup> It was shown that the response behavior of the mixed potential depends on whether Tafel type, mass transport limited, and/or linear Butler–Volmer kinetics is observed for the electrochemical reactions.<sup>230</sup> This means that the non-

Nernstian behavior clearly comes from the reaction kinetic control and not equilibrium thermodynamic control at the sensing electrode. Clearly, interfacial properties of electrode materials, geometry, morphology, and solid electrolytes will influence the mixed potential response.<sup>93</sup> In the final analysis, it is difficult to maintain several kinetic rates invariant over long periods of time and, therefore, difficult to prepare sensors with low drift, although significant progress has been made.

## 6.5. High-Temperature Solid Electrolyte H<sub>2</sub> Sensors

### 6.5.1. Solid Electrolytes for High-Temperature H<sub>2</sub> Sensors

Typical solid electrolytes for high-temperature H<sub>2</sub> sensors include YSZ and perovskites that become sufficiently conductive only when the temperature exceeds 400 °C.<sup>167,172,202–206</sup> Over a wide range of temperatures, they have a high ionic conductivity and high activity for gas sensing. Often having high melting and/or decomposition temperatures, they can provide microstructural and morphological stability to improve the reliability and long-term performance of sensors. The perovskite structure has two differently sized cations, which makes it amenable to a variety of dopant additions. This doping flexibility allows controlling the transport and catalytic properties to optimize sensor performance for particular applications.<sup>206</sup>

The most well-known are perovskite structured oxides, including SrCeO<sub>3</sub>, SrCeO<sub>3</sub>/Yb, SrCeO<sub>3</sub>/In, BaCeO<sub>3</sub>, BaCeO<sub>3</sub>/Gd, SrZrO<sub>3</sub>, BaZrO<sub>3</sub>, and CaZrO<sub>3</sub>, which have high thermal stability and exhibit appreciable proton conduction with low activation energy at elevated temperatures (>700 °C) in steam and hydrogen atmospheres<sup>177,197,207–210</sup> and have been used for hydrogen sensors.<sup>178</sup> The conductivity of these ion conducting materials is strongly dependent on the temperature,<sup>54</sup> and data on proton conductance for several perovskites are presented in Figure 32. As a rule, the embedding of the fourth element is used to control the conductivity; for example, in the case of SrCeO<sub>3</sub>/Yb, doping with 5% of Yb<sup>3+</sup> achieved the maximum of ionic conductivity.

These proton conductors are ceramic materials and typically do not have high porosity but rather can reach 96–99% of the theoretical density.<sup>90</sup> Because of the exceptional thermal and chemical stability of the materials, a hydrogen sensor for molten metals has been developed and widely used in the process control in the metal melting industry.<sup>171,176,211</sup> In order to produce high-quality castings, it is necessary to reduce the hydrogen concentration in the molten metals during the casting process to an acceptable level, and a hydrogen sensor provides important process control data.<sup>176</sup>

One novel protonic conductor includes BaZr<sub>0.4</sub>Ce<sub>0.4</sub>In<sub>0.2</sub>O<sub>3</sub> (BZCI), a material that has practical durability in the presence of steam and has relatively high conductivity.<sup>184</sup> This material was able to produce a very stable H<sub>2</sub> sensor at 800 and 1000 °C in a wet but pure hydrogen atmosphere. The crystal structure and the composition of all samples did not change during a test with hydrogen. The actual EMFs almost coincided with the theoretical values below 800 °C but were lower than the theoretical values at 1000 °C. Protonic conduction in BZCI was confirmed below 800 °C and seems to decrease at higher temperature.

Many of the oxides discussed above (SrCeO<sub>3</sub>, BaCeO<sub>3</sub>) easily react with carbon dioxide to form carbonates of the alkaline earth elements and therefore are not good candidates

for applications in sensors exposed to CO<sub>2</sub>, including ambient atmosphere sensors.<sup>84,212</sup> Barium cerate ceramics (BaCe<sub>0.8</sub>Gd<sub>0.2</sub>O<sub>3</sub>, i.e., BCG) also were affected by steam or CO<sub>2</sub> and have met with problems in practical use.<sup>181–183,213</sup> The SrCeO<sub>3</sub>/Yb reacts with 10% CO<sub>2</sub> at temperatures below 800 °C, and this reaction can take place already at 500 °C.<sup>186</sup> Research has demonstrated that cerates such as BaCeO<sub>3</sub> are thermodynamically unstable when a critical H<sub>2</sub>O vapor pressure is exceeded.<sup>212</sup> It was established that BaCeO<sub>3</sub> in an H<sub>2</sub>O vapor containing environment (~430 Torr H<sub>2</sub>O) decomposed into CeO<sub>2</sub> and Ba(OH)<sub>2</sub> in relatively short periods of time at temperatures less than 900 °C and that doped BaCeO<sub>3</sub> decomposed at a faster rate than the undoped BaCeO<sub>3</sub>. It was assumed that the rapid decomposition of both powder and sintered samples is the result of the high solubility of H<sub>2</sub>O in BaCeO<sub>3</sub>, which accelerates the kinetics of decomposition.

The zirconates, such as CaZrO<sub>3</sub> and BaZrO<sub>3</sub>, are less reactive with CO<sub>2</sub> than cerates and are more stable in H<sub>2</sub>O- and CO<sub>2</sub>-containing atmospheres.<sup>207,214</sup> The Y-doped BaZrO<sub>3</sub> has been reported to exhibit high proton conductivity and good chemical stability.<sup>215,216</sup> Furthermore, it has been demonstrated<sup>217</sup> that strontium cerate is not stable in a simulated coal gasification atmosphere containing 0.0033 vol % H<sub>2</sub>S at 800 °C, since SrS and CeO<sub>2</sub> are formed. Consideration of stability issues, therefore, causes the majority of practical H<sub>2</sub> sensors to use the YSZ electrolyte.

Recently, nonstoichiometric complex or mixed perovskite-type oxides of the formula A<sub>2</sub>B(1)<sub>1+x</sub>B(2)<sub>1-x</sub>O<sub>6-δ</sub> and A<sub>3</sub>B(1)<sub>1+x</sub>B(2)<sub>2-x</sub>O<sub>9-δ</sub> have been demonstrated to become proton conductors upon exposure to H<sub>2</sub>O vapor.<sup>218,219</sup> Among them, the A<sub>3</sub>B(1)<sub>1+x</sub>B(2)<sub>2-x</sub>O<sub>9-δ</sub> (A = Sr, Ba) compounds are particularly interesting because of their excellent protonic conductivity.<sup>220</sup> In addition, unlike Ce-based perovskites, these compounds have a wide band gap<sup>221</sup> and are superior insulators without producing detectable electronic conduction under either oxidizing or reducing gas mixtures up to 1000 °C.<sup>220</sup>

A high-temperature solid electrolyte suitable for use in H<sub>2</sub> sensors includes Sn<sub>0.9</sub>In<sub>0.1</sub>P<sub>2</sub>O<sub>7</sub>.<sup>86</sup> The EMF of sensors prepared from this material varied linearly with the logarithm of the H<sub>2</sub> concentration, and the EMF was minimally affected by the water-vapor concentration.<sup>86</sup> The results presented by Mukundan et al.<sup>169</sup> also provoke interest. Pt/Ce<sub>0.8</sub>Gd<sub>0.2</sub>O<sub>1.9</sub>/Au mixed-potential sensors were used to detect H<sub>2</sub> in a gas mixture of H<sub>2</sub>–air. The sensor response was maximum for H<sub>2</sub> and negligible for methane; other gases followed the trend methane < propane < CO, propylene < hydrogen.

### 6.5.2. Practical High-Temperature H<sub>2</sub> Sensors

An example of a high-temperature solid-state mixed potential gas sensor designed for hydrogen detection and aimed at commercialization is given in Figure 34.

The H<sub>2</sub> sensors were fabricated by using a half-open, yttrium-stabilized-zirconia tube (YSZ, 8 mol % Y<sub>2</sub>O<sub>3</sub> doped, NKT).<sup>93,195</sup> The tube was 30 mm in length and 5 and 8 mm in inner and outer diameter, respectively. This design is essentially the same structure as that used for potentiometric YSZ oxygen sensors except that the sensing electrode on the outer surface is provided with a porous ZnO layer. The Pt mesh is designed to work as an electron-collector. Pt black and Pt mesh were pressed on the inner surface of the YSZ tube at the closed end to form a reference electrode. This RE was always exposed to static atmospheric air. An oxide



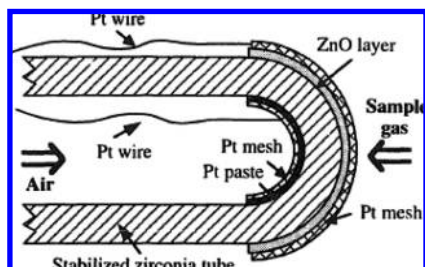


**Figure 34.** Mixed-potential type H<sub>2</sub> sensor using a YSZ- and ZnO-Pt electrode. (a) Device structure with the ZnO layer deposited around the YSZ tube. (Reprinted from ref 93, Copyright 1996, with permission from Elsevier.)

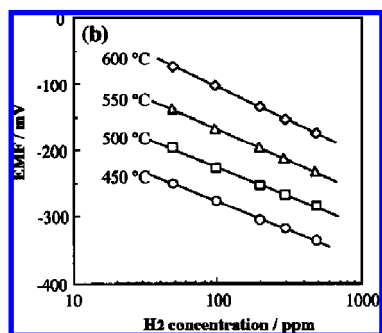


**Figure 35.** Mixed-potential H<sub>2</sub> sensor using a YSZ- and ZnO-electrode. EMF as a function of concentration of H<sub>2</sub> in air. (Reprinted from ref 93, Copyright 1996, with permission from Elsevier.)

powder paste containing  $\alpha$ -terpineol and ethyl cellulose was applied beltlike (width, 10 mm; total area, 2.5 cm<sup>2</sup>) on the outside of the tube, followed by calcination at 650 °C for 2 h, to form the sensing oxide layer. The oxide layer thus formed was porous and about 30  $\mu$ m thick. This device generated a fairly large EMF response to H<sub>2</sub> in air at temperatures in the range 450–600 °C, as shown in Figure 35.

The EMF response is seen to be linear to the logarithm of H<sub>2</sub> concentration, but the slopes are about  $-100$  mV/decade, inconsistent with the behavior of an equilibrium type device<sup>93</sup> and more typical of a mixed-potential device. The EMF appears to decrease rapidly with a rise in temperature, and this seems to result from the enhancement of catalytic oxidation of H<sub>2</sub> on the sensing electrode with temperature. In this particular device with the ZnO electrode, the EMF response is still large at 600 °C, being capable of detecting 50 ppm H<sub>2</sub> in air. The 90% response and recovery time to 200 ppm H<sub>2</sub> at 600 °C for this device are 5 and 10 s, respectively. The stability of this sensor (Figure 36), exemplified by both air and H<sub>2</sub> EMF responses, provides encouraging results for the design of elevated temperature H<sub>2</sub> sensors.

Other approaches to the design of high-temperature H<sub>2</sub> sensors have been reported, and one is shown in Figure 37. The goal of this approach is to simplify and miniaturize the sensor structure.

The chip type device was fabricated by using a small bar of yttrium stabilized zirconia (8 YSZ, 6  $\times$  2  $\times$  1.5 mm<sup>3</sup>), as shown in Figure 37, and applying two kinds of oxide pastes, one at each end of the zirconia bar, leaving about 1 mm of space in between, followed by calcining at 650 °C for 2 h, to form a couple of belt-shaped oxide electrodes (width, about 2 mm; thickness, about 30 nm). A Pt wire was wound around each oxide electrode as an electrical collector.<sup>94</sup> The

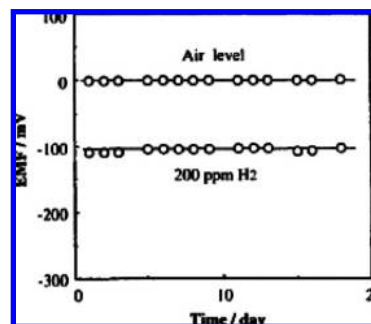


**Figure 36.** Long-term stability of the ZnO-attached YSZ-based device at 600 °C. (Reprinted from ref 93, Copyright 1996, with permission from Elsevier.)

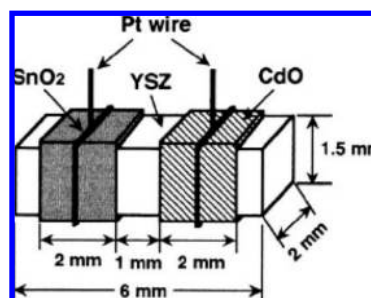


**Figure 37.** Chip type YSZ-based device attached with CdO and SnO<sub>2</sub> electrodes: schematic view of the device structure. (Reprinted from ref 94, Copyright 1998, with permission from Elsevier.)

sensing characteristics illustrate that the EMF varied almost logarithmically with the concentration of H<sub>2</sub> in the range of 20–200 ppm. Furthermore, the authors operated the chip-type device at 600 °C for approximately 400 h and the EMF was relatively stable during the test period. Due to favorable sensing characteristics, the YSZ-based device has the potential to be used as a H<sub>2</sub> sensor that can operate in high-temperature combustion exhaust without the requirement for a reference gas.

### 6.5.3. Role of Sensing Electrodes in High-Temperature H<sub>2</sub> Sensors

Typical examples of high-temperature potentiometric solid electrolyte H<sub>2</sub> sensors that use YSZ solid electrolytes are summarized in Table 6. Various combinations of solid electrolytes and electrodes have been tested for H<sub>2</sub> sensing. Certainly one key to the search for improved performance is the choice of the sensing electrode material.

Noble metals (Pt, Pd, Au, etc.) were first used as sensing electrode (SE) materials.<sup>233,235,236</sup> While the response of a Pt electrode was found to be stable at both 600 and 550 °C, the Au electrode had stability problems at 600 °C due to the changing morphology of the gold film,<sup>169</sup> and in general, the noble metal Pt was more acceptable as a sensing electrode for the mixed-potential type H<sub>2</sub> gas sensors.<sup>187</sup> The rapid recrystallization rate of gold electrodes at elevated temperatures has made Au electrodes unstable in high-temperature long-term operation. Unfortunately, sensors using the Pt electrodes exhibited small EMF responses to target gases at operating temperatures above ca. 500 °C and gave poor gas selectivity at lower temperature below ca. 400 °C unless covered with an additional catalyst layer. In order to get over these difficulties, a search for sensing electrode materials was carried out to include other noble metals and noble alloys. However, other metals often do not have the required

**Table 6. Examples of High-Temperature Potentiometric Solid Electrolyte H<sub>2</sub> Sensors**

target gas	sensor structure		operation	gas temp	ref
	(RE)	(SE)			
H <sub>2</sub>	Pt/YSZ/	Au-Pt-(H <sub>2</sub> +air)	550 °C	0–10 000 ppm	87
H <sub>2</sub>	Pt/YSZ/	ZnO-Pt-(H <sub>2</sub> +air)	400–600 °C	50–500 ppm	93
H <sub>2</sub>	Pt/YSZ/	Pt(CuO–ZnO/Al <sub>2</sub> O <sub>3</sub> )-(H <sub>2</sub> +air)	420 °C	0–1400 ppm	165
H <sub>2</sub>	Pt/YSZ/	Pt-(H <sub>2</sub> +air)	550 °C	0.05–1%	166
H <sub>2</sub>	Na <sub>x</sub> WO <sub>3</sub> /YSZ/	Pt-(H <sub>2</sub> –air)			232
H <sub>2</sub>	Au-LaMnO <sub>3</sub> /YSZ/	Tb-YSZ-Au-(H <sub>2</sub> –air)	600 °C	20–1000 ppm	188
H <sub>2</sub>	Pt/YSZ/	Au-(H <sub>2</sub> –air)	<500 °C		233
H <sub>2</sub>	Ag/YSZ/	ITO-(H <sub>2</sub> +N <sub>2</sub> )	460 °C	50–2000 ppm	95
H <sub>2</sub>	LaMO <sub>3</sub> /YSZ/	(Pt–Al <sub>2</sub> O <sub>3</sub> )-(H <sub>2</sub> –air)	400–500 °C	2000 ppm	234

<sup>a</sup> YSZ, yttria stabilized zirconia; RE, reference electrode; SE, sensing electrode.

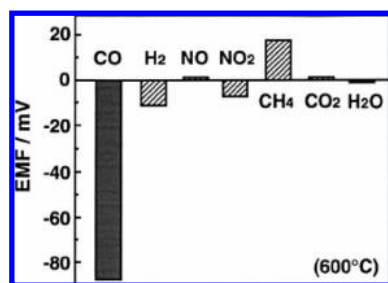


**Figure 38.** Cross-sensitivities to various gases at 600 °C for the tubular YSZ-based device using CdO and SnO<sub>2</sub> electrodes. (Gas concentration CO, H<sub>2</sub>, NO, NO<sub>2</sub>, CH<sub>4</sub>; 200 ppm each, CO<sub>2</sub>; 10000 ppm, H<sub>2</sub>O; 1.5 kPa). (Reprinted from ref 94, Copyright 1998, with permission from Elsevier.)

activity; for example, a Ni-sensing electrode was considerably less sensitive to hydrogen.<sup>76</sup>

Sensors using Pt-based alloy electrodes can provide higher EMF responses to H<sub>2</sub> at temperatures of about 550 °C.<sup>87</sup> Among the Pt-based alloys investigated, a Pt–Au alloy electrode had the highest response to H<sub>2</sub>. The increased gas sensitivities of the sensors with alloy electrodes were considered to be due to a reduction in the catalytic activity for the gas phase oxidation of H<sub>2</sub> by alloying Pt with Au, Ag, Cu, Ni, and Rh. Tests of a non-Nernstian type zirconia sensor with a Pt–Au sensing electrode<sup>88</sup> also established improved selectivity for CO against H<sub>2</sub>.

Using metal oxides for electrode modification provided improved results for H<sub>2</sub> sensing.<sup>165</sup> The use of refractory oxide electrodes for metal electrodes offers promise in improving both the selectivity and the long-term stability of hydrogen sensors.<sup>93,94,231</sup> YSZ-based sensors with metal oxide electrodes such as SnO<sub>2</sub> or CdO can be operated at the rather high temperatures of 485–700 °C, and certain formulations can give relatively good sensing performances for HC's or H<sub>2</sub>, even under rather severe operating conditions.<sup>237</sup>

ITO, SnO<sub>2</sub>, and CdO were used also by Miura et al.<sup>94</sup> and Martin et al.<sup>95</sup> as sensing electrodes in devices configured as shown in Figure 37. Some results from these sensors (CdO/YSZ/SnO<sub>2</sub>) are summarized in Figure 38.

Although results have shown that the SnO<sub>2</sub> and CdO metal oxides can be used in the sensor system CdO/YSZ/SnO<sub>2</sub> for H<sub>2</sub> detection, this approach was even more effective for the design of a CO sensor. The response of CdO/YSZ/SnO<sub>2</sub>-based sensors to H<sub>2</sub> (Figure 38) is considerably smaller than the response to CO. Conversely, the results illustrate that it is possible to detect CO sensitively and selectively in the presence of H<sub>2</sub>, which is also an important problem. It is scientifically interesting that devices with single oxide electrodes (SnO<sub>2</sub>/YSZ/SnO<sub>2</sub> or CdO/YSZ/CdO) have a sensitivity to CO that is almost always smaller than the

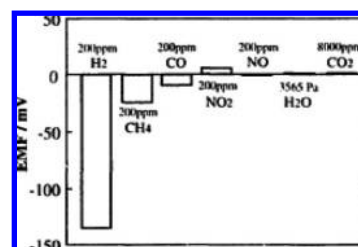


**Figure 39.** Sensitivities of the ZnO-electrode device to various gases at 600 °C. (Reprinted from ref 93, Copyright 1996, with permission from Elsevier.)

**Table 7. EMF Response to H<sub>2</sub> and CO at 600 °C for the YSZ-Electrolyte Device Using Various Oxides (Data Extracted from Refs 61 and 94)**

oxides	EMF (mV)	
	200 ppm H <sub>2</sub>	200 ppm CO
AuO	–136	–9
ZnO	–125	–44
CdO	–104	–126
SnO <sub>2</sub>	–95	–50
In <sub>2</sub> O <sub>3</sub>	–70	–47
Sb <sub>2</sub> O <sub>3</sub>	–15	–7
WO <sub>3</sub>	–7	0
TiO <sub>2</sub>	–7	0
MoO <sub>3</sub>	–5	–1
Fe <sub>2</sub> O <sub>3</sub>	–4	–2
Pt (only)	–3	–1
CuO	–1	0
Mn <sub>2</sub> O <sub>3</sub>	0	0
Co <sub>3</sub> O <sub>4</sub>	0	0
Cr <sub>2</sub> O <sub>3</sub>	0	0
NiO	0	0
PbO <sub>2</sub>	0	0

sensitivity to H<sub>2</sub>. Also, for the same devices, the EMF signal was less than that when noble metals are used as electrodes. Simultaneous sensitivity to CO and H<sub>2</sub> provides interesting responses, but not a selective H<sub>2</sub> sensor. Using ITO with a thickness of 2–13 μm as the sensing electrode succeeded in decreasing the RH influence on the operating characteristics of sensor devices.<sup>91</sup> The thicker ITO electrodes resulted in a smaller response due to the increased rates of hydrogen/oxygen recombination, which dilutes the effective H<sub>2</sub> concentration reaching the sensing region of the electrode.

Detailed studies of the metal oxide influence on YSZ H<sub>2</sub> sensors' analytical characteristics were conducted.<sup>93</sup> In Table 7, the EMF response is shown to be clearly dependent on the oxides used. The maximum H<sub>2</sub> response was obtained with ZnO electrodes, and similar examinations were carried out for the response to CO (also see Table 7). The response to CO was visible with ZnO, In<sub>2</sub>O<sub>3</sub>, and SnO<sub>2</sub>, but it was much smaller than the response to H<sub>2</sub>. The EMF was linear

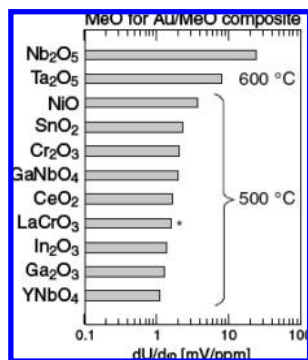


**Figure 40.** Hydrogen sensitivity of YSZ-based devices with composite electrodes (Au/20 mass % MeO) at  $\varphi(\text{H}_2) = 10$  ppmv,  $\varphi(\text{O}_2) = 1.5$  vol %. The REs were prepared from commercially available Pt-paste.<sup>238</sup> (Reprinted from ref 229, Copyright 2006, with permission from Elsevier.)

with the logarithm of the  $\text{H}_2$  concentration in the range of 50–500 ppm at each temperature.

The oxide electrode sensors exhibited an excellent selectivity to  $\text{H}_2$  in the presence of  $\text{NO}$ ,  $\text{NO}_2$ ,  $\text{CH}_4$ ,  $\text{CO}_2$ , and  $\text{H}_2\text{O}$ , as well as good stability during 450 h of testing at 600 °C (Figure 39). In the device with a Pt-sensing electrode, for comparison, the EMF response was not observed above 500 °C. Among the various oxides tested for the sensing electrodes, the EMF response to a fixed concentration of  $\text{H}_2$  (200 ppm in air) at fixed temperature (600 °C) was in the following order:  $\text{ZnO} \gg \text{SnO}_2 > \text{In}_2\text{O}_3 \gg \text{TiO}_2$ , with many transition metal oxides such as  $\text{Fe}_2\text{O}_3$ ,  $\text{Cr}_2\text{O}_3$ ,  $\text{NiO}$ ,  $\text{Mn}_3\text{O}_4$ , and  $\text{Co}_3\text{O}_4$  giving insignificant or no response. These results suggest that semiconducting oxides with modest catalytic activity tend to make the best sensing electrodes.

Composite electrodes, made of Au and metal oxides (MeO), have been studied.<sup>81,96,97</sup> Compared to electrodes made of mixed oxides or perovskites, electrodes made of these composites show elevated sensitivities to a variety of hydrocarbons and  $\text{H}_2$  (Figure 40).

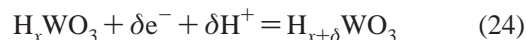
Comparing different materials, the slope ( $dU/d\varphi$ ) of the potential/concentration plot at  $\varphi(\text{H}_2) = 10$  ppmv was calculated by regression. The decreasing catalytic activity of the electrode materials is closely correlated with increasing sensitivity.<sup>238</sup> At 600 °C, the composite materials Au–MeO with  $\text{Nb}_2\text{O}_5$  and  $\text{Ta}_2\text{O}_5$  have the highest sensitivities to  $\text{H}_2$ , and the  $\text{Nb}_2\text{O}_5$  sensor had a sensitivity  $> 20$  mV/ppmv and a potential value (EMF) of 600 mV at 800 ppmv  $\text{H}_2$ . The calibration curve for Au/CeO electrodes exhibits the typical logarithmic behavior of a potentiometric sensor. The Eu– $\text{NbO}_4$ /Au composite electrode had higher sensitivity, but the signal drifts even at constant  $\text{H}_2$ -concentration and the rate of the electrochemical oxidation depends on the time of exposure to hydrogen. This observation is not unique and was also observed at some composite electrodes containing  $\text{TbNbO}_4$ , and it can be due, at least in part, to the elevated  $\text{H}_2$ -solubility in these materials. The perovskite  $\text{LaCr}_{0.8}\text{Ga}_{0.2}\text{O}_{3-\delta}$  provides an example of an electrode material with very low sensitivity to  $\text{H}_2$ , and this is more typical of these composites' analytical characteristics from data reported originally with regard to the detection of hydrocarbons (HCs).<sup>229</sup> In summary, the above-mentioned research has shown that Au– $\text{Nb}_2\text{O}_5$  and Au– $\text{Ta}_2\text{O}_5$  are good candidates for sensing electrodes in  $\text{H}_2$  sensors.

Research aimed at optimization of electrodes for YSZ-based potentiometric gas sensors has produced some unique formulations.<sup>234</sup> The  $\text{LaMnO}_3$ ,  $\text{La}_{0.7}\text{Sr}_{0.3}\text{MnO}_3$ ,  $\text{ZnM}_2\text{O}_4$  (M

= Mn, Co), and  $\text{MnFe}_2\text{O}_4$  electrodes on YSZ had higher sensitivity to CO than to  $\text{H}_2$ . In these studies, only a  $\text{ZnFe}_2\text{O}_4$  formulation had a higher sensitivity to  $\text{H}_2$  than to CO. Analysis of the catalytic activity of these materials revealed that the oxide electrode materials also had a higher catalytic activity for CO oxidation than for  $\text{H}_2$  oxidation. On the other hand,  $\text{ZnFe}_2\text{O}_4$  had higher catalytic activity for  $\text{H}_2$  oxidation than for CO oxidation. This has led to the conclusion that the gas selectivity of YSZ-based potentiometric sensors is a direct reflection of the relative catalytic activity of electrode materials.<sup>234</sup> And this result underscores the importance of the choice of materials for electrodes for sensor development.

Nanotechnology has apparently contributed to the hydrogen sensor stability because the use of nanocomposites of Au– $\text{MeO}_x$  seems to resolve the instability of Au electrodes.<sup>81</sup> For example, electrodes made from Au– $\text{Ga}_2\text{O}_3$ , containing 20 mass %  $\text{Ga}_2\text{O}_3$  nanoparticles, in a potentiometric YSZ sensor, kept working with stability up to 850 °C. These Au– $\text{Ga}_2\text{O}_3$  nanocomposite electrodes were prepared by using thick film technology and were sintered at between 900 and 950 °C.

Considerable success in sensing  $\text{H}_2$  was demonstrated with electrodes of metal(IV) hydrides.<sup>89</sup> If a  $\text{MeH}_x$  is unable to catalyze electrode processes, any possible interference due to the diffusion of gaseous hydrogen from the sensing to the reference compartment is avoided. Therefore, even highly hydrogen-permeable membranes of protonic conductors can be used with these electrode materials as well as very thin films which can significantly lower device electrical resistance and facilitate the design of simple and miniaturized sensors. Noncatalytic metal hydrides with very low hydrogen pressure include  $\text{ZrH}_x$  and  $\text{TiH}_x$  ( $P_{\text{H}_2} \sim 10^{-10}$  and  $10^{-17}$  atm, respectively, at room temperature). In practice, however, research has shown that the  $\text{TiH}_x$  electrode, especially at higher temperature, tends to become covered by a layer of oxide, making it increasingly less reversible. Further, although sufficient for a reference electrode, its exchange current density is only of the order of  $0.3 \mu\text{A}/\text{cm}^2$ .<sup>77</sup> The candidate material for the sensor electrode must have two main characteristics: (a) a viable electron concentration and (b) the capability to reversibly insert protons that come from the electrolyte.<sup>77</sup> Another possible candidate of questionable stability includes tungsten bronze ( $\text{H}_x\text{WO}_3$ ), which is an electron conductor and can exchange protons through the following electrochemical reaction:



Finally, experiments have also shown that the NiO electrode anodically doped with Ni(III) can be used in this capacity, and such electrodes exhibit both reversibility and stability of potential.

#### 6.5.4. Advantages of High-Temperature Solid Electrolyte $\text{H}_2$ Sensors

Specific advantages of high-temperature solid state potentiometric hydrogen sensors can include accuracy, sensitivity, rugged construction, the possibility for miniaturization, and the wide concentration range that can be measured. The use of ceramic solid electrolytes in electrochemical gas sensors at elevated temperatures allows for the detection of  $\text{H}_2$  under harsh conditions, where typical aqueous electrolytes, liquids, or polymeric materials cannot be used. The high operating temperature frequently reduces the RH influence that is bothersome in many sensing applications.



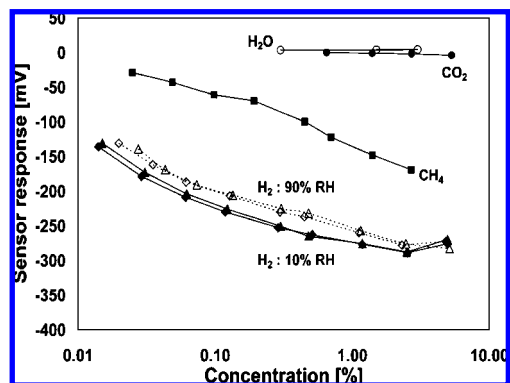


**Figure 41.** Response at 500 °C of an aged sensor with an  $\sim 13$   $\mu\text{m}$  ITO electrode; H<sub>2</sub> in 10% (closed symbols) and  $\sim 90\%$  (open symbols) RH. The two curves at each humidity level represent before (diamonds) and after (triangles) 18 h at 90% relative humidity. Responses to CH<sub>4</sub>, CO<sub>2</sub>, and H<sub>2</sub>O are also shown. (From ref 91. Copyright 2005. Reproduced by permission of The Electrochemical Society.)

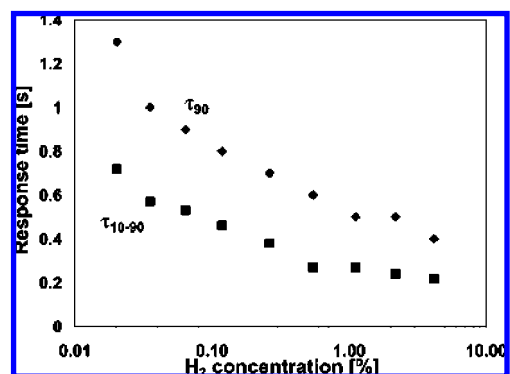


**Figure 42.** Sensor response times as a function of H<sub>2</sub> concentration measured from the baseline to 90% of the full response  $\tau_{(90)}$  and from 10 to 90% of the full response  $\tau_{(10-90)}$ . (From ref 91. Copyright 2005. Reproduced by permission of The Electrochemical Society.)

These advantages can be clearly seen if one considers the performance of potentiometric sensors using the ITO/YSZ/Pt system.<sup>91</sup> In Figure 41, the response to H<sub>2</sub> at 500 °C for a sensor with a 13  $\mu\text{m}$  ITO electrode is shown after aging in air for over 100 h at 500 °C. These measurements were carried out in the atmosphere with 10% (closed symbols) and 90% (open symbols) relative humidity. Each pair of curves represents measurements taken before and after 18 h at 90% relative humidity. These data indicate that the sensor is fairly insensitive to relative humidity in the 10–90% range, with a change in response of  $\leq 10\%$  (decreasing with increasing humidity) and no visible hysteresis on cycling the humidity. In addition, the sensor response is stable and reproducible in this humidity range over the duration of the test.

Figure 41 also illustrates the sensor response to CH<sub>4</sub>, H<sub>2</sub>O, and CO<sub>2</sub> over varying concentration ranges. The reported CO<sub>2</sub> concentrations represent an excess above the ambient air level ( $\sim 1\%$ ). It can be seen that the sensor is not responsive to H<sub>2</sub>O and CO<sub>2</sub> over the ranges tested. In contrast, the sensor responds to CH<sub>4</sub>, although with a smaller response than to H<sub>2</sub>. As a rule, high-temperature sensors have a fast rate of response (see Figure 42). Response times of 2 s<sup>57</sup> or even less than 1 s (at 500 °C) have been observed.<sup>91</sup> Such a response may be acceptable for hydrogen leak sensor applications.<sup>6</sup>

However, it is still not possible to achieve complete selectivity with high-temperature H<sub>2</sub> sensor measurements. Various gases other than H<sub>2</sub> can also be detected (Figure 41) whenever they produce or consume protons through any electrode reaction. Typical examples are CO and NH<sub>3</sub>,<sup>187</sup> and especially various combustible hydrogen-containing gases including hydrocarbons.<sup>91</sup> Research has shown that the easiest way of resolving of this problem is the creation of additional passive filters, preventing penetration of unwanted reacting molecules and yet allowing the fast diffusing and very penetrating hydrogen to access the sensing surface. This would also suggest the use of time dependent thermal, chemical, or electrical properties to sort out the various specific molecular interactions, as can be utilized in sensor arrays.<sup>255</sup> For example, a Pd film has been used as a barrier to prevent chemical attack of the solid electrolyte by aggressive gases but allow hydrogen permeation for sensing.<sup>90</sup> A solid Teflon membrane was used on low-temperature sensors,<sup>60</sup> and certain ceramics and glasses only a few hundred nanometers thick (e.g., SiO<sub>2</sub> or Si<sub>3</sub>N<sub>4</sub>) can also make an effective barrier for gases while allowing hydrogen to pass. While Pd is a most suitable material for a barrier, Pd can change crystal form in H<sub>2</sub> (this effect is reduced by alloys with Ni or Ag) and can also change permeation rate with deposits on its surface. It remains a challenge to engineer a barrier that does not grossly slow the response time (theoretical calculations show a 10 s slower response is expected if a Pd protection cap with a thickness of 0.25 mm is used) but immensely increases the lifetime while retaining the sensitivity and stability of the measurement.

## 6.6. Conductometric Solid Electrolyte H<sub>2</sub> Sensors

Conductometric solid electrolyte H<sub>2</sub> sensors are a class of devices with atmosphere-sensitive conductivity,<sup>172</sup> and in order to be utilized, the materials (solid electrolyte) need to have their stoichiometry (and therefore electrical conductivity) change as a function of gas composition. The conductivity is defined by the transport properties and the impurity levels in oxides, which in turn can be described, to a first approximation, by the defect equilibrium and diffusion rates.<sup>168</sup> The conductivity response to a change in gas composition is important and should be considered as a criterion in the selection of a sensor material. The sensor temperature will affect the time response of conductometric sensors because ions drift faster at higher temperatures and the conductometric sensor responds more rapidly to changes in the H<sub>2</sub> content of the sample gases at elevated temperatures. Therefore, current conductometric sensors are generally equipped with a heater to maintain the solid electrolyte at a constant, controlled, and/or elevated temperature.

Most of the available solid electrolytes can be used for the design of conductometric sensors. However, only a very limited number of solid electrolytes have been evaluated as H<sub>2</sub> sensors,<sup>138,168,172</sup> and most of these are from the family of perovskite materials.<sup>205</sup> Conductometric solid electrolyte-based H<sub>2</sub> sensors typically have a configuration similar to standard semiconductor gas sensors with Pt contacts embedded in the electrolyte.<sup>235,239–241</sup> In contrast to amperometric sensors, the conductometric gas sensor electrodes are designed simply for measurement of the conductivity change taking place in solid electrolytes under hydrogen gas. In this case, an open porosity of the solid electrolyte is advantageous and allows rapid gas interaction with the solid. There are

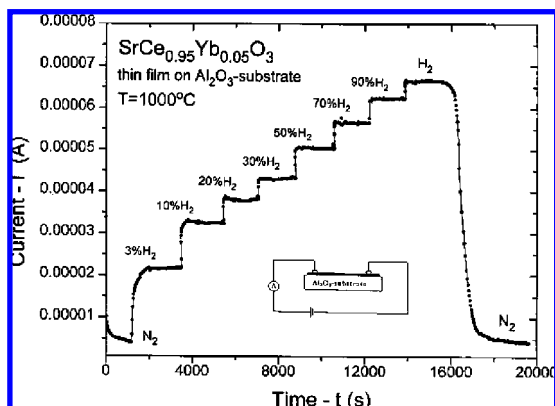


**Figure 43.** The conductance of  $\text{SrCe}_{0.95}\text{Yb}_{0.05}\text{O}_3$  thin films at 1000 °C changes as the ambient changes from  $\text{N}_2$  to  $\text{H}_2$ . (Reprinted with permission from ref 172. Copyright 1998 Elsevier.)

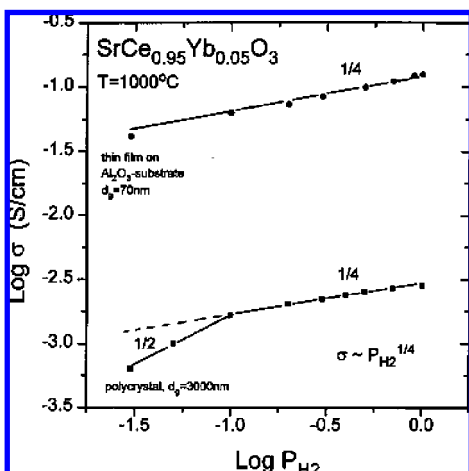


**Figure 44.** Comparison of the electrical conductivity of nano- and microcrystalline  $\text{SrCe}_{0.95}\text{Yb}_{0.05}\text{O}_3$  as a function of hydrogen concentration at 1000 °C. (Reprinted from ref 172, Copyright 1998, with permission from Elsevier.)

several reported constructions of the above-mentioned sensor, and discussion of mechanisms of operation can be found.<sup>235,239–245</sup>

The perovskite solid electrolyte material's conductivity is sensitive to the change in  $\text{H}_2$  gas concentration (Figure 43). The conductivity of  $\text{SrCe}_{0.95}\text{Yb}_{0.05}\text{O}_3$  follows a  $(P_{\text{H}_2})^{1/4}$  or  $(P_{\text{H}_2})^{1/2}$  dependence over the hydrogen activity of  $10^{-2} < P_{\text{H}_2} < 10^0$ . The response characteristics, such as sensitivity and equilibration time, are affected by the microstructure of the films.<sup>172</sup> Measurements show that, for the  $\text{SrCe}_{0.95}\text{Yb}_{0.05}\text{O}_3$  films (Figure 44), the amplitude of the conductivity determined for nanocrystalline films was approximately 2 orders

of magnitude higher than that for microcrystalline materials. The effect is probably related to the fact that the conductivity of nanocrystalline specimens is determined by the grain boundary conduction, where a much higher rate of diffusion exists compared to that of the bulk.<sup>172</sup>

A plot of the temporal response to hydrogen pulses of the material  $\text{SrCe}_{0.95}\text{Yb}_{0.05}\text{O}_3$  as a conductometric sensor is shown in Figure 45 at an elevated temperature. Even at high temperature, the rate of response is relatively slow. There must be a stoichiometric but reversible reaction that is a function of hydrogen concentration to account for this change in conductivity of the solid electrolyte. Both the time of response and time of recovery depend on hydrogen concentration in the gas blend and can exceed 10 min at concentrations  $< 10\%$ . The response time is also not exactly symmetrical, illustrating the fact that the rise and decay are most likely two different chemical reactions with different rates and rate determining steps. Sensors with thick films can have even slower responses,<sup>174</sup> undoubtedly due to slower mass transport in thicker structures. The  $\text{CH}_4$  conductometric sensors designed using a proton conductor, such as  $\text{CaZrO}_3$ ,<sup>246</sup> and CO sensors designed using  $\text{NdCoO}_3$  were also quite slow in response.<sup>247</sup> Slow response is a fundamental property of perovskite type solid electrolytes most likely caused by the relatively low rates for ion diffusion in these materials. In this survey and review, the solid electrolyte conductometric sensors do not have any particular advantage over either classical electrochemical sensors or the typical semiconductor (HMOX chemiresistor) sensors that operate at a considerably lower temperature and typically have a faster response.<sup>239–245</sup> The future of perovskite materials in conductometric sensors seems to be focused not on hydrogen gas sensors but on investigations of sensors for oxygen, alcohol, CO, and hydrocarbons.<sup>204,206,247–250</sup> At the present, it is apparent that the functional mechanism of these sensors is most commonly a surface one rather than a bulk effect.

## 7. Outlook

There are no doubts that an ideal sensor for any widespread application must have both the correct analytical performance and appropriate logistical properties to be successful. However, we have to note that there is no universal sensor and no universal electrochemical sensor, not even for a single simple gas such as hydrogen. As shown in this review, electrochemical  $\text{H}_2$  sensors can be stable, require very little power, and have good signal/noise in many practical applications. In many designs, sensors have linear operating characteristics, practical selectivity, excellent repeatability,

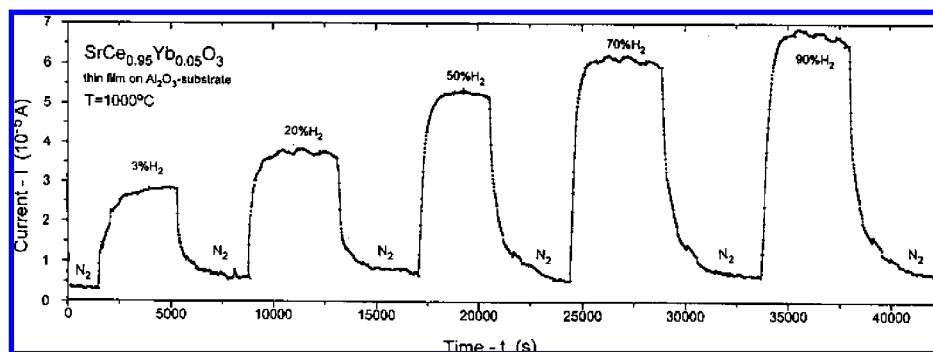


**Figure 45.** The conductance of  $\text{SrCe}_{0.95}\text{Yb}_{0.05}\text{O}_3$  thin film as a function of time after switching gases between  $\text{N}_2$  and  $\text{N}_2\text{-H}_2$  at 1000 °C. (Reprinted from ref 172, Copyright 1998, with permission from Elsevier.)

and accuracy. However, at the same time, like virtually any sensor, electrochemical H<sub>2</sub> sensors are not completely specific. We should define practical selectivity as not causing false positive or negative readings that interfere with the application. For example, if the sensor improves safety by saving lives, property, or time and causes so few false alarms (e.g., 1 in 10,000) and the cost of the false alarms is low compared to life and operational savings, then benefits outweigh any issue caused by the lack of selectivity and the selectivity is sufficient for that application.

Most electrochemical H<sub>2</sub> sensors have a limited temperature range of operation and are sensitive to changes in temperature. Humidity extremes can destabilize most sensors. Sensors can have limited storage life and slow start-up if depolarized. However, the presence of disadvantages does not outweigh the advantages of having low-power, sensitive electrochemical H<sub>2</sub> sensors in many field applications.

There are many creative and innovative solutions to hydrogen monitoring in specific cases that have been provided by electrochemical sensors. Electrochemical sensors compete well with the myriad of optical, electronic, mechanical, and thermal sensing techniques and particularly when the sensitivity must be combined with low cost and low power. In general, electrochemical sensors can be much less expensive than optical, mechanical, or thermal sensors that include spectrometers or complex electronics, and electrochemical sensors can still be amenable to microfabrication batch processes.<sup>251</sup> Unlike catalytic and semiconductor sensors, the electrochemical sensor can often provide a response at room temperature, where the power required is much lower. Electrochemical sensors can often operate in the absence of oxygen on the sensing side whereas the availability of oxygen is essential for pellistor and semiconductor sensors. In applications such as cover gas monitoring in Fast Reactors, where there is no oxygen on the sensing side, the solid–electrolyte proton conductor hydrogen sensor can be used. Thus, one can state that electrochemical hydrogen sensors have and will continue to have an important impact on the market for hydrogen sensors.

Many of the electrochemical H<sub>2</sub> sensors discussed herein have either advantages or shortcomings in one or more applications. Potentiometric sensors have a wide dynamic range but lack accuracy at higher concentrations because of their logarithmic response. Amperometric sensors are usually optimized for hydrogen detection in a considerably more narrow concentration range but have a simple linear response. Ultimately, the choice of the specific sensor will be conditioned by the requirements the application makes of the measuring system.

The many alternatives illustrated herein show the possibilities but have not completely solved all the problems of hydrogen sensors. New electrode materials with greater stability are possible. New electrolytes not yet utilized to any significant extent, such as ionic liquids, need to make a contribution. The structure of the material, i.e. nanostructures, has just begun to emerge as electrodes and electrolytes. The geometry of the sensor and control of each interface is critical, and new MEMS sensors need to emerge for H<sub>2</sub> sensing.<sup>252</sup> Finally, the operating modes for these sensors have not really been explored. Time dependent signals and sensor arrays can solve many of the selectivity problems that are still present in today's hydrogen sensors.

Overall, there is a growing need for hydrogen sensors for safety, security, process control, and medical diagnosis. The

applications will dictate the challenges remaining and put the pressure on sensor developers for improvements. The improvements will evolve through the application of human creativity and the basic knowledge of materials, structure, fabrication, and operation methods illustrated by the scientific and engineering reports cited in this review. The most difficult applications defy all types of sensor technologies, including electrochemical sensors. The issues yet to be solved include sensor stability and durability when operating in severe environments, e.g. environments that exist in places such as gasifiers and combustion processes. But great progress has been made. The results reviewed herein illustrate the insight we have today and provide the fundamental knowledge needed to move forward. This is to say, there are more practical opportunities for monitoring today than ten years ago, and one can envision practical solutions that integrate new materials, structures, and technology over the next ten years to produce ever better electrochemical sensors and sensor systems.

## 8. Acknowledgments

G.K. is thankful to the Korean Brain Pool Program for support of his research. J.S. is thankful for support from SRI International for this work.

## 9. References

- (1) Linden, D., Ed. *Hand-book of Fuel Cell and Batteries*; MacGraw-Hill: 1995.
- (2) Hunter, G. W. *A Survey and Analysis of Experimental Hydrogen Sensors*; NASA Technical Memorandum 106300; 1992.
- (3) Hunter, G. W. *A Survey and Analysis of Commercially Available Hydrogen Sensors*; NASA Technical Memorandum 105878; 1992.
- (4) Hunter, G. W.; Makel, D. B.; Jansa, E. D.; Patterson, G.; Cova, P. J.; Liu, C. C.; Wu, Q. H.; Powers, W. T. *A Hydrogen Leak Detection System for Aerospace and Commercial Applications*; NASA Technical Memorandum 1070363; 1995.
- (5) Weiller, B. H.; Barrie, J. D.; Aitchison, K. A.; Chaffee, P. D. *Mater. Res. Soc. Symp. Proc.* **1995**, *360*, 535.
- (6) Glass, R. S., Milliken, J., Howden, K., Sullivan, R., Eds. *Sensor Needs and Requirements for Proton-Exchange Membrane Fuel Cell Systems and Direct-Injection Engines*; Lawrence Livermore National Laboratory, UCRL-ID-137767, Livermore, CA (2000), p 11.
- (7) Arnason, B.; Sigfusson, T. I. *Int. J. Hydrogen Energy* **2000**, *25*, 389.
- (8) Kordesch, K.; Simader, G. *Fuel Cells and their Applications*; VCH Publishers, Inc., New York, 1996.
- (9) Stetter, J. R.; Maclay, G. J. Carbon Nanotubes and Sensors: A Review. In *Advanced Micro and Nano Systems*, Volume I; Baltes, H., Brand, O., Fedder, G. K., Hierold, C., Korvink, J. O., Tabata, O., Eds.; Wiley-VCH Verlag-GmbH and Co.: Weinheim, Germany, 2004; Chapter 10, p357.
- (10) Pavlenko, V. F. *Gasanalyzers*; Mashinostroenie: Moscow-Leningrad, 1965 (in Russian).
- (11) Brajnikov, V. V. *Detectors for chromatography*; Mashinostroenie: Moscow, 1992 (in Russian).
- (12) Ishihara, T.; Matsubara, S. *J. Electroceram.* **1998**, *2*, 215.
- (13) Aroutiounian, V. *Int. J. Hydrogen Energy* **2007**, *32*, 1145.
- (14) Christofides, C.; Mandelis, A. *J. Appl. Phys.* **1990**, *68*, R1.
- (15) Lundstrom, I.; Sundgren, H.; Winquist, F.; Eriksson, M.; Krantz-Rulcker, C.; Lloyd-Spez, A. *Sens. Actuators, B* **2007**, *121*, 247.
- (16) Ando, M. *TrAC, Trends Anal. Chem.* **2006**, *25*, 937.
- (17) Wilson, D. M.; Hoyt, S.; Janata, J.; Booksh, K.; Obando, L. *IEEE Sensors J.* **2001**, *1*, 256.
- (18) Janata, J.; Josowicz, M.; Vanysek, P.; DeVaney, D. M. *Anal. Chem.* **1998**, *70*, 179R.
- (19) Brett, C. M. A. *Pure Appl. Chem.* **2001**, *73*, 1969.
- (20) Limoges, B.; Degrand, C.; Brossier, P. *J. Electroanal. Chem.* **1996**, *402*, 175.
- (21) Shi, M.; Anson, F. C. *J. Electroanal. Chem.* **1996**, *415*, 41.
- (22) www.transducertech.com website, note 5 year lifetime graph of room temperature lab use of an aqueous electrochemical sensors for CO.
- (23) (a) Stetter, J. R.; Blurton, K. F. *Rev. Sci. Instrum.* **1976**, *47*, 691. (b) Stetter, J. R.; Blurton, K. F. *Ind. Eng. Chem.: Product R&D* **1977**, *16*, 22. (c) Vaihinger, S.; Goepel, W.; Stetter, J. R. *Sens. Actuators*,



- B* 1991, 4, 337–43. (d) Chang, S. C.; Stetter, J. R.; Cha, C. S. *Talanta* 1993, 40, 461. (e) Stetter, J. R.; Li, J. *Chem. Rev.* 2008, 108, 352.
- (24) Janata, J. *Principles of Chemical Sensors*; Plenum Press: New York, 1989.
- (25) Mari, C. M.; Terzaghi, G.; Bertolini, M.; Barbi, G. B. *Sens. Actuators, B* 1992, 8, 41.
- (26) Weppner, W. *Sens. Actuators* 1987, 12, 107.
- (27) Knake, R.; Jacquinet, P.; Hodgson, A. W. E.; Hauser, P. C. *Anal. Chim. Acta* 2005, 549, 1.
- (28) Cao, Z.; Buttner, W. J.; Stetter, J. R. *Electroanalysis* 1992, 4, 253.
- (29) Bontempelli, G.; Comisso, N.; Toniolo, R.; Schiavon, G. *Electroanalysis* 1997, 9, 433.
- (30) Alber, K. S.; Cox, J. A.; Kulesza, P. J. *Electroanalysis* 1997, 9, 97.
- (31) Opekar, F.; Stulik, K. *Anal. Chim. Acta* 1999, 385, 151.
- (32) Opekar, F.; Stulik, K. *Crit. Rev. Anal. Chem.* 2002, 32, 253.
- (33) Yamazoe, N.; Miura, N. *J. Electroceramics* 1998, 2, 243.
- (34) Bobacka, J.; Ivaska, A.; Lewenstam, A. *Chem. Rev.* 2008, 108, 329.
- (35) Bakker, E.; Buhlmann, P.; Pretsch, E. *Chem. Rev.* 1997, 97, 3083.
- (36) Buhlmann, P.; Pretsch, E.; Bakker, E. *Chem. Rev.* 1998, 98, 1593.
- (37) Reinhardt, G.; Mayer, R.; Rosch, M. *Solid State Ionics* 2002, 150, 79.
- (38) Hodgson, A. W. E.; Jacquinet, P.; Jordan, L. R.; Hauser, P. C. *Electroanalysis* 1999, 11, 782.
- (39) Holzinger, M.; Maier, J.; Sitte, W. *Solid State Ionics* 1997, 94, 217.
- (40) Kulesza, P. J.; Cox, J. A. *Electroanalysis* 1998, 10, 73.
- (41) Ishihara, T.; Fukuyama, M.; Dutta, A.; Kabemura, K.; Nishiguchi, H.; Takita, Y. *J. Electrochem. Soc.* 2003, 150, H241.
- (42) Cao, Z.; Stetter, J. R. In *Opportunities for Innovation: Chemical and Biological Sensors*; Madou, M., Joseph, J. P., Eds.; U.S. Department of Commerce: 1991.
- (43) Lu, X.; Wu, S.; Wang, L.; Su, Z. *Sens. Actuators, B* 2005, 107, 812.
- (44) Sakthivel, M.; Weppner, W. *Sens. Actuators, B* 2006, 113, 998.
- (45) Nikolova, V.; Nikolov, I.; Andreev, P.; Najdenov, V.; Vitanov, T. *J. Appl. Electrochem.* 2000, 30, 705.
- (46) Barsan, N.; Stetter, J. R.; Findlay, M.; Göpel, W. *Anal. Chem.* 1999, 71, 2512.
- (47) Ramesh, C.; Velayutham, G.; Murugesan, N.; Ganesan, V.; Dhathathreyan, K. S.; Periaswami, G. *J. Solid State Electrochem.* 2003, 8, 511.
- (48) Sakthivel, M.; Weppner, W. *J. Solid State Electrochem.* 2007, 11, 561.
- (49) Blurton, K. F.; Stetter, J. R. *J. Chromatogr.* 1978, 155, 35.
- (50) Stetter, J. R.; Sedlak, J. M.; Blurton, K. F. *J. Chromatogr. Sci.* 1977, 15, 125.
- (51) Ollison, W. M.; Penrose, W. M.; Stetter, J. R. *Anal. Chim. Acta* 1995, 313, 209.
- (52) Sakthivel, M.; Weppner, W. *Sensors* 2006, 6, 284.
- (53) Stetter, J. R. *Proc. Electrochem. Soc.* 1993, 93, 193.
- (54) Sundmacher, K.; Rihko-Struckmann, L. K.; Galvita, V. *Catal. Today* 2005, 104, 185.
- (55) Bakker, E.; Pretsch, E. *TrAC, Trends Anal. Chem.* 2005, 24, 199.
- (56) Pretsch, E. *TrAC, Trends Anal. Chem.* 2007, 26, 46.
- (57) Okamura, K.; Ishiji, T.; Iwaki, M.; Suzuki, Y.; Takahashi, K. *Surf. Coat. Technol.* 2007, 201, 8116.
- (58) Liu, Y.-C.; Hwang, B.-J.; Chen, Y.-L. *Electroanalysis* 2002, 14, 556.
- (59) Lizcano-Valbuena, W. H.; Perez, J.; Paganin, V. A.; Gonzalez, E. R. *Ecl. Quím., Sao Paulo* 2005, 30, 74.
- (60) Chao, Y.; Buttner, W. J.; Yao, S.; Stetter, J. R. *Sens. Actuators, B* 2005, 106, 784.
- (61) Sakthivel, M.; Weppner, W. *Int. J. Hydrogen Energy* 2008, 33, 905.
- (62) Ramesh, C.; Murugesan, N.; Krishnaiah, M. V.; Ganesan, V.; Periaswami, G. *J. Solid State Electrochem.* (Published online: 13 November 2007).
- (63) Opekar, F.; Langmaier, J.; Samec, Z. *J. Electroanal. Chem.* 1994, 379, 301.
- (64) Samec, Z.; Opekar, F.; Crijns, G. J. E. F. *Electroanalysis* 1995, 7, 1054.
- (65) Opekar, F. *J. Electroanal. Chem.* 1989, 260, 451.
- (66) Bouchet, R.; Rosini, S.; Vitter, G.; Siebert, E. *Sens. Actuators, B* 2001, 76, 610.
- (67) Bonanos, N. *Solid State Ionics* 2001, 145, 265 Bonanos.
- (68) Hitchman, M. L. *Measurements of Dissolved Oxygen*; Wiley: 1978.
- (69) Mosley, P. T.; Norris, J.; Williams, D. E., Eds. *Techniques and Mechanisms in Gas Sensing*; Adam Hilger: New York, 1991.
- (70) Vielstich, W.; Lamm, A.; Gasteiger, H. A., Eds. *Handbook of Fuel Cell—Fundamentals, technology and Applications*, Vol. 2, Part 3; John Wiley: Chichester, 2003.
- (71) Bay, H. W.; Blurton, K. F.; Lieb, H. C.; Oswin, H. G. *Int. Lab.* 1972, 1, 37.
- (72) La Conti, A. B.; Maget, H. J. R. *J. Electrochem. Soc.* 1971, 118, 506.
- (73) Paganin, V. A.; Ticianelli, E. A.; Gonzalez, E. R. *J. Appl. Electrochem.* 1996, 26, 297.
- (74) Rosini, S.; Siebert, E. *Electrochim. Acta* 2005, 50, 2943.
- (75) Ren, X.; Wilson, M. S.; Gottesfeld, S. *J. Electrochem. Soc.* 1996, 143, L12.
- (76) Ponomareva, V. G.; Lavrova, G. V.; Hairetdinov, E. F. *Sens. Actuators, B* 1997, 40, 95.
- (77) Alberti, G.; Palombari, R.; Pierri, F. *Solid State Ionics* 1997, 97, 359.
- (78) Treglaziov, I.; Leonova, L.; Dobrovolsky, Y.; Ryabov, A.; Vakulenko, A.; Vassiliev, S. *Sens. Actuators, B* 2005, 106, 164.
- (79) Maffei, N.; Kuriakose, A. K. *Sens. Actuators, B* 2004, 98, 73.
- (80) Zosel, J.; Schiffel, G.; Gerlach, F.; Ahlborn, K.; Sasum, U.; Vashook, V.; Guth, U. *Solid State Ionics* 2006, 177, 2301.
- (81) Westphal, D.; Jakobs, S.; Guth, U. *Ionics* 2001, 7, 182.
- (82) Miura, N.; Yamazoe, N. *Solid State Ionics* 1992, 53–56, 975.
- (83) Katahira, K.; Matsumoto, H.; Iwahara, H.; Koide, K.; Iwamoto, T. *Sens. Actuators, B* 2001, 73, 130.
- (84) Sakthivel, M.; Weppner, W. *Sens. Actuators, B* 2007, 125, 435.
- (85) Chehab, S. F.; Canaday, J. D.; Kuriakose, A. K.; Wheat, T. A.; Ahmad, A. *Solid State Ionics* 1991, 45, 299.
- (86) Tomita, A.; Namekata, Y.; Nagao, M.; Hibino, T. *J. Electrochem. Soc.* 2007, 154, J172.
- (87) Vogel, A.; Baier, G.; Schule, V. *Sens. Actuators, B* 1993, 15, 147.
- (88) Deublein, G.; Liaw, B. Y.; Robert, A.; Huggins, R. A. *Solid State Ionics* 1988, 28–30, 1660.
- (89) Alberti, G.; Casciola, M. *Solid State Ionics* 2001, 145, 3.
- (90) Jacobs, A.; Vangrunderbeek, J.; Beckers, H.; De Schumr, F.; Luyten, J.; Van Landschoot, R.; Schoonman, J. *Fuel Process. Technol.* 1993, 36, 251.
- (91) Martin, L. P.; Glass, R. S. *J. Electrochem. Soc.* 2005, 152, H43.
- (92) Colombari, Ph. *Ann. Chim. Sci. Mater.* 1999, 24, 1.
- (93) Lu, G.; Miura, N.; Yamazoe, N. *Sens. Actuators, B* 1996, 35, 130.
- (94) Miura, N.; Raisen, T.; Lu, G.; Yamazoe, N. *Sens. Actuators, B* 1998, 47, 84.
- (95) Martin, L. P.; Pham, A.-Q.; Glass, R. S. *Solid State Ionics* 2004, 175, 527.
- (96) Hibino, T.; Kakimoto, S.; Sano, M. *J. Electrochem. Soc.* 1999, 146, 3361.
- (97) Zosel, J.; Müller, R.; Vashook, V.; Guth, U. *Solid State Ionics* 2004, 175, 531.
- (98) Hamann, C.; Hamnett, A.; Vielstich, W. *Electrochemistry*; Wiley-VCH: Weinheim, 1998.
- (99) Bagotsky, V. S.; Osetrova, N. V. *J. Electroanal. Chem.* 1973, 43, 233.
- (100) Gasteiger, H. A.; Markovic, N. M.; Ross, P. N. *J. Phys. Chem.* 1995, 99, 8290.
- (101) De Mello, R. M. Q.; Ticianelli, E. A. *Electrochim. Acta* 1997, 42, 1031.
- (102) Harrison, J. A.; Khan, Z. A. *J. Electroanal. Chem.* 1971, 30, 327.
- (103) Stonehart, P. *Ber. Bunsen-Ges. Phys. Chem.* 1990, 94, 913.
- (104) Sawyer, D. T.; Seo, E. T. *J. Electroanal. Chem.* 1963, 5, 23.
- (105) Roh, S.; Stetter, J. R. *J. Electrochem. Soc.* 2003, 150, H272.
- (106) Dabill, D. W.; Gentry, S. J.; Holland, H. B.; Jones, A. *J. Catal.* 1978, 53, 164.
- (107) Bui, P. A.; Vlachos, D. C.; Westmoreland, P. R. *Ind. Eng. Chem. Res.* 1997, 36, 2558.
- (108) Park, Y. K.; Aghalayam, P.; Vlachos, D. G. *J. Phys. Chem., A* 1999, 103, 8101.
- (109) McCandless, F. P. *Ind. Eng. Process Des. Dev.* 1972, 11, 470.
- (110) Hartel, G.; Rompf, F.; Puschel, T. *J. Membr. Sci.* 1996, 113, 115.
- (111) De Vos, R. M.; Verweij, H. *Science* 1998, 279, 1710.
- (112) Hartel, G.; Puschel, T. *J. Membr. Sci.* 1999, 162, 1.
- (113) Pages, X.; Rouessac, V.; Cot, D.; Nabias, G.; Durand, J. *Sep. Purif. Technol.* 2001, 25, 399.
- (114) Orme, C. J.; Stone, M. L.; Benson, M. T.; Peterson, E. S. *Sep. Sci. Technol.* 2003, 38, 3225.
- (115) Wesselingh, J. A.; Krishna, R. *Mass Transfer in Multicomponent Mixtures*; Delft University Press: Delft, The Netherlands, 2000; Chapter 21, p 233.
- (116) Yao, S.; Wang, M. *J. Electrochem. Soc.* 2002, 149, H28.
- (117) Ives, D. J. G.; Janz, G. J., Eds. *Reference Electrodes: Theory and Practice*; Academic Press: New York, 1961; Chapter 4, p 179.
- (118) (a) Anderson, G.; Hadden, D. *The Gas Monitoring Handbook*; Avocet Press Inc.: 1999. (b) Chou, J. *Hazardous Gas Monitors: A Practical Guide to Selection, Operation, and Applications*; McGraw-Hill Professional: 1999. (c) Elter, P. M., Cassinelli, M. E., Eds.; *NIOSH Manual of Analytical Methods*, 4th ed.; M.E. U.S. Department of Health and Human Services, Cincinnati, OH, 1994..
- (119) Liu, Y. C.; Hwang, B. J.; Tzeng, I. J. *J. Electrochem. Soc.* 2002, 149, H173.
- (120) (a) Samec, Z.; Opekar, F.; Gjeff, C. *Electroanalysis* 1995, 7, 1054. (b) Opekar, F.; Stulik, K. *Anal. Chim. Acta* 1999, 385, 151.
- (121) Bobacka, J. *Electroanalysis* 2006, 18, 7.
- (122) Zawodzinski, T. A.; Springer, T. E.; Uribe, F.; Gottesfeld, S. *Solid State Ionics* 1993, 60, 199.

- (123) Anantaraman, A. V.; Gardner, C. L. *J. Electroanal. Chem.* **1996**, *414*, 115.
- (124) Opekar, F. *Electroanalysis* **1992**, *4*, 133.
- (125) Yasuda, A.; Doi, K.; Yamaga, N.; Fujioka, T.; Kusanagi, S. *J. Electrochem. Soc.* **1992**, *139*, 3224.
- (126) Yan, H.; Liu, C. *Sens. Actuators, B* **1993**, *10*, 133.
- (127) Bouchet, R.; Siebert, E. *Solid State Ionics* **1999**, *118*, 287.
- (128) Bouchet, R.; Siebert, E.; Vitter, G. *J. Electrochem. Soc.* **2000**, *147*, 3125.
- (129) Bouchet, R.; Rosini, S.; Vitter, G.; Siebert, E. *J. Electrochem. Soc.* **2002**, *149*, H119.
- (130) Ramesh, C.; Velayutham, G.; Murugesan, N.; Ganesan, V.; Manivannan, V.; Periaswami, G. *Ionics* **2004**, *10*, 50.
- (131) Michalska, A. *Anal. Bioanal. Chem.* **2006**, *384*, 391.
- (132) Wroblewski, W.; Dybko, A.; Malinowska, E.; Brzozka, Z. *Talanta* **2004**, *63*, 33.
- (133) Lukow, S. R.; Kounaves, S. P. *Electroanalysis* **2005**, *17*, 1441.
- (134) Josowicz, M. *Analyst* **1995**, *120*, 1019.
- (135) Maksymiuk, K. *Electroanalysis* **2006**, *18*, 1537.
- (136) Maffei, N. A. K.; Kuriakose, A. K. *Sens. Actuators, B* **1999**, *56*, 243.
- (137) Vork, F. T. A.; Janssen, L. J. J.; Barendrecht, E. *Electrochim. Acta* **1986**, *31*, 1569.
- (138) Inaba, T.; Saji, K.; Takahashi, H. *Electrochemistry* **1999**, *67*, 458.
- (139) Ogumi, Z.; Inatomi, K.; Hinatsu, J. T.; Takehara, Z. I. *Electrochim. Acta* **1992**, *37*, 1295.
- (140) Millet, P.; Durand, R.; Dartyge, E.; Tourillon, G.; Fontaine, A. *J. Electrochem. Soc.* **1993**, *140*, 1373.
- (141) Bouchet, R.; Siebert, E.; Vitter, G. *J. Electrochem. Soc.* **2000**, *147*, 3548.
- (142) Park, C. O.; Akbar, S. A.; Weppner, W. *J. Mater. Sci.* **2003**, *38*, 4639.
- (143) Liu, J.; Weppner, W. *Sens. Actuators, B* **1992**, *6*, 270.
- (144) Mika, M.; Paidar, M.; Klapste, B.; Masinova, M.; Bouzek, K.; Vondrak, J. *J. Phys. Chem. Sol.* **2007**, *68*, 775.
- (145) Sondheimer, S. J.; Bunce, N. J.; Fyfe, C. A. *J. Macromol. Sci. Rev. Macromol. Chem. C* **1986**, *26*, 353.
- (146) Opekar, F.; Svozil, D. *J. Electroanal. Chem.* **1995**, *385*, 269.
- (147) Bay, H. W.; Blurton, K. F.; Lieb, H. C.; Oswin, H. G. *Nature* **1972**, *240*, 52.
- (148) Hoare, J. P. *The Electrochemistry of Oxygen*; Wiley: New York, 1968.
- (149) Hrnčirova, P.; Opekar, F. *Sens. Actuators, B* **2002**, *81*, 329.
- (150) Miura, N.; Harada, T.; Yamazoe, N. *J. Electrochem. Soc.* **1989**, *136*, 1215.
- (151) *Proton conductors: Solid membranes and gels-materials and devices*; Colombari, Ph., Ed.; Cambridge, London, 1992.
- (152) Kleperis, J.; Bayars, G.; Vaivars, G.; Kranevskis, A.; Lūsis, A. *Sov. Electrochem.* **1992**, *28*, 1181.
- (153) Kumar, R. V.; Fray, D. J. *Sens. Actuators* **1988**, *15*, 185.
- (154) Ukshe, E.; Leonova, L. *Sov. Electrochem.* **1992**, *28*, 1166.
- (155) Zhuykov, S. *Int. J. Hydrogen Energy* **1996**, *21*, 749.
- (156) Miura, N.; Yamazoe, N. In *Chemistry of Solid State Materials 2: Proton Conductors*; Colombari, P., Ed.; Cambridge University Press: Cambridge, 1992; p 527.
- (157) Velasco, G.; Schneli, J. Ph.; Croset, M. *Sens. Actuators* **1982**, *2*, 371.
- (158) Miura, N.; Kato, H.; Yamazoe, N.; Seiyama, T. In *Proceedings of International Meeting of Chemical Sensors*, Fukuoka, Japan; Kodansha/Elsevier: Tokyo/Amsterdam, 1983, p 233.
- (159) Miura, N.; Harada, T.; Shimizu, Y.; Yamazoe, N. *Sens. Actuators, B* **1990**, *1*, 125.
- (160) Alberti, G.; Palombari, R. *Solid State Ionics* **1989**, *35*, 153.
- (161) Alberti, G.; Carbone, A.; Palombari, R. *Sens. Actuators, B* **2001**, *75*, 125.
- (162) Dobrovolsky, Yu.; Leonova, L.; Vakulenko, *Solid State Ionics* **1996**, *86–88*, 1017.
- (163) Nogami, M.; Matsumura, M. *Daiko, Sens. Actuators, B* **2006**, *120*, 266.
- (164) Mellander, B.-E.; Zhu, B. *Solid State Ionics* **1993**, *61*, 105.
- (165) Tan, Y.; Tan, T. C. *J. Electrochem. Soc.* **1994**, *141*, 461.
- (166) Shimizu, F.; Yamazoe, N. T.; Seiyama, T. *Chem. Lett.* **1978**, *7*, 299.
- (167) Hashimoto, A.; Hibino, T.; Mori, K.; Sano, M. *Sens. Actuators, B* **2001**, *81*, 55.
- (168) Kurita, N.; Fukatsu, N.; Ohashi, T. *J. Jpn. Inst. Met.* **1994**, *58*, 782.
- (169) Mukundan, R.; Brosha, E. L.; Brown, D. R.; Garzon, F. G. *J. Electrochem. Soc.* **2000**, *147*, 1583.
- (170) Matsumoto, H.; Suzuki, T.; Iwahara, H. *Solid State Ionics* **1999**, *116*, 99.
- (171) Nishimura, R.; Toba, K.; Yamakawa, K. *Corros. Sci.* **1996**, *38*, 611.
- (172) Kosacki, I.; Anderson, H. U. *Sens. Actuators, B* **1998**, *48*, 263.
- (173) Katohira, K.; Matsumoto, H.; Iwahara, H.; Koide, K.; Iwamoto, T. *Sens. Actuators, B* **2000**, *67*, 189.
- (174) Kosacki, I.; Anderson, H. U. *Solid State Ionics* **1997**, *97*, 429.
- (175) De Schutter, F.; Vangrunderbeek, J.; Luyten, J.; Kosacki, I.; Van Landschoot, R.; Schram, J.; Schoonman, J. *Solid State Ionics* **1992**, *57*, 77.
- (176) Yajima, T.; Koide, K.; Takai, H.; Fukatsu, N.; Iwahara, H. *Solid State Ionics* **1995**, *79*, 333.
- (177) Yajima, T.; Iwahara, H.; Koide, K.; Yamamoto, K. *Sens. Actuators, B* **1991**, *5*, 145.
- (178) Yajima, T.; Koide, K.; Fukatsu, N.; Ohashi, T.; Iwahara, H. *Sens. Actuators, B* **1993**, *13–14*, 697.
- (179) Iwahara, H.; Uchida, H.; Ogaki, K.; Nagato, H. *J. Electrochem. Soc.* **1991**, *138*, 295.
- (180) Bonanos, N.; Ellis, B.; Mahmood, M. N. *Solid State Ionics* **1991**, *44*, 305.
- (181) Taniguchi, N.; Gamo, T. *Denki Kagaku ovobi Kogyo Butsuri Kagaku* **1994**, *62*, 326.
- (182) Lander, J. J. *J. Am. Chem. Soc.* **1951**, *73*, 5794.
- (183) Iwahara, H. In *Proton Conductors*; Colombari, Ph., Ed.; Cambridge University Press: 1992; Chapter 34.
- (184) Taniguchi, N.; Kuroha, T.; Nishimura, C.; Iijima, K. *Solid State Ionics* **2005**, *176*, 2979.
- (185) Du, Y.; Nowick, A. S. *Solid State Ionics* **1996**, *91*, 85.
- (186) Wang, W.; Virkar, A. V. *J. Power Sources* **2005**, *142*, 1.
- (187) Miura, N.; Lu, G.; Yamazoe, N. *Solid State Ionics* **2000**, *136–137*, 533.
- (188) Brosha, E. L.; Mukundan, R.; Brown, R. D.; Garzon, F. H. *Sens. Actuators, B* **2002**, *87*, 47.
- (189) Daiko, Y.; Kasuga, T.; Nogami, M. *J. Sol–Gel Sci. Technol.* **2003**, *26*, 1041.
- (190) Kriksunov, L. B.; Macdonald, D. D. *Sens. Actuators, B* **1996**, *32*, 57.
- (191) Ding, K. *Geochim. Cosmochim. Acta* **1995**, *59*, 4769.
- (192) Fukatsu, N.; Kurita, N. *Ionics* **2005**, *11*, 54.
- (193) Zheng, M.; Zhen, X. *Metall. Mater. Trans., B* **1993**, *24*, 789.
- (194) Miura, N.; Kato, H.; Ozawa, Y.; Yamazoe, N.; Seiyama, T. *Chem. Lett.* **1984**, *11*, 1905.
- (195) Lu, G.; Miura, N.; Yamazoe, N. *J. Electrochem. Soc.* **1996**, *143*, L154.
- (196) Deniard-Courant, S.; Piffard, Y.; Barboux, P.; Livage, J. *Solid State Ionics* **1988**, *27*, 189.
- (197) Nowick, A. S.; Du, Y.; Liang, K. C. *Solid State Ionics* **1999**, *125*, 303.
- (198) Thangadurai, V.; Weppner, W. *J. Mater. Chem.* **2001**, *11*, 636.
- (199) Schaak, R. E.; Mallouk, T. E. *J. Solid State Chem.* **2000**, *155*, 46.
- (200) Toda, K.; Kameo, Y.; Kurita, S.; Sato, M. *J. Alloys Compd.* **1996**, *234*, 19.
- (201) Thangadurai, V.; Weppner, W. *Ionics* **2001**, *7*, 22.
- (202) Schober, T. *Solid State Ionics* **2003**, *162–163*, 277.
- (203) Iwahara, H. *Solid State Ionics* **1995**, *77*, 289.
- (204) Post, M. L.; Tunney, J. J.; Yang, D.; Du, X.; Singleton, D. L. *Sens. Actuators, B* **1999**, *59*, 190.
- (205) Tejuca, L. J.; Fierro, J. L. G., Eds. *Properties and Applications of Perovskite-Type Oxides*; Marcel Dekker: New York, 1993.
- (206) Fergus, J. W. *Sens. Actuators, B* **2007**, *123*, 1169.
- (207) Iwahara, H.; Yajima, T.; Hibino, T.; Ozaki, K. *Solid State Ionics* **1993**, *61*, 65.
- (208) Norby, T. *Nature* **2001**, *410*, 877.
- (209) Zheng, M.; Chen, X. *Solid State Ionics* **1994**, *70*, 595.
- (210) Wakamura, K. *J. Phys. Chem. Solids* **2005**, *66*, 133.
- (211) Fukatsu, N.; Kurita, N.; Koide, K.; Ohashi, T. *Solid State Ionics* **1998**, *113–115*, 219.
- (212) Tanner, C. W.; Virkar, A. V. *J. Electrochem. Soc.* **1996**, *143*, 1386.
- (213) Scholten, M. J.; Schoonman, J.; Van Miltenburg, J. C.; Oonk, H. A. J. *Solid State Ionics* **1993**, *61*, 83.
- (214) Yajima, T.; Iwahara, H.; Uchida, H.; Koide, K. *Solid State Ionics* **1990**, *40/41*, 914.
- (215) Kreuer, K. D. *Solid State Ionics* **1999**, *125*, 285.
- (216) Kreuer, K. D. *Annu. Rev. Mater. Res.* **2003**, *33*, 333.
- (217) Luyten, J.; De Schutter, F.; Schram, J.; Schoonman, J. *Solid State Ionics* **1991**, *46*, 117.
- (218) Liang, K. C.; Nowick, A. S. *Solid State Ionics* **1993**, *61*, 77.
- (219) Liang, K. C.; Du, Y.; Nowick, A. S. *Solid State Ionics* **1994**, *69*, 117.
- (220) Du, Y.; Nowick, A. S. In *Solid State Ionics IV*; Nazri, G.-A., Tarascon, J.-M., Schreiber, M., Eds.; MRS Symp. Proc.; 1995; Vol. 369, p 289.
- (221) Lecomte, J.; Loup, J. P.; Bossert, G.; Hervieu, M.; Raveau, B. *Solid State Ionics* **1984**, *12*, 113.
- (222) Fleming, W. J. *J. Electrochem. Soc.* **1977**, *124*, 21.
- (223) Okamoto, H.; Obayashi, H.; Kudo, T. *Solid State Ionics* **1980**, *1*, 319.
- (224) Okamoto, H.; Obayashi, H.; Kudo, T. *Solid State Ionics* **1981**, *3–4*, 453.
- (225) Okamoto, H.; Kawamura, G.; Kudo, T. *J. Catal.* **1984**, *87*, 1.

- (226) Li, N.; Tan, T. C.; Zeng, H. C. *J. Electrochem. Soc.* **1993**, *140*, 1068.
- (227) Can, Z. Y.; Narita, H.; Mizusaki, J.; Tagawa, H. *Solid State Ionics* **1995**, *79*, 344.
- (228) Mukundan, R.; Brosha, E. L.; Garzon, F. H. *J. Electrochem. Soc.* **2003**, *150*, H279.
- (229) Zosel, J.; Schiffel, G.; Gerlach, F.; Ahlborn, K.; Sasum, U.; Vashook, V.; Guth, U. *Solid State Ionics* **2006**, *177*, 2301.
- (230) Garzon, F. H.; Mukundan, R.; Brosha, E. L. *Solid State Ionics* **2000**, *136–137*, 633.
- (231) Miura, N.; Lu, G.; Yamazoe, N.; Kurosawa, H.; Hasei, M. *J. Electrochem. Soc.* **1996**, *143*, L33.
- (232) Chu, W. F.; Leonhard, V.; Erdmann, H.; Ilgenstein, M. *Sens. Actuators, B* **1991**, *4*, 321.
- (233) Mukundan, R.; Brosha, E. L. D.; Brown, D.; Garzon, F. *Electrochem. Soc. Lett.* **1999**, *2*, 412.
- (234) Sorita, R.; Kawano, T. *Sens. Actuators, B* **1996**, *35–36*, 274.
- (235) Moseley, P. T.; Tofield, B. C., Eds. *Solid State Gas Sensors*; Adam Hilger: Bristol, 1987.
- (236) Hibino, T.; Kuwahara, Y.; Wang, S.; Kakimoto, S.; Sano, M. *Electrochem. Soc. Lett.* **1998**, *1*, 197.
- (237) Nakatou, M.; Miura, N. *Solid State Ionics* **2005**, *176*, 2511.
- (238) Zosel, J.; Westphal, D.; Jakobs, S.; Müller, R.; Guth, U. *Solid State Ionics* **2002**, *152–153*, 525.
- (239) Williams, D. E. *Sens. Actuators, B* **1999**, *57*, 1.
- (240) *Chemical Sensor Technology*; Yamazoe, N., Ed.; Elsevier: Amsterdam, 1991; Vol. 3.
- (241) Korotcenkov, G. *Sens. Actuators, B* **2007**, *121*, 664.
- (242) Barsan, N.; Weimar, U. *J. Electroceram.* **2001**, *7*, 143.
- (243) Korotcenkov, G. *Mater. Sci. Eng., R* **2008**, *61*, 1.
- (244) Korotcenkov, G. *Mater. Sci. Eng., B* **2007**, *139*, 1.
- (245) Korotcenkov, G. *Sens. Actuators, B* **2005**, *107*, 209.
- (246) Suzuki, Y.; Awano, M.; Kondo, N.; Ohji, T. *J. Eur. Ceram. Soc.* **2002**, *22*, 1177.
- (247) Malavasi, L.; Tealdi, C.; Flor, G.; Chiodelli, G.; Cervetto, V.; Montenero, A. M.; Borella, M. *Sens. Actuators, B* **2005**, *105*, 407.
- (248) Sahner, K.; Moos, R.; Matam, M.; Tunney, J. J.; Post, M. *Sens. Actuators, B* **2005**, *108*, 102.
- (249) Post, M. L.; Sanders, B. W. *Electrochem. Soc. Symp. Proc.* **1993**, *93*, 358.
- (250) Liu, X.; Cheng, B.; Hu, J.; Qin, H.; Jiang, M. *Sens. Actuators, B* **2008**, *129*, 53.
- (251) (a) Maclay, G. J.; Buttner, W. J.; Stetter, J. R. *IEEE Trans. Electron Devices* **1988**, *35*, 793. (b) Buttner, W. J.; Stetter, J. R.; Maclay, G. J. *Sens. Mater.* **1990**, *2*, 99.
- (252) Bryzek, J.; Roundy, S.; Bircumshaw, B.; Chung, C.; Castellino, K.; Vestel, M.; Stetter, J. R. *IEEE Circuits Devices* **2006**, *22* (2), 8.

CR800339K